Supplementary Information

Electrochemical ring-contraction synthesis of [60]fullerene-fused indanes from [60]fullerene-fused tetrahydroisoquinolines

Jian-Feng Li,[a‡] Wan-Qing Gao,[b‡] Zheng-Chun Yin,[*b] Wen-Jie Qiu,[a] Xinmin Huang,[a] Ming-Wei Liu[a] and Guan-Wu Wang[*ab]

[a]Department of Chemistry, University of Science and Technology of China, Hefei, Anhui 230026, P. R. China.
E-mail: gwang@ustc.edu.cn

[b]Key Laboratory of Functional Molecular Solids, Ministry of Education, Anhui Laboratory of Molecule-Based Materials and School of Chemistry and Materials Science, Anhui Normal University, Wuhu, Anhui 241002, P. R. China
E-mail: zcyin@ahnu.edu.cn

Table of Contents

1. General information

All electrochemical reactions were performed under argon (99.999%, containing 1.0 ppm of O_2 as determined by a trace oxygen analyzer) bubbling through a latex tube at 25 °C using a Shanghai Chenhua CHI630D workstation. Tetra-*n*-butylammonium perchlorate (TBAP) was recrystallized from absolute ethanol and dried in a vacuum at 50 °C prior to use. A conventional three-electrode cell was used for cyclic voltammetry (CV) and differential pulse voltammetry (DPV) measurements and consisted of a 2-mm diameter platinum disc working electrode, a platinum wire auxiliary electrode and a saturated calomel reference electrode (SCE). Controlled potential electrolysis (CPE) was carried out on a potentiostat/galvanostat using an "H"-type cell consisting of two platinum gauze electrodes (15 mm × 30 mm, serving as working and counter electrodes, respectively) and a SCE. The SCE was separated from the bulk of the solution by a fritted-glass bridge of low porosity, which contained the solvent/supporting electrolyte mixture. Compounds **1a-h** were synthesized according to the procedure developed by our group.[1] Other chemicals were purchased from commercial sources and used as received. ^{1}H NMR and ^{13}C NMR spectra were recorded on a Bruker ASCEND III–400 or a Bruker ASCEND III–500 spectrometer. ^{1}H NMR chemical shifts were determined relative to TMS (δ 0.00 ppm) or residual $CHCl_2CHCl_2$ (δ 5.88 ppm). ^{13}C NMR chemical shifts were determined relative to TMS (δ 0.00 ppm) or residual $CHCl_2CHCl_2$ (δ 72.86 ppm). Because $CDCl_2CDCl_2$ was not available in the solvent library of either the Bruker ASCEND III–400 or the Bruker ASCEND III–500 spectrometer, CD_2Cl_2 was selected as the closest alternative. Data for ^{1}H NMR and ^{13}C NMR are reported as follows: chemical shift (δ, ppm), multiplicity (s = singlet, d = doublet, t = triplet, m = multiplet). High-resolution mass spectra were obtained on a Bruker UltrafleXtreme MALDI-TOF/TOF instrument. UV-vis spectra were obtained on a SHIMADZU UV-3600PLUS instrument.

CVs and DPVs of compounds **1** and **3**: Compounds **1** and **3** dissolved in anhydrous 1,2-dichlorobenzene (1,2-$C_6H_4Cl_2$) solution containing 0.1 M TBAP under an argon atmosphere at room temperature. CV measurement was then undertaken at a scan rate of 50 mV s^{-1}. The parameters of DPV: step potential: 4 mV; pulse amplitude: 50 mV; pulse duration: 0.05 s; pulse period: 0.5 s.

Synthesis of dianion $\mathbf{1}^{2-}$: 0.015 mmol of **1a–h** dissolved in 15 mL of anhydrous 1,2-$C_6H_4Cl_2$ solution containing 0.1 M TBAP were added into an "H"-type cell. After bubbling with Ar/O_2 through a latex tube for 20 min at 25 °C, the solution was electroreduced by CPE at –1.34, –1.36, –1.34, –1.33, –1.31, –1.36, –1.35 V and –1.34 V *vs*. SCE, respectively. When the theoretical number of coulombs (2.89 C) was reached, the electrolysis was terminated after ca. 2 h, and the solution of $\mathbf{1}^{2-}$ was obtained.

Vis/NIR spectral measurement of the dianion of **1a**: 3.6 mg (3.6 μmol) of **1a** was electroreduced by CPE at –1.34 V *vs*. SCE in 15 mL of anhydrous 1,2-$C_6H_4Cl_2$ solution containing 0.1 M TBAP under argon bubbling. The electrolysis was terminated when the theoretical number of coulombs required for a full conversion of **1a** to $\mathbf{1a}^{2-}$ was reached. A dark brown-colored solution was obtained after the electrolysis, which is the typical color for C_{60} anionic species with two electrons distributed on the fullerene

skeleton. The resulted solution was transferred to a 10-mm quartz cuvette under argon for the Vis/NIR measurement.

2. CV diagrams of compounds 1a–h

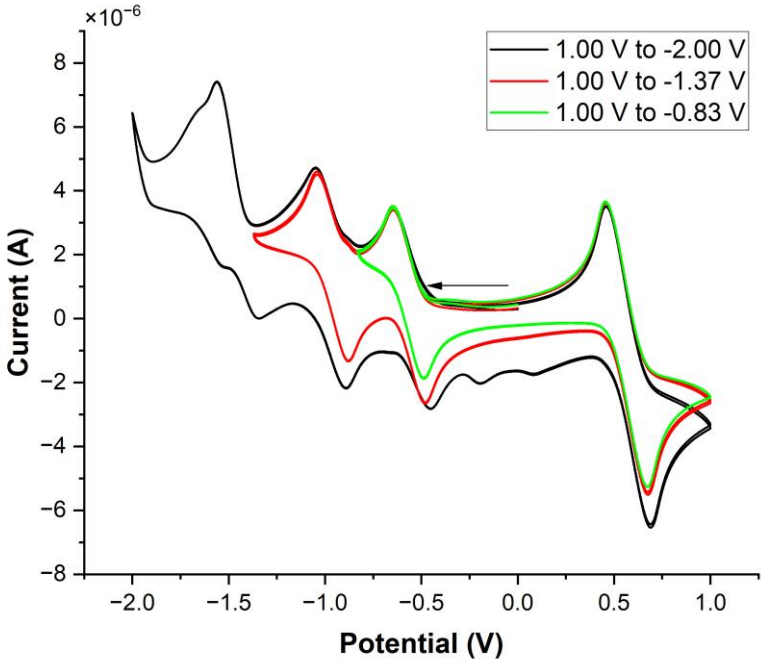

Fig. S1 CV of compound **1a** (scanning rate: 50 mV s^{-1}).

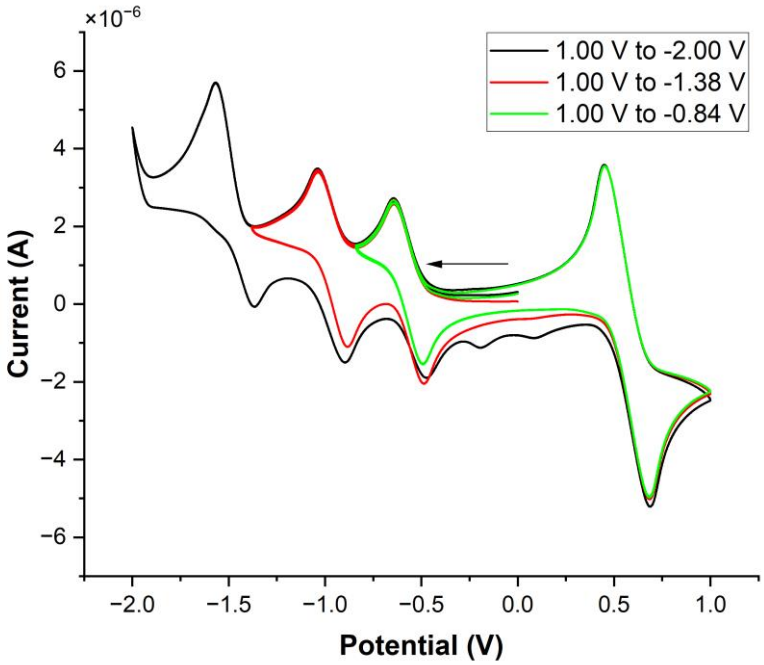

Fig. S2 CV of compound **1b** (scanning rate: 50 mV s^{-1}).

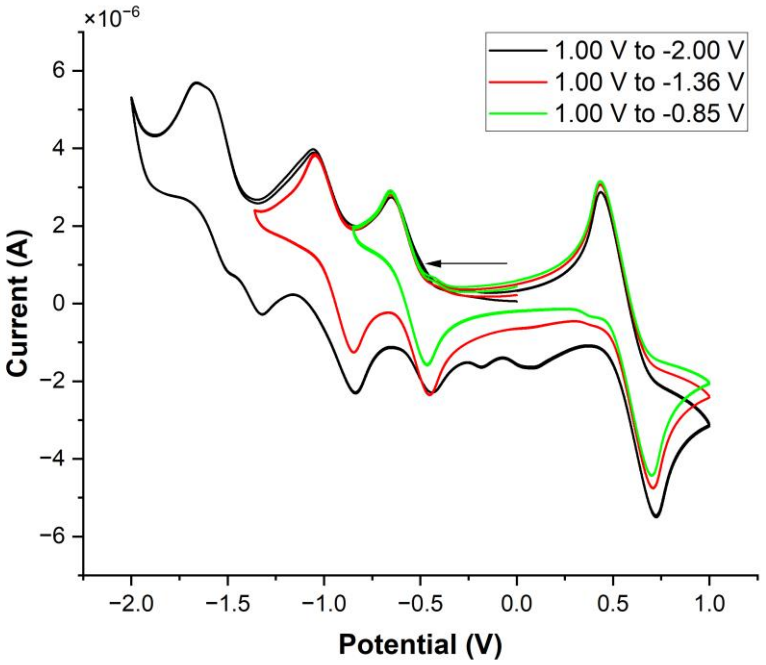

Fig. S3 CV of compound **1c** (scanning rate: 50 mV s^{-1}).

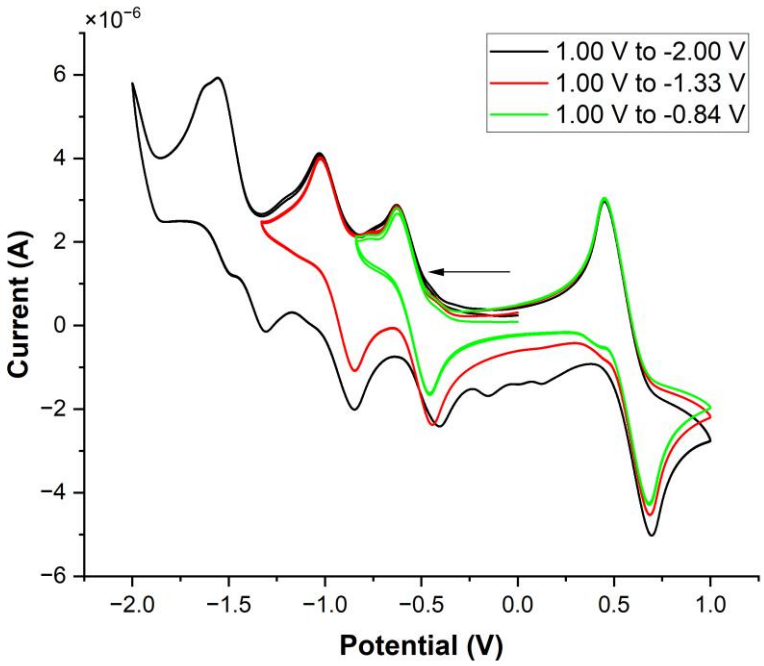

Fig. S4 CV of compound **1d** (scanning rate: 50 mV s^{-1}).

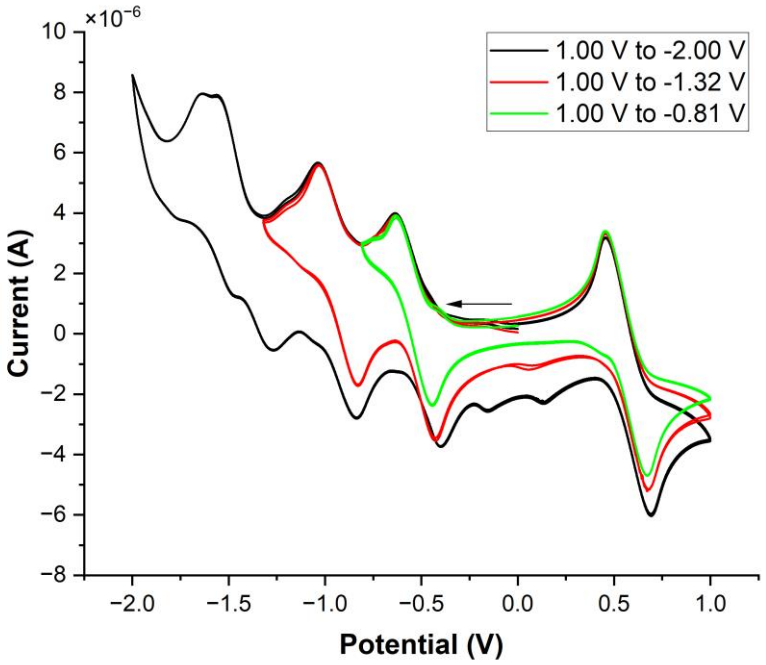

Fig. S5 CV of compound **1e** (scanning rate: 50 mV s^{-1}).

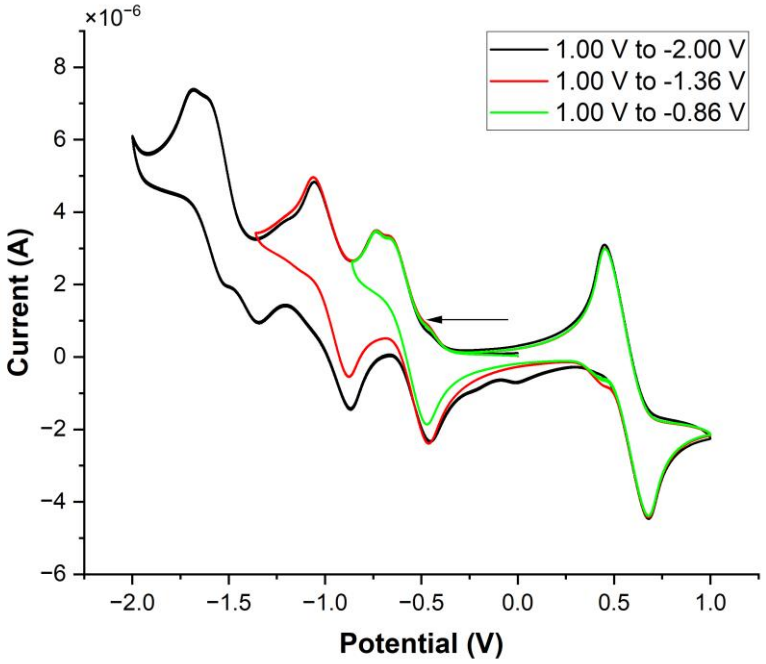

Fig. S6 CV of compound **1f** (scanning rate: 50 mV s^{-1}).

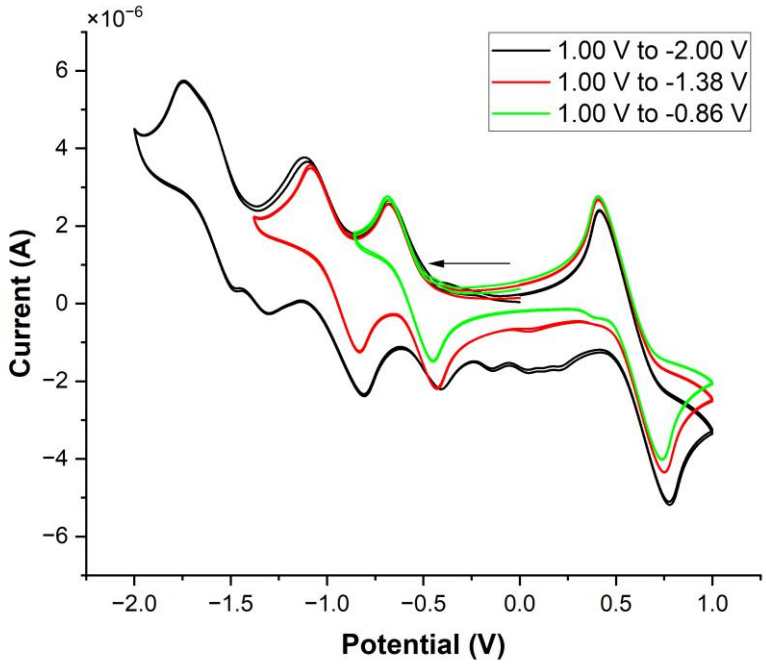

Fig. S7 CV of compound **1g** (scanning rate: 50 mV s^{-1}).

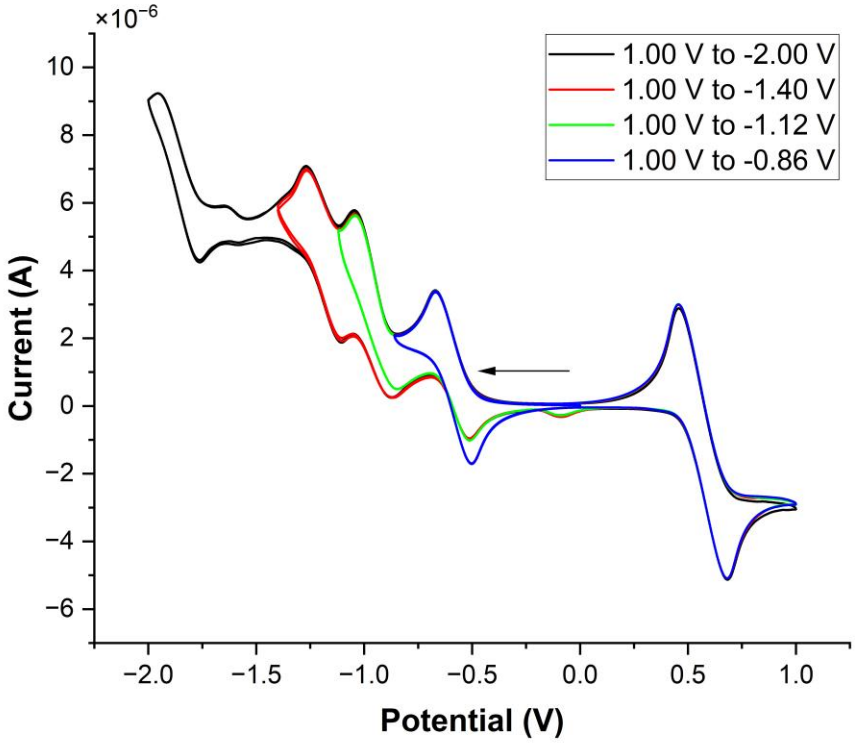

Fig. S8 CV of compound **1h** (scanning rate: 50 mV s^{-1}).

3. Syntheses and spectral data of compounds 3aa–ha

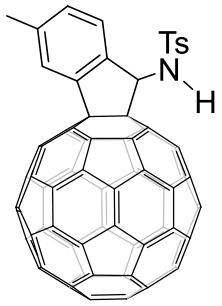

3aa

Synthesis and spectral data of 3aa: After the electrolysis of **1a** (14.9 mg, 0.015 mmol), the dianion $\mathbf{1a}^{2-}$ was stirred at 70 °C for 3 h under Ar/O_2 bubbling through a latex tube, then trifluoroacetic acid (TFA, 3.4 μL, 0.045 mmol) was added, and the reaction was stirred at 25 °C for 15 min, the resulting mixture was directly filtered through a silica gel column (200–300 mesh) plug with CS_2/ethyl acetate (5:1, v/v) to remove supporting electrolyte and insoluble materials, and then evaporated in vacuum to remove the solvent. Next, the residue was further separated on a silica gel column (300–400 mesh) with CS_2/CH_2Cl_2 (3:1, v/v) as the eluent to afford product **3aa** (9.9 mg, 66%) as an amorphous brown solid and the solubility of **3aa** in chloroform is 4.0 mg mL^{-1}; ^{1}H NMR (400 MHz, 1:1 CS_2/$CDCl_2CDCl_2$) δ 7.84 (s, 1H), 7.75 (d, J = 8.1 Hz, 2H), 7.57 (d, J = 7.9 Hz, 1H), 7.39 (d, J = 7.9 Hz, 1H), 7.11 (d, J = 8.1 Hz, 2H), 6.72 (d, J = 10.2 Hz, 1H), 5.77 (d, J = 10.2 Hz, 1H), 2.49 (s, 3H), 2.29 (s, 3H); ^{13}C NMR (101 MHz, 1:1 CS_2/$CDCl_2CDCl_2$) (all 1C unless indicated) δ 154.84, 153.57, 152.19, 150.61, 146.28, 146.10, 145.33, 145.16, 145.10 (2C), 145.04, 144.98, 144.85 (4C), 144.46, 144.43, 144.29, 144.21, 144.13, 144.10, 144.06 (2C), 144.03 (2C), 143.99, 143.85, 143.32, 143.22, 143.16 (aryl *C*), 142.99 (2C), 141.88, 141.86, 141.49 (aryl *C*), 141.42, 141.40, 141.09 (2C), 140.99, 140.93, 140.89, 140.84, 140.80, 140.74, 140.56 (3C), 140.48, 140.41, 140.21, 140.01 (2C), 139.46, 139.28, 138.00 (aryl *C*), 136.90 (aryl *C*), 135.26 (aryl *C*), 135.19, 133.92, 133.48, 133.29, 130.19 (aryl *C*), 128.77 (2C, aryl *C*), 126.30 (2C, aryl *C*), 125.79 (aryl *C*), 125.09 (aryl *C*), 73.89 (sp^3-*C* of C_{60}), 67.46, 20.60, 20.52; UV–vis ($CHCl_3$) λ_{max}/nm (log ε) 257 (5.00), 311 (4.54), 431 (4.30), 699 (3.74) (the characteristic absorptions at approximately 430 nm and 700 nm in the UV–vis data are consistent with the literature[2]); MALDI-TOF MS m/z calcd for $C_{75}H_{15}NO_2S$ $[M]^-$ 993.0829, found 993.0836.

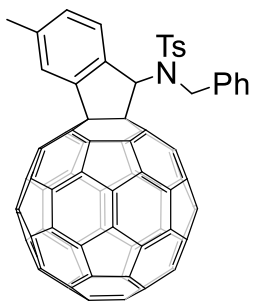

3ab

Synthesis and spectral data of 3ab: After the electrolysis of **1a** (14.9 mg, 0.015 mmol), the dianion $\mathbf{1a}^{2-}$ was stirred at 70 °C for 3 h under Ar/O_2 bubbling through a latex tube,

then benzyl bromide (35.6 μL, 0.300 mmol) was added, and the reaction was stirred at 25 °C for 2 h, the resulting mixture was directly filtered through a silica gel column (200–300 mesh) plug with CS_2/ethyl acetate (5:1, v/v) to remove supporting electrolyte and insoluble materials, and then evaporated in vacuum to remove the solvent. Next, the residue was further separated on a silica gel column (300–400 mesh) with CS_2/CH_2Cl_2 (2:1, v/v) as the eluent to afford product **3ab** (7.1 mg, 44%) as an amorphous brown solid; ^{1}H NMR (500 MHz, $CDCl_3$) δ 7.95 (s, 1H), 7.79 (d, J = 8.1 Hz, 2H), 7.57 (s, 1H), 7.25 (d, J = 8.1 Hz, 2H), 7.21 (d, J = 8.0 Hz, 1H), 7.19–7.16 (m, 1H), 7.13–7.11 (m, 4H), 7.04 (d, J = 8.0 Hz, 1H), 4.99 (d, J = 15.4 Hz, 1H), 4.79 (d, J = 15.4 Hz, 1H), 2.53 (s, 3H), 2.43 (s, 3H); ^{13}C NMR (126 MHz, $CDCl_3$) (all 1C unless indicated) δ 156.82, 154.41, 153.92, 152.76, 147.45, 147.36 (2C), 146.32, 146.29, 146.25, 146.20, 146.16, 146.10, 146.05, 146.03, 145.99, 145.93, 145.83, 145.76, 145.51, 145.38, 145.34, 145.32 (2C), 145.23 (2C), 145.17 (2C), 144.62, 144.59, 144.43, 144.34, 143.87 (aryl *C*), 143.50 (aryl *C*), 143.09, 143.07, 142.72, 142.62 (2C), 142.58, 142.43, 142.41, 142.16, 142.07, 142.01, 141.99, 141.91, 141.88, 141.87, 141.80, 141.65, 141.31, 141.00 (aryl *C*), 140.55, 140.36, 139.40, 139.22, 138.18 (aryl *C*), 137.17, 136.62 (aryl *C*), 136.10, 134.29, 134.27, 133.87 (aryl *C*), 130.40 (aryl *C*), 129.86 (2C, aryl *C*), 129.61 (2C, aryl *C*), 128.21 (2C, aryl *C*), 127.75 (aryl *C*), 127.67 (2C, aryl *C*), 127.58 (aryl *C*), 126.47 (aryl *C*), 75.91 (sp^3-*C* of C_{60}), 74.33, 74.26 (sp^3-*C* of C_{60}), 50.63, 21.64 (2C); UV–vis ($CHCl_3$) λ_{max}/nm (log ε) 257 (4.97), 311 (4.52), 431 (4.13), 702 (3.27) (the characteristic absorptions at approximately 430 nm and 700 nm in the UV–vis data are consistent with the literature[2]); MALDI-TOF MS *m*/*z* calcd for $C_{82}H_{21}NO_2S$ $[M]^-$ 1083.1298, found 1083.1305.

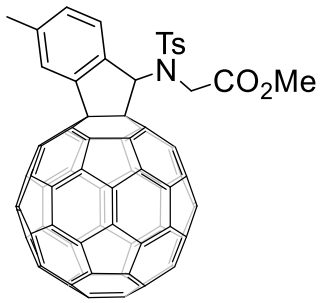

3ac

Synthesis and spectral data of 3ac: After the electrolysis of **1a** (14.9 mg, 0.015 mmol), the dianion $\mathbf{1a}^{2-}$ was stirred at 70 °C for 3 h under Ar/O_2 bubbling through a latex tube, then sodium hydride (NaH, 3.6 mg, 0.150 mmol) and methyl bromoacetate (28.4 μL, 0.300 mmol) was added and the reaction was stirred at 25 °C for 2 h, the resulting mixture was directly filtered through a silica gel column (200–300 mesh) plug with CS_2/ethyl acetate (5:1, v/v) to remove supporting electrolyte and insoluble materials, and then evaporated in vacuum to remove the solvent. Next, the residue was further separated on a silica gel column (300–400 mesh) with CS_2/CH_2Cl_2 (2:1, v/v) as the eluent to afford product **3ac** (11.1 mg, 69%) as an amorphous brown solid; ^{1}H NMR (400 MHz, $CDCl_3$) δ 8.08 (d, J = 8.1 Hz, 2H), 7.96 (s, 1H), 7.77 (d, J = 7.9 Hz, 1H), 7.45 (d, J = 7.9 Hz, 1H), 7.26 (s, 1H), 7.18 (d, J = 8.1 Hz, 2H), 4.54 (d, J = 17.9 Hz, 1H), 4.37 (d, J = 17.9 Hz, 1H), 3.66 (s, 3H), 2.56 (s, 3H), 2.34 (s, 3H); ^{13}C NMR (101 MHz, $CDCl_3$) (all 1C unless indicated) δ 169.37 (*C*=O), 156.32, 154.61, 153.84, 152.59, 147.87, 147.49, 147.35, 146.35, 146.33, 146.30, 146.24, 146.14, 146.09 (2C), 146.06 (2C), 145.74, 145.72, 145.67, 145.57, 145.34 (3C), 145.31 (2C), 145.25, 145.19, 145.00,

144.59 (aryl *C*), 144.56, 144.51, 144.39, 144.37, 143.33 (aryl *C*), 143.09, 143.07, 142.75, 142.70, 142.67, 142.61, 142.41, 142.31, 142.21, 142.06, 142.02 (2C), 141.84, 141.81 (3C), 141.55, 141.50 (aryl *C*), 141.33, 140.62, 140.54, 139.10, 139.06, 136.82 (aryl *C*), 136.28, 134.84, 134.67, 134.07, 133.51 (aryl *C*), 130.98 (aryl *C*), 129.60 (2C, aryl *C*), 129.08 (2C, aryl *C*), 127.55 (aryl *C*), 126.47 (aryl *C*), 74.96 (sp^3-*C* of C_{60}), 74.11 (sp^3-*C* of C_{60}), 73.80, 52.36, 47.46, 21.68, 21.67; UV–vis ($CHCl_3$) λ_{max}/nm (log ε) 257 (4.99), 310 (4.53), 431 (4.13), 699 (3.24) (the characteristic absorptions at approximately 430 nm and 700 nm in the UV–vis data are consistent with the literature[2]); MALDI-TOF MS m/z calcd for $C_{78}H_{19}NO_4S$ $[M]^-$ 1065.1040, found 1065.1048.

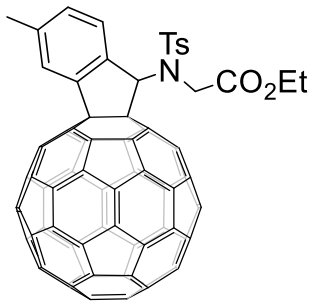

3ad

Synthesis and spectral data of 3ad: After the electrolysis of **1a** (14.9 mg, 0.015 mmol), the dianion $\mathbf{1a}^{2-}$ was stirred at 70 °C for 3 h under Ar/O_2 bubbling through a latex tube, then NaH (3.6 mg, 0.150 mmol) and ethyl bromoacetate (33.3 μL, 0.300 mmol) was added and the reaction was stirred at 25 °C for 2 h, the resulting mixture was directly filtered through a silica gel column (200–300 mesh) plug with CS_2/ethyl acetate (5:1, v/v) to remove supporting electrolyte and insoluble materials, and then evaporated in vacuum to remove the solvent. Next, the residue was further separated on a silica gel column (300–400 mesh) with CS_2/CH_2Cl_2 (2:1, v/v) as the eluent to afford product **3ad** (12.2 mg, 75%) as an amorphous brown solid; ^{1}H NMR (400 MHz, $CDCl_3$) δ 8.09 (d, J = 8.1 Hz, 2H), 7.96 (s, 1H), 7.81 (d, J = 7.9 Hz, 1H), 7.46 (d, J = 7.9 Hz, 1H), 7.25 (s, 1H), 7.17 (d, J = 8.1 Hz, 2H), 4.52 (d, J = 17.9 Hz, 1H), 4.34 (d, J = 17.9 Hz, 1H) 4.20–4.04 (m, 2H), 2.56 (s, 3H), 2.33 (s, 3H), 1.24 (t, J = 7.2 Hz, 3H); ^{13}C NMR (101 MHz, $CDCl_3$) (all 1C unless indicated) δ 168.86 (*C*=O), 156.30, 154.59, 153.82, 152.59, 147.86, 147.47, 147.32, 146.31, 146.30, 146.27, 146.21, 146.12, 146.06 (3C), 146.03, 145.70 (2C), 145.62, 145.57, 145.32, 145.31, 145.29, 145.27 (2C), 145.23, 145.16, 144.96, 144.56 (aryl *C*), 144.53, 144.50, 144.36, 144.34, 143.29 (aryl *C*), 143.08, 143.04, 142.73, 142.67, 142.64, 142.58, 142.39, 142.28, 142.19, 142.02, 142.00, 141.99, 141.82, 141.78 (2C), 141.77, 141.51, 141.46 (aryl *C*), 141.34, 140.60, 140.51, 139.04 (2C), 136.77 (aryl *C*), 136.25, 134.86, 134.64, 134.02, 133.56 (aryl *C*), 130.99 (aryl *C*), 129.56 (2C, aryl *C*), 129.13 (2C, aryl *C*), 127.59 (aryl *C*), 126.42 (aryl *C*), 74.91 (sp^3-*C* of C_{60}), 74.08 (sp^3-*C* of C_{60}), 73.74, 61.47, 47.58, 21.67 (2C), 14.21; UV–vis ($CHCl_3$) λ_{max}/nm (log ε) 257 (5.00), 311 (4.55), 431 (4.18), 703 (2.60) (the characteristic absorptions at approximately 430 nm and 700 nm in the UV–vis data are consistent with the literature[2]); MALDI-TOF MS m/z calcd for $C_{79}H_{21}NO_4S$ $[M]^-$ 1079.1197, found 1079.1208.

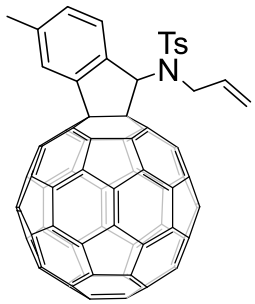

3ae

Synthesis and spectral data of 3ae: After the electrolysis of **1a** (14.9 mg, 0.015 mmol), the dianion **1a**$^{2-}$ was stirred at 70 °C for 3 h under Ar/O_2 bubbling through a latex tube, then allyl bromide (26.0 μL, 0.300 mmol) was added and the reaction was stirred at 25 °C for 2 h, the resulting mixture was directly filtered through a silica gel column (200–300 mesh) plug with CS_2/ethyl acetate (5:1, v/v) to remove supporting electrolyte and insoluble materials, and then evaporated in vacuum to remove the solvent. Next, the residue was further separated on a silica gel column (300–400 mesh) with CS_2/CH_2Cl_2 (3:1, v/v) as the eluent to afford product **3ae** (7.9 mg, 51%) as an amorphous brown solid; ^{1}H NMR (400 MHz, $CDCl_3$) δ 7.97 (s, 1H), 7.93 (d, J = 8.2 Hz, 2H), 7.45 (s, 1H), 7.36 (d, J = 7.9 Hz, 1H), 7.30 (d, J = 8.2 Hz, 2H), 7.24 (d, J = 7.9 Hz, 1H), 5.78–5.66 (m, 1H), 5.13 (dd, J = 17.1, 1.3 Hz, 1H), 5.05 (dd, J = 10.1, 1.3 Hz, 1H), 4.30 (d, J = 6.7 Hz, 2H), 2.54 (s, 3H), 2.44 (s, 3H); ^{13}C NMR (101 MHz, $CDCl_3$) (all 1C unless indicated) δ 156.62, 154.56, 154.05, 153.25, 147.47, 147.43, 147.39, 146.36, 146.33, 146.30, 146.21, 146.13 (2C), 146.11, 146.09, 146.02, 145.96, 145.80, 145.78, 145.68, 145.58, 145.38, 145.36, 145.33 (2C), 145.25 (2C), 145.21, 144.66, 144.58, 144.45, 144.40, 143.88 (aryl *C*), 143.51 (aryl *C*), 143.14, 143.11, 142.73, 142.68, 142.67, 142.62, 142.43, 142.38, 142.23, 142.13, 142.08, 142.07, 142.03, 141.93, 141.85, 141.74 (2C), 141.38, 141.18 (aryl *C*), 140.62, 140.50, 139.56, 139.48, 138.49 (aryl *C*), 136.82, 135.48, 134.61 (aryl *C*), 134.57, 134.43 (CH_2*C*H=CH_2), 134.33, 130.62 (aryl *C*), 129.80 (2C, aryl *C*), 127.88 (2C, aryl *C*), 127.18 (aryl *C*), 126.56 (aryl *C*), 118.49 (CH_2CH=*C*H_2), 75.90 (sp^3-*C* of C_{60}), 74.23, 74.17 (sp^3-*C* of C_{60}), 50.40, 21.67, 21.66; UV–vis ($CHCl_3$) λ_{max}/nm (log ε) 257 (4.96), 311 (4.52), 431 (4.15), 700 (2.64) (the characteristic absorptions at approximately 430 nm and 700 nm in the UV–vis data are consistent with the literature[2]); MALDI-TOF MS m/z calcd for $C_{78}H_{19}NO_2S$ [M]$^-$ 1033.1142, found 1033.1154.

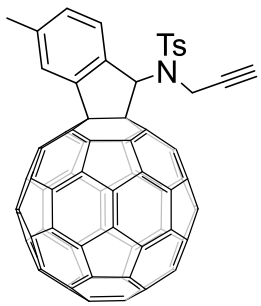

3af

Synthesis and spectral data of 3af: After the electrolysis of **1a** (14.9 mg, 0.015 mmol), the dianion **1a**$^{2-}$ was stirred at 70 °C for 3 h under Ar/O_2 bubbling through a latex tube,

then propargyl bromide (25.9 μL, 0.300 mmol) was added and the reaction was stirred at 25 °C for 2 h, the resulting mixture was directly filtered through a silica gel column (200–300 mesh) plug with CS_2/ethyl acetate (5:1, v/v) to remove supporting electrolyte and insoluble materials, and then evaporated in vacuum to remove the solvent. Next, the residue was further separated on a silica gel column (300–400 mesh) with CS_2/CH_2Cl_2 (3:1, v/v) as the eluent to afford product **3af** (6.5 mg, 42%) as an amorphous brown solid; ^{1}H NMR (500 MHz, $CDCl_3$) δ 8.05 (d, J = 8.3 Hz, 2H), 7.97 (s, 1H), 7.44 (d, J = 7.9 Hz, 1H), 7.39 (d, J = 7.9 Hz, 1H), 7.38 (s, 1H), 7.27 (d, J = 8.3 Hz, 2H), 4.51 (dd, J = 18.0, 2.4 Hz, 1H), 4.47 (dd, J = 18.0, 2.4 Hz, 1H), 2.52 (s, 3H), 2.42 (s, 3H), 2.18 (t, J = 2.4 Hz, 1H); ^{13}C NMR (101 MHz, $CDCl_3$) (all 1C unless indicated) δ 156.43, 154.66, 153.75, 152.63, 147.56, 147.50, 147.38, 146.35, 146.33, 146.32, 146.22, 146.13 (2C), 146.10 (2C), 146.04, 145.85, 145.78, 145.72, 145.67, 145.53, 145.35 (2C), 145.33, 145.30, 145.28, 145.22 (2C), 144.63, 144.52, 144.42, 144.40, 144.23 (aryl *C*), 143.34 (aryl *C*), 143.11, 143.10, 142.72, 142.68, 142.66, 142.62, 142.43, 142.34, 142.26, 142.09, 142.08, 142.03, 141.94, 141.84, 141.80, 141.76, 141.74, 141.59, 141.43 (aryl *C*), 140.62, 140.51, 139.42, 139.40, 137.68 (aryl *C*), 136.89, 135.09, 134.79, 134.31, 133.27 (aryl *C*), 130.75 (aryl *C*), 129.66 (2C, aryl *C*), 128.25 (2C, aryl *C*), 127.62 (aryl *C*), 126.52 (aryl *C*), 79.28 (CH_2C≡CH), 75.44 (sp^3-*C* of C_{60}), 74.12, 74.10 (sp^3-*C* of C_{60}), 73.15 (CH_2C≡*C*H), 36.20, 21.70, 21.69; UV–vis ($CHCl_3$) λ_{max}/nm (log ε) 257 (4.99), 311 (4.54), 431 (4.16), 698 (2.59) (the characteristic absorptions at approximately 430 nm and 700 nm in the UV–vis data are consistent with the literature[2]); MALDI-TOF MS m/z calcd for $C_{78}H_{17}NO_2S$ $[M]^-$ 1031.0985, found 1031.0995.

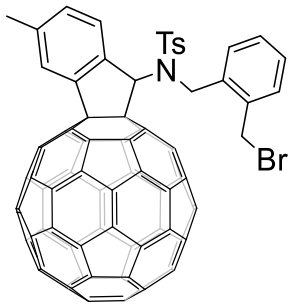

3ag

Synthesis and spectral data of 3ag: After the electrolysis of **1a** (14.9 mg, 0.015 mmol), the dianion $\mathbf{1a}^{2-}$ was stirred at 70 °C for 3 h under Ar/O_2 bubbling through a latex tube, then 1,2-bis(bromomethyl) benzene (40.4 μL, 0.300 mmol) was added and the reaction was stirred at 25 °C for 2 h, the resulting mixture was directly filtered through a silica gel column (200–300 mesh) plug with CS_2/ethyl acetate (5:1, v/v) to remove supporting electrolyte and insoluble materials, and then evaporated in vacuum to remove the solvent. Next, the residue was further separated on a silica gel column (300–400 mesh) with CS_2/CH_2Cl_2 (2:1, v/v) as the eluent to afford product **3ag** (8.9 mg, 50%) as an amorphous brown solid; ^{1}H NMR (400 MHz, $CDCl_3$) δ 7.99 (d, J = 8.0 Hz, 2H), 7.94 (s, 1H), 7.55 (s, 1H), 7.44 (d, J = 8.0 Hz, 2H), 7.32 (d, J = 7.9 Hz, 1H), 7.21 (d, J = 7.5 Hz, 1H), 7.16 (t, J = 7.5 Hz, 1H), 6.99 (t, J = 7.6 Hz, 1H), 6.81 (d, J = 7.6 Hz, 1H), 6.76 (d, J = 7.9 Hz, 1H), 5.21 (d, J = 15.5 Hz, 1H), 4.73 (d, J = 15.5 Hz, 1H), 4.68 (d, J = 10.4 Hz, 1H), 4.16 (d, J = 10.4 Hz, 1H), 2.55 (s, 3H), 2.54 (s, 3H); ^{13}C NMR (101 MHz, $CDCl_3$) (all 1C unless indicated) δ 156.82, 154.12, 153.38, 152.23, 147.48, 147.45,

147.37, 146.50, 146.31, 146.28, 146.16, 146.14, 146.09, 146.04, 146.02, 145.97, 145.85, 145.82, 145.58, 145.44, 145.40, 145.31, 145.28, 145.23 (4C), 145.16, 144.68, 144.60, 144.42 (2C), 144.33 (aryl *C*), 144.14 (aryl *C*), 143.08, 143.04, 142.69, 142.60, 142.56 (2C), 142.46, 142.45, 142.15, 142.00, 141.96, 141.94, 141.90 (2C), 141.86, 141.64, 141.57, 141.23 (aryl *C*), 141.00, 140.52, 140.17, 139.44, 139.21, 137.50 (aryl *C*), 137.30, 136.99 (aryl *C*), 136.21, 134.66 (aryl *C*), 134.57, 134.20, 133.06 (aryl *C*), 131.53 (aryl *C*), 130.67 (aryl *C*), 130.49 (aryl *C*), 130.26 (2C, aryl *C*), 128.90 (aryl *C*), 128.64 (aryl *C*), 127.82 (2C, aryl *C*), 127.31 (aryl *C*), 126.76 (aryl *C*), 75.88 (sp^3-*C* of C_{60}), 74.82, 73.93 (sp^3-*C* of C_{60}), 46.39, 31.61, 21.75, 21.64; UV–vis ($CHCl_3$) λ_{max}/nm (log ε) 257 (5.00), 311 (4.54), 430 (4.30), 698 (3.75) (the characteristic absorptions at approximately 430 nm and 700 nm in the UV–vis data are consistent with the literature[2]); MALDI-TOF MS m/z calcd for $C_{83}H_{22}NO_2S^{79}Br$ $[M]^-$ 1175.0560, found 1175.0569.

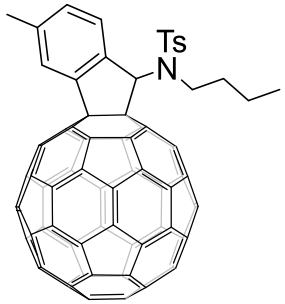

3ah

Synthesis and spectral data of 3ah: After the electrolysis of **1a** (14.9 mg, 0.015 mmol), the dianion $\mathbf{1a}^{2-}$ was stirred at 70 °C for 3 h under Ar/O_2 bubbling through a latex tube, then *n*-butyl iodide (85.4 μL, 0.750 mmol) was added and the reaction was stirred at 70 °C for 1 h, the resulting mixture was directly filtered through a silica gel column (200–300 mesh) plug with CS_2/ethyl acetate (5:1, v/v) to remove supporting electrolyte and insoluble materials, and then evaporated in vacuum to remove the solvent. Next, the residue was further separated on a silica gel column (300–400 mesh) with CS_2/CH_2Cl_2 (4:1, v/v) as the eluent to afford product **3ah** (9.7 mg, 62%) as an amorphous brown solid and the solubility of **3ah** in chloroform is 53.8 mg mL^{-1}; ^1H NMR (500 MHz, 1:1 $CS_2/CDCl_2CDCl_2$) δ 7.87 (s, 1H), 7.80 (d, J = 8.0 Hz, 2H), 7.29 (d, J = 8.1 Hz, 1H), 7.25 (s, 1H), 7.23 (d, J = 8.1 Hz, 1H), 7.19 (d, J = 8.0 Hz, 2H), 3.59–3.49 (m, 1H), 3.44–3.35 (m, 1H), 2.47 (s, 3H), 2.33 (s, 3H), 1.68–1.56 (m, 2H), 1.12–0.99 (m, 2H), 0.69 (tt, J = 7.4, 1.5 Hz, 3H); ^{13}C NMR (126 MHz, $CDCl_3$) (all 1C unless indicated) δ 156.74, 154.74, 154.14, 153.22, 147.46, 147.39, 147.36, 146.34, 146.31, 146.30, 146.21, 146.10 (3C), 146.02, 146.00, 145.88, 145.80 (2C), 145.71, 145.53, 145.35 (2C), 145.32, 145.25 (2C), 145.20, 145.17, 144.62, 144.55, 144.44, 144.41, 143.84 (aryl *C*), 143.26 (aryl *C*), 143.13, 143.10, 142.73, 142.67 (2C), 142.62, 142.39, 142.34, 142.23, 142.14, 142.07, 142.03 (2C), 141.83, 141.80, 141.75, 141.64, 141.28, 141.02 (aryl *C*), 140.60, 140.51, 139.38, 139.25, 138.64 (aryl *C*), 136.61, 135.31, 134.73 (aryl *C*), 134.54, 134.19, 130.59 (aryl *C*), 129.86 (2C, aryl *C*), 127.69 (2C, aryl *C*), 127.17 (aryl *C*), 126.47 (aryl *C*), 75.69 (sp^3-*C* of C_{60}), 74.47, 74.25 (sp^3-*C* of C_{60}), 47.98, 32.20, 21.66, 21.64, 20.63, 13.65; UV–vis ($CHCl_3$) λ_{max}/nm (log ε) 257 (5.02), 311 (4.56), 431 (4.32), 701 (3.76) (the characteristic absorptions at approximately 430 nm and 700 nm in the UV–vis data are consistent with the

literature[2]); MALDI-TOF MS m/z calcd for $C_{79}H_{23}NO_2S$ $[M]^-$ 1049.1455, found 1049.1450.

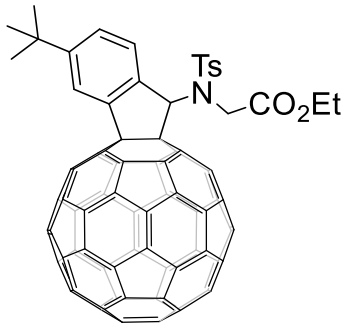

3bd

Synthesis and spectral data of 3bd: After the electrolysis of **1b** (15.5 mg, 0.015 mmol), the dianion $\mathbf{1b}^{2-}$ was stirred at 70 °C for 3 h under Ar/O_2 bubbling through a latex tube, then NaH (3.6 mg, 0.150 mmol) and ethyl bromoacetate (33.3 μL, 0.300 mmol) was added and the reaction was stirred at 25 °C for 2 h, the resulting mixture was directly filtered through a silica gel column (200–300 mesh) plug with CS_2/ethyl acetate (5:1, v/v) to remove supporting electrolyte and insoluble materials, and then evaporated in vacuum to remove the solvent. Next, the residue was further separated on a silica gel column (300–400 mesh) with CS_2/CH_2Cl_2 (2:1, v/v) as the eluent to afford product **3bd** (11.5 mg, 68%) as an amorphous brown solid; ^{1}H NMR (400 MHz, $CDCl_3$) δ 8.12 (s, 1H), 8.10 (d, J = 8.0 Hz, 2H), 7.83 (d, J = 8.2 Hz, 1H), 7.69 (d, J = 8.2 Hz, 1H), 7.25 (s, 1H), 7.18 (d, J = 8.0 Hz, 2H), 4.54 (d, J = 18.0 Hz, 1H), 4.36 (d, J = 18.0 Hz, 1H), 4.20–4.04 (m, 2H), 2.34 (s, 3H), 1.45 (s, 9H), 1.24 (t, J = 7.1 Hz, 3H); ^{13}C NMR (101 MHz, $CDCl_3$) (all 1C unless indicated) δ 168.89 (*C*=O), 156.45, 154.90 (aryl *C*), 154.74, 153.93, 152.68, 147.96, 147.48, 147.34, 146.33, 146.31, 146.28, 146.23, 146.13, 146.08 (3C), 146.05, 145.73 (2C), 145.65, 145.54, 145.33 (2C), 145.31 (3C), 145.24, 145.18, 144.96, 144.57, 144.55 (aryl *C*), 144.53, 144.38, 144.35, 143.11, 143.07, 142.90 (aryl *C*), 142.75, 142.69, 142.65, 142.60, 142.42, 142.31, 142.21, 142.03 (3C), 141.83 (2C), 141.80, 141.79, 141.54, 141.37, 140.68, 140.59, 139.08 (2C), 136.80 (aryl *C*), 136.31, 134.90, 134.75, 134.06, 133.57 (aryl *C*), 129.56 (2C, aryl *C*), 129.16 (2C, aryl *C*), 127.64 (aryl *C*), 127.33 (aryl *C*), 122.36 (aryl *C*), 75.00 (sp^3-*C* of C_{60}), 74.39 (sp^3-*C* of C_{60}), 73.76, 61.45, 47.67, 35.34, 31.52 (3C), 21.67, 14.25; UV–vis ($CHCl_3$) λ_{max}/nm (log ε) 257 (4.99), 310 (4.51), 431 (4.17), 701 (3.38) (the characteristic absorptions at approximately 430 nm and 700 nm in the UV–vis data are consistent with the literature[2]); MALDI-TOF MS m/z calcd for $C_{82}H_{27}NO_4S$ $[M]^-$ 1121.1666, found 1121.1658.

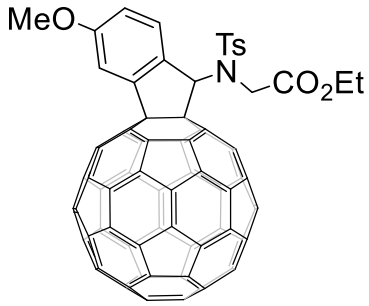

3cd

Synthesis and spectral data of 3cd: After the electrolysis of **1c** (15.1 mg, 0.015 mmol), the dianion $\mathbf{1c}^{2-}$ was stirred at 100 °C for 3 h under Ar/O_2 bubbling through a latex tube, then NaH (3.6 mg, 0.150 mmol) and ethyl bromoacetate (33.3 μL, 0.300 mmol) was added and the reaction was stirred at 25 °C for 2 h, the resulting mixture was directly filtered through a silica gel column (200–300 mesh) plug with CS_2/ethyl acetate (5:1, v/v) to remove supporting electrolyte and insoluble materials, and then evaporated in vacuum to remove the solvent. Next, the residue was further separated on a silica gel column (300–400 mesh) with CS_2/CH_2Cl_2 (2:1, v/v) as the eluent to afford product **3cd** (7.3 mg, 45%) as an amorphous brown solid; ^{1}H NMR (500 MHz, $CDCl_3$) δ 8.09 (d, J = 8.1 Hz, 2H), 7.82 (d, J = 8.6 Hz, 1H), 7.61 (d, J = 2.4 Hz, 1H), 7.21 (s, 1H), 7.20 (dd, J = 8.6, 2.4 Hz, 1H), 7.18 (d, J = 8.1 Hz, 2H), 4.52 (d, J = 17.9 Hz, 1H), 4.37 (d, J = 17.9 Hz, 1H), 4.19–4.06 (m, 2H), 3.95 (s, 3H), 2.34 (s, 3H), 1.25 (t, J = 7.2 Hz, 3H); ^{13}C NMR (126 MHz, $CDCl_3$) (all 1C unless indicated) δ 168.90 (*C*=O), 162.29 (aryl *C*), 156.14, 154.30, 153.66, 152.55, 147.83, 147.48, 147.36, 146.34, 146.32, 146.30, 146.22, 146.13, 146.08 (2C), 146.04, 145.93, 145.71 (2C), 145.61, 145.54, 145.38, 145.35, 145.33, 145.32, 145.30, 145.25, 145.17, 145.01, 144.82 (aryl *C*), 144.55, 144.53, 144.51 (2C), 144.35 (aryl *C*), 143.10, 143.06, 142.75, 142.69, 142.66, 142.60, 142.42, 142.31, 142.15, 142.02 (2C), 141.99, 141.85, 141.78 (2C), 141.76, 141.54, 141.35, 140.64, 140.54, 139.11, 139.08, 136.89 (aryl *C*), 136.23, 135.01, 134.68, 134.03, 129.57 (2C, aryl *C*), 129.10 (2C, aryl *C*), 128.88 (aryl *C*), 127.83 (aryl *C*), 117.23 (aryl *C*), 109.95 (aryl *C*), 75.22 (sp^3-*C* of C_{60}), 74.06 (sp^3-*C* of C_{60}), 73.45, 61.47, 55.86, 47.42, 21.66, 14.23; UV–vis ($CHCl_3$) λ_{max}/nm (log ε) 256 (5.00), 311 (4.53), 431 (4.13), 701 (2.52) (the characteristic absorptions at approximately 430 nm and 700 nm in the UV–vis data are consistent with the literature[2]); MALDI-TOF MS m/z calcd for $C_{79}H_{21}NO_5S$ $[M]^-$ 1095.1146, found 1095.1135.

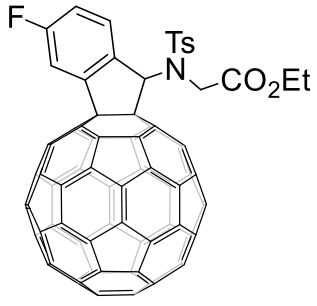

3dd

Synthesis and spectral data of 3dd: After the electrolysis of **1d** (15.0 mg, 0.015 mmol), the dianion $\mathbf{1d}^{2-}$ was stirred at 100 °C for 3 h under Ar/O_2 bubbling through a latex tube,

then NaH (3.6 mg, 0.150 mmol) and ethyl bromoacetate (33.3 μL, 0.300 mmol) was added and the reaction was stirred at 25 °C for 2 h, the resulting mixture was directly filtered through a silica gel column (200–300 mesh) plug with CS_2/ethyl acetate (5:1, v/v) to remove supporting electrolyte and insoluble materials, and then evaporated in vacuum to remove the solvent. Next, the residue was further separated on a silica gel column (300–400 mesh) with CS_2/CH_2Cl_2 (2:1, v/v) as the eluent to afford product **3dd** (9.9 mg, 61%) as an amorphous brown solid; ^{1}H NMR (500 MHz, $CDCl_3$) δ 8.06 (d, J = 8.2 Hz, 2H), 7.92 (dd, J = 8.6, 5.0 Hz, 1H), 7.82 (dd, J = 8.2, 2.5 Hz, 1H), 7.33 (td, J = 8.5, 2.5 Hz, 1H), 7.21 (s, 1H), 7.17 (d, J = 8.2 Hz, 2H), 4.49 (d, J = 17.9 Hz, 1H), 4.35 (d, J = 17.9 Hz, 1H), 4.21–4.05 (m, 2H), 2.34 (s, 3H), 1.25 (t, J = 7.2 Hz, 3H); ^{13}C NMR (126 MHz, 1:1 $CS_2/CDCl_3$) (all 1C unless indicated) δ 168.55 (*C*=O), 164.77 (aryl *C*, d, $J_{C\text{-}F}$ = 251.2 Hz), 155.66, 153.65, 153.00, 151.99, 147.58, 147.47, 147.34, 146.35, 146.33, 146.31, 146.23, 146.12, 146.08, 146.07, 146.04, 145.70, 145.59 (2C), 145.52 (aryl *C*, d, $J_{C\text{-}F}$ = 8.1 Hz), 145.51, 145.46, 145.40, 145.31 (2C), 145.26, 145.21, 145.18, 145.15, 145.02, 144.50, 144.48 (3C), 144.30 (aryl *C*), 143.09, 143.05, 142.76, 142.70, 142.66, 142.60, 142.38, 142.27, 142.03, 141.99, 141.97, 141.89, 141.81 (2C), 141.79, 141.74, 141.52, 141.28, 140.70, 140.61, 139.10, 139.06, 136.80 (aryl *C*), 136.16, 135.07, 134.72, 133.93, 132.07 (aryl *C*, d, $J_{C\text{-}F}$ = 2.3 Hz), 129.76 (aryl *C*, d, $J_{C\text{-}F}$ = 9.0 Hz), 129.55 (2C, aryl *C*), 129.08 (2C, aryl *C*), 117.59 (aryl *C*, d, $J_{C\text{-}F}$ = 23.1 Hz), 112.75 (aryl *C*, d, $J_{C\text{-}F}$ = 23.2 Hz), 75.05 (sp^3-*C* of C_{60}), 73.69 (sp^3-*C* of C_{60}), 73.12, 61.49, 47.49, 21.65, 14.22; UV–vis ($CHCl_3$) λ_{max}/nm (log ε) 257 (4.99), 312 (4.51), 431 (4.18), 701 (3.39) (the characteristic absorptions at approximately 430 nm and 700 nm in the UV–vis data are consistent with the literature[2]); MALDI-TOF MS m/z calcd for $C_{78}H_{18}FNO_4S$ $[M]^-$ 1083.0946, found 1083.0934.

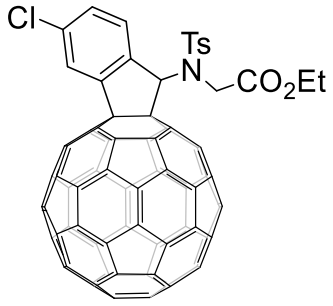

3ed

Synthesis and spectral data of 3ed: After the electrolysis of **1e** (15.2 mg, 0.015 mmol), the dianion $\mathbf{1e}^{2-}$ was stirred at 110 °C for 3 h under Ar/O_2 bubbling through a latex tube, then NaH (3.6 mg, 0.150 mmol) and ethyl bromoacetate (33.3 μL, 0.300 mmol) was added and the reaction was stirred at 25 °C for 2 h, the resulting mixture was directly filtered through a silica gel column (200–300 mesh) plug with CS_2/ethyl acetate (5:1, v/v) to remove supporting electrolyte and insoluble materials, and then evaporated in vacuum to remove the solvent. Next, the residue was further separated on a silica gel column (300–400 mesh) with CS_2/CH_2Cl_2 (2:1, v/v) as the eluent to afford product **3ed** (11.9 mg, 72%) as an amorphous brown solid; ^{1}H NMR (500 MHz, 1:1 $CS_2/CDCl_3$) δ 8.12 (d, J = 2.0 Hz, 1H), 8.05 (d, J = 8.2 Hz, 2H), 7.87 (d, J = 8.4 Hz, 1H), 7.58 (dd, J = 8.4, 2.0 Hz, 1H), 7.19 (s, 1H), 7.17 (d, J = 8.2 Hz, 2H), 4.47 (d, J = 17.8 Hz, 1H), 4.33 (d, J = 17.8 Hz, 1H), 4.17–4.04 (m, 2H), 2.34 (s, 3H), 1.25 (t, J = 7.1 Hz, 3H); ^{13}C NMR (126 MHz, 1:1 $CS_2/CDCl_3$) (all 1C unless indicated) δ 168.44 (*C*=O), 155.55,

153.59, 152.85, 151.83, 147.51, 147.41, 147.28, 146.30, 146.29, 146.26, 146.19, 146.07, 146.04, 146.02, 146.00, 145.66, 145.56, 145.54, 145.46, 145.42, 145.37, 145.26 (2C), 145.21, 145.15, 145.10 (2C), 144.97 (2C, including one aryl *C*), 144.46 (2C), 144.44, 144.42, 144.25 (aryl *C*), 143.04, 143.01, 142.71, 142.65, 142.61, 142.56, 142.33, 142.22, 141.99, 141.95, 141.93, 141.84, 141.78, 141.76, 141.75, 141.70, 141.48, 141.22, 140.65, 140.56, 139.05, 139.00, 137.23 (aryl *C*), 136.66 (aryl *C*), 136.10, 135.14 (aryl *C*), 134.98, 134.68, 133.88, 130.13 (aryl *C*), 129.53 (2C, aryl *C*), 129.21 (aryl *C*), 129.06 (2C, aryl *C*), 126.17 (aryl *C*), 74.76 (sp^3-*C* of C_{60}), 73.57 (sp^3-*C* of C_{60}), 73.19, 61.49, 47.51, 21.65, 14.21; UV–vis ($CHCl_3$) λ_{max}/nm (log ε) 257 (4.99), 311 (4.52), 431 (4.13), 701 (2.62) (the characteristic absorptions at approximately 430 nm and 700 nm in the UV–vis data are consistent with the literature[2]); MALDI-TOF MS m/z calcd for $C_{78}H_{18}{}^{35}ClNO_4S$ $[M]^-$ 1099.0651, found 1099.0642.

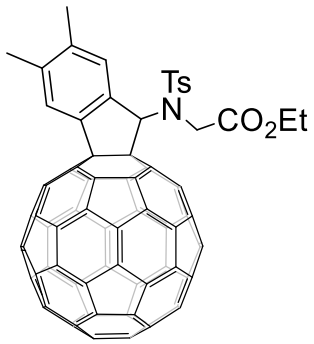

3fd

Synthesis and spectral data of 3fd: After the electrolysis of **1f** (15.1 mg, 0.015 mmol), the dianion $\mathbf{1f}^{2-}$ was stirred at 70 °C for 3 h under Ar/O_2 bubbling through a latex tube, then NaH (3.6 mg, 0.150 mmol) and ethyl bromoacetate (33.3 μL, 0.300 mmol) was added and the reaction was stirred at 25 °C for 2 h, the resulting mixture was directly filtered through a silica gel column (200–300 mesh) plug with CS_2/ethyl acetate (5:1, v/v) to remove supporting electrolyte and insoluble materials, and then evaporated in vacuum to remove the solvent. Next, the residue was further separated on a silica gel column (300–400 mesh) with CS_2/CH_2Cl_2 (2:1, v/v) as the eluent to afford product **3fd** (10.3 mg, 63%) as an amorphous brown solid; ^{1}H NMR (400 MHz, $CDCl_3$) δ 8.09 (d, J = 8.2 Hz, 2H), 7.90 (s, 1H), 7.63 (s, 1H), 7.22 (s, 1H), 7.16 (d, J = 8.2 Hz, 2H), 4.53 (d, J = 18.0 Hz, 1H), 4.31 (d, J = 18.0 Hz, 1H), 4.19–4.04 (m, 2H), 2.48 (s, 3H), 2.46 (s, 3H), 2.32 (s, 3H), 1.24 (t, J = 7.1 Hz, 3H); ^{13}C NMR (101 MHz, $CDCl_3$) (all 1C unless indicated) δ 168.84 (*C*=O), 156.49, 154.75, 153.85, 152.72, 147.90, 147.43, 147.28, 146.28, 146.24, 146.21, 146.17, 146.11, 146.08, 146.02 (2C), 146.00, 145.67 (2C), 145.60, 145.52, 145.27, 145.25 (2C), 145.22, 145.19, 145.13, 145.11, 144.87, 144.57 (aryl *C*), 144.50, 144.47, 144.35, 144.31, 143.04, 143.01, 142.70, 142.63, 142.59, 142.53, 142.36, 142.24, 142.21, 142.06, 141.95 (2C), 141.77 (2C), 141.75, 141.74, 141.44, 141.33, 140.79 (aryl *C*), 140.56, 140.47, 140.34 (aryl *C*), 139.11 (aryl *C*), 138.99 (2C), 136.66 (aryl *C*), 136.20, 134.72, 134.65, 134.01, 133.82 (aryl *C*), 129.56 (2C, aryl *C*), 129.18 (2C, aryl *C*), 128.03 (aryl *C*), 126.72 (aryl *C*), 74.84 (sp^3-*C* of C_{60}), 73.95 (sp^3-*C* of C_{60}), 73.88, 61.44, 47.64, 21.65, 20.36, 20.26, 14.23; UV–vis ($CHCl_3$) λ_{max}/nm (log ε) 257 (5.00), 311 (4.51), 431 (4.15), 703 (3.39) (the characteristic absorptions at approximately 430 nm and 700 nm in the UV–vis data are consistent with the literature[2]); MALDI-TOF MS m/z calcd for $C_{80}H_{23}NO_4S$ $[M]^-$ 1093.1353, found 1093.1345.

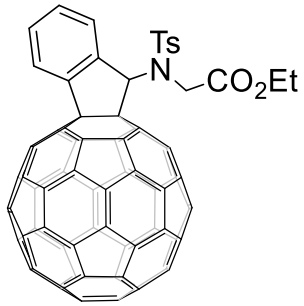

3gd

Synthesis and spectral data of 3gd: After the electrolysis of **1g** (14.7 mg, 0.015 mmol), the dianion $\mathbf{1g}^{2-}$ was stirred at 70 °C for 3 h under Ar/O_2 bubbling through a latex tube, then NaH (3.6 mg, 0.150 mmol) and ethyl bromoacetate (33.3 μL, 0.300 mmol) was added and the reaction was stirred at 25 °C for 2 h, the resulting mixture was directly filtered through a silica gel column (200–300 mesh) plug with CS_2/ethyl acetate (5:1, v/v) to remove supporting electrolyte and insoluble materials, and then evaporated in vacuum to remove the solvent. Next, the residue was further separated on a silica gel column (300–400 mesh) with CS_2/CH_2Cl_2 (2:1, v/v) as the eluent to afford product **3gd** (10.3 mg, 64%) as an amorphous brown solid; ^{1}H NMR (500 MHz, 1:1 $CS_2/CDCl_3$) δ 8.14 (d, J = 7.5 Hz, 1H), 8.06 (d, J = 8.3 Hz, 2H), 7.90 (d, J = 7.8 Hz, 1H), 7.69 (t, J = 7.4 Hz, 1H), 7.61 (t, J = 7.5 Hz, 1H), 7.24 (s, 1H), 7.16 (d, J = 8.3 Hz, 2H), 4.47 (d, J = 17.9 Hz, 1H), 4.31 (d, J = 17.9 Hz, 1H), 4.15–4.02 (m, 2H), 2.35 (s, 3H), 1.23 (t, J = 7.1 Hz, 3H); ^{13}C NMR (126 MHz, 1:1 $CS_2/CDCl_3$) (all 1C unless indicated) δ 168.46 (*C*=O), 156.11, 154.34, 153.57, 152.36, 147.75, 147.36, 147.23, 146.24 (2C), 146.20, 146.14, 146.04, 145.98 (2C), 145.94, 145.83, 145.64, 145.57, 145.50, 145.37, 145.29, 145.26, 145.24, 145.22, 145.19, 145.15, 145.06, 144.92, 144.45, 144.42, 144.26, 144.24 (2C, including one aryl *C*), 143.01, 142.98, 142.96 (aryl *C*), 142.67, 142.61, 142.57, 142.51, 142.33, 142.21, 142.10, 141.94, 141.91, 141.90, 141.76, 141.72, 141.70 (2C), 141.45, 141.24, 140.56, 140.45, 139.00, 138.95, 136.84 (aryl *C*), 136.71 (aryl *C*), 136.15, 134.81, 134.56, 133.93, 130.97 (aryl *C*), 129.65 (aryl *C*), 129.43 (2C, aryl *C*), 129.11 (2C, aryl *C*), 127.94 (aryl *C*), 126.03 (aryl *C*), 74.57 (sp^3-*C* of C_{60}), 74.08 (sp^3-*C* of C_{60}), 73.84, 61.33, 47.57, 21.62, 14.22; UV–vis ($CHCl_3$) λ_{max}/nm (log ε) 257 (5.01), 311 (4.54), 431 (4.22), 701 (3.43) (the characteristic absorptions at approximately 430 nm and 700 nm in the UV–vis data are consistent with the literature[2]); MALDI-TOF MS m/z calcd for $C_{78}H_{19}NO_4S$ $[M]^-$ 1065.1040, found 1065.1033.

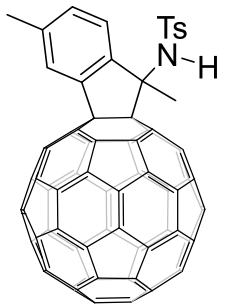

3ha

Synthesis and spectral data of 3ha: After the electrolysis of **1h** (14.9 mg, 0.015 mmol), the dianion **1h**$^{2-}$ was stirred at 25 °C for 2 h under Ar/O_2 bubbling through a latex tube, then TFA (3.4 μL, 0.045 mmol) was added, and the reaction was stirred at 25 °C for 15 min, the resulting mixture was directly filtered through a silica gel column (200–300 mesh) plug with CS_2/ethyl acetate (5:1, v/v) to remove supporting electrolyte and insoluble materials, and then evaporated in vacuum to remove the solvent. Next, the residue was further separated on a silica gel column (300–400 mesh) with CS_2/CH_2Cl_2 (3:1, v/v) as the eluent to afford product **3ha** (9.2 mg, 62%) as an amorphous brown solid; ^{1}H NMR (400 MHz, $CDCl_3$) δ 7.93 (s, 1H), 7.83 (d, J = 8.2 Hz, 2H), 7.58 (d, J = 8.0 Hz, 1H), 7.38 (dd, J = 8.0, 0.9 Hz, 1H), 7.29 (d, J = 8.2 Hz, 2H), 5.92 (s, 1H), 2.54 (s, 3H) , 2.51 (s, 3H) , 2.44 (s, 3H); ^{13}C NMR (101 MHz, $CDCl_3$) δ 155.99, 155.34, 154.83, 154.16, 147.57, 147.40, 146.67, 146.34, 146.31, 146.27, 146.15, 146.11, 146.08 (2C), 146.07, 146.04, 145.97, 145.75, 145.55, 145.53, 145.49, 145.32, 145.30 (2C), 145.26 (3C), 145.21, 144.56 (aryl *C*), 144.52, 144.48, 143.55 (aryl *C*), 143.12, 143.11, 142.72 (aryl *C*), 142.66 (2C), 142.50, 142.40, 142.22, 142.15, 142.08, 142.06, 141.99 (2C), 141.98, 141.92 (2C), 141.86, 141.80, 141.76, 141.72, 141.66, 140.86 (aryl *C*), 140.60, 140.53, 140.11 (aryl *C*), 139.35, 139.26, 136.25, 135.53, 135.18, 135.07, 130.91 (aryl *C*), 129.68 (2C, aryl *C*), 127.34 (2C, aryl *C*), 126.19 (aryl *C*), 125.84 (aryl *C*), 81.50, 75.95 (sp^3-*C* of C_{60}), 74.07 (sp^3-*C* of C_{60}), 29.77, 21.63, 21.60; UV–vis ($CHCl_3$) λ_{max}/nm (log ε) 257 (4.98), 309 (4.49), 431 (4.18), 700 (3.36) (the characteristic absorptions at approximately 430 nm and 700 nm in the UV–vis data are consistent with the literature[2]); MALDI-TOF MS m/z calcd for $C_{76}H_{17}NO_2S$ $[M]^-$ 1007.0985, found 1007.0988.

Scale-up synthesis of 3ah: Compound **1a** (149.2 mg, 0.150 mmol) was dissolved in 30 mL of anhydrous 1,2-$C_6H_4Cl_2$ solvent containing 0.1 M TBAP. Then the solution was electroreduced by CPE at –1.34 V under argon bubbling at 25 °C. When the theoretical number of coulombs (29.0 C) was reached, the electrolysis was terminated after ca. 17 h, and the solution of **1a**$^{2-}$ was obtained. The dianion **1a**$^{2-}$ was stirred at 70 °C for 3 h under Ar/O_2 bubbling, then *n*-butyl iodide (854.0 μL, 7.50 mmol) was added, and the reaction was stirred at 25 °C for 2 h, the resulting mixture was directly filtered through a silica gel column (200–300 mesh) plug with CS_2/ethyl acetate (5:1, v/v) to remove supporting electrolyte and insoluble materials, and then evaporated in vacuum to remove the solvent. Next, the residue was further separated on a silica gel column (300–400 mesh) with CS_2/CH_2Cl_2 (4:1, v/v) as the eluent to afford product **3ah** (35.5 mg, 23%) as an amorphous brown solid.

4. X-ray crystallography of compound 3aa

Black block crystals of **3aa** were obtained by slow evaporation of a saturated solution in CS_2/CH_3OH at 25 °C. Single-crystal X-ray diffraction data were collected on a diffractometer (XtaLAB PRO 007HF (Cu), Rigaku) equipped with a CCD area detector using graphite-monochromated CuKα radiation (λ = 1.54184 Å) in the scan range 9.15° < 2θ < 158.68°. The structure was solved with intrinsic phasing using SHELXT and refined with full-matrix least-squares refinement using the SHELXL program within OLEX2. Crystallographic data have been deposited in the Cambridge Crystallographic Data Centre as deposition number CCDC 2527512.

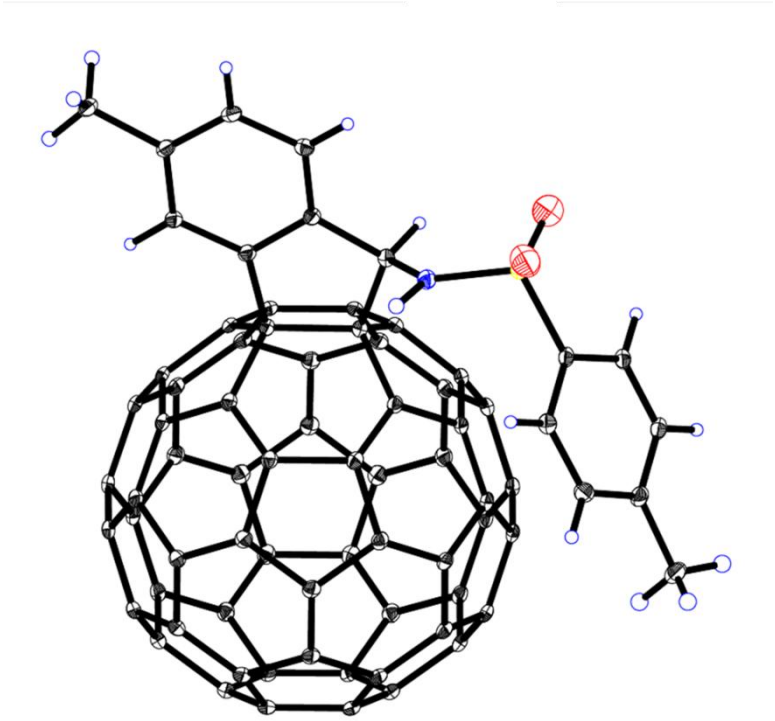

Fig. S9 ORTEP diagram of **3aa** with thermal ellipsoids shown at 20% probability. The CS_2 molecule is omitted for clarity.

Table S1 Crystal data of 3aa.

Identification code	2527512
Empirical formula	$C_{76}H_{15}NO_2S_3$
Formula weight	1070.07
Temperature/K	111(2)
Crystal system	triclinic
Space group	P-1
a/Å	9.89343(15)
b/Å	13.8418(2)
c/Å	16.4878(3)
α/°	104.5485(16)
β/°	98.8265(15)
γ/°	96.0111(14)
Volume/Å^3	2135.24(7)
Z	2
ρ_{calc}g/cm^3	1.664
μ/mm^{-1}	2.111
F(000)	1084.0
Crystal size/mm^3	0.15 × 0.12 × 0.08
Radiation	Cu Kα (λ = 1.54184)
2θ range for data collection/°	9.15 to 158.68
Index ranges	-12 ≤ h ≤ 12, -13 ≤ k ≤ 17, -20 ≤ l ≤ 21
Reflections collected	27839
Independent reflections	8997 [R_{int} = 0.0382, R_{sigma} = 0.0424]
Data/restraints/parameters	8997/0/744
Goodness-of-fit on F^2	1.086
Final R indexes [I>=2σ (I)]	R_1 = 0.0509, wR_2 = 0.1374
Final R indexes [all data]	R_1 = 0.0613, wR_2 = 0.1442
Largest diff. peak/hole / e Å^{-3}	0.60/-0.70

5. Control experiments

When the 1.0 ppm Ar/O_2 bubbling flow rate was measured to be approximately 2.4 mL s^{-1} via the water displacement method, the reaction yield of **3aa** was 66%. Increasing the Ar/O_2 bubbling flow rate to 4.6 mL s^{-1} or reducing it to 0.5 mL s^{-1} gave yields of 65% and 62%, respectively (Scheme S1a).

Then, the electrolyzed reaction mixture was transferred into a Schlenk tube under an Ar atmosphere without bubbling and stirred at 70 °C for 3 h, and product **3aa** was isolated in 53% yield. When the reaction time was further extended to 6 h under the same conditions, the yield decreased slightly to 52%. For comparison, the electrolyzed reaction mixture was transferred into a Schlenk tube and subjected to three consecutive freeze–pump–thaw cycles. The mixture was then stirred under an Ar atmosphere without bubbling at 70 °C for 3 h, and only a 15% yield was obtained (Scheme S1b). These results indicated that O_2 was essential for this transformation, and the O_2 required for the reaction mainly originates from dissolved O_2 in the solution, which could not be fully removed by argon bubbling.

Subsequently, the latex tube used for Ar bubbling was replaced with a fluorinated ethylene propylene (FEP) tube to better avoid atmospheric O_2 permeation through the tube. The electrolyzed reaction mixture was stirred at 70 °C for 3 h, and **3aa** was isolated in 54% yield. Prolongation of the bubbling time to 6 h gave a yield of 57% (Scheme S1c). These results indicated that partial O_2 for full conversion arose from O_2 permeation through the latex tube into the reaction system during the Ar/O_2 bubbling process.

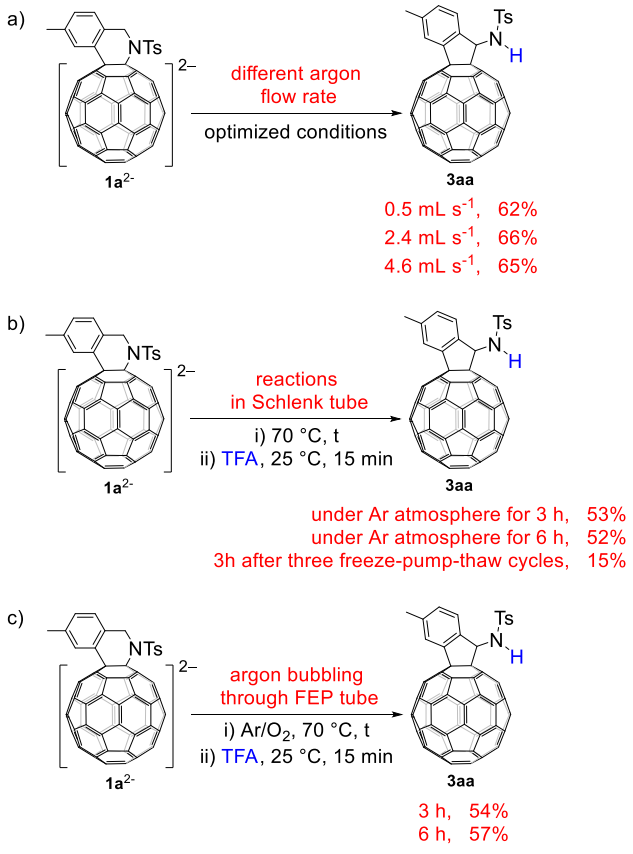

Scheme S1 Control experiments.

The calculation of O_2 permeation through the latex tubing is based on the widely accepted solution-diffusion model for gas transport in polymers,[3] described by the following equation:

$$J = \frac{P^G(p_o - p_e)}{l}$$

where J is the O_2 flux through the tube wall per unit wall area per time O_2 ($cm^3\ cm^{-2}\ s^{-1}$), P^G is the O_2 permeability coefficient of latex ($cm^2 \cdot s^{-1} \cdot cmHg^{-1}$, 1 Barrer = 10^{-10} $cm^2 \cdot s^{-1} \cdot cmHg^{-1}$), p_o is the O_2 partial pressure outside the tube (cmHg), p_e is the O_2 partial pressure inside the tube (cmHg), and l is the wall thickness (cm).

The O_2 permeability coefficient P^G of the latex tube is taken as 24 Barrer, based on the value reported in the literature.[4] The latex tube used in our setup had an inner diameter of 6 mm, an outer diameter of 9 mm, and a total length of 2 m. The O_2 partial pressure in ambient air is 0.21 atm, which corresponds to 15.96 cmHg. The carrier gas inside the tube is high-purity argon containing 1.0 ppm O_2, so the internal O_2 partial pressure is taken as 0 cmHg. Thus, by substituting the numerical values into the formula, the value of J in the latex tube is calculated as follows:

$$J = \frac{24 \times 10^{-10}\ cm^2\ s^{-1}\ cmHg^{-1} \times 15.96\ cmHg^{-1}}{(0.9 - 0.6)\ /\ 2\ cm} = 2.55 \times 10^{-7}\ cm^3\ cm^{-2}\ s^{-1}$$

To facilitate understanding of the calculation process, we defined the O_2 permeation quantity as Q, the inner surface area of the latex tube as A, and the bubbling time as t. Then we obtained the following formula:

$$J = \frac{Q}{A \times t}$$

Therefore, under our experimental conditions, the O_2 permeation quantity per hour in the latex tube is calculated as follows:

$$\begin{aligned} Q = J \times A \times t &= 2.55 \times 10^{-7}\ cm^3\ cm^{-2}\ s^{-1} \times (\pi \times 0.6 \times 200)\ cm^2 \times 3600\ s \\ &= 0.35\ cm^3 \end{aligned}$$

This corresponds to 0.014 mmol h^{-1} of O_2 permeating through the latex tube into the reaction system. The calculated amount of permeated O_2 is sufficient to complete the remaining conversion.

6. NMR spectra of compounds 3aa–ha

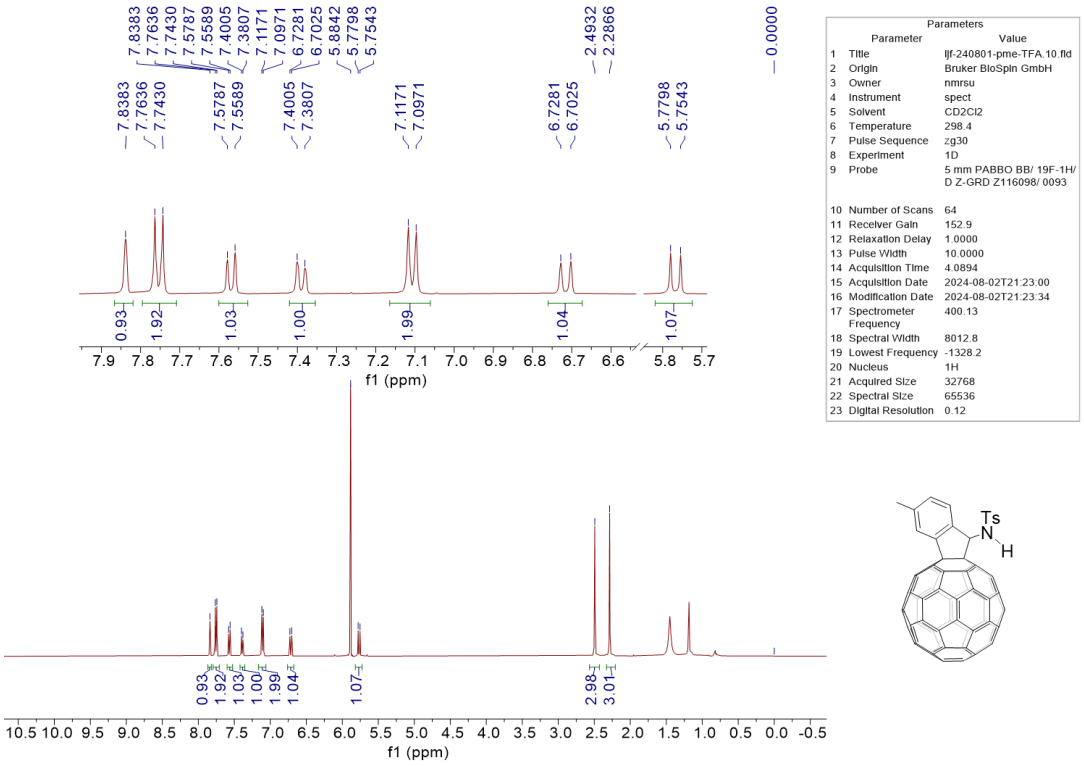

Fig. S10 ^{1}H NMR (400 MHz, 1:1 CS_2/$CDCl_2CDCl_2$) of compound **3aa**.

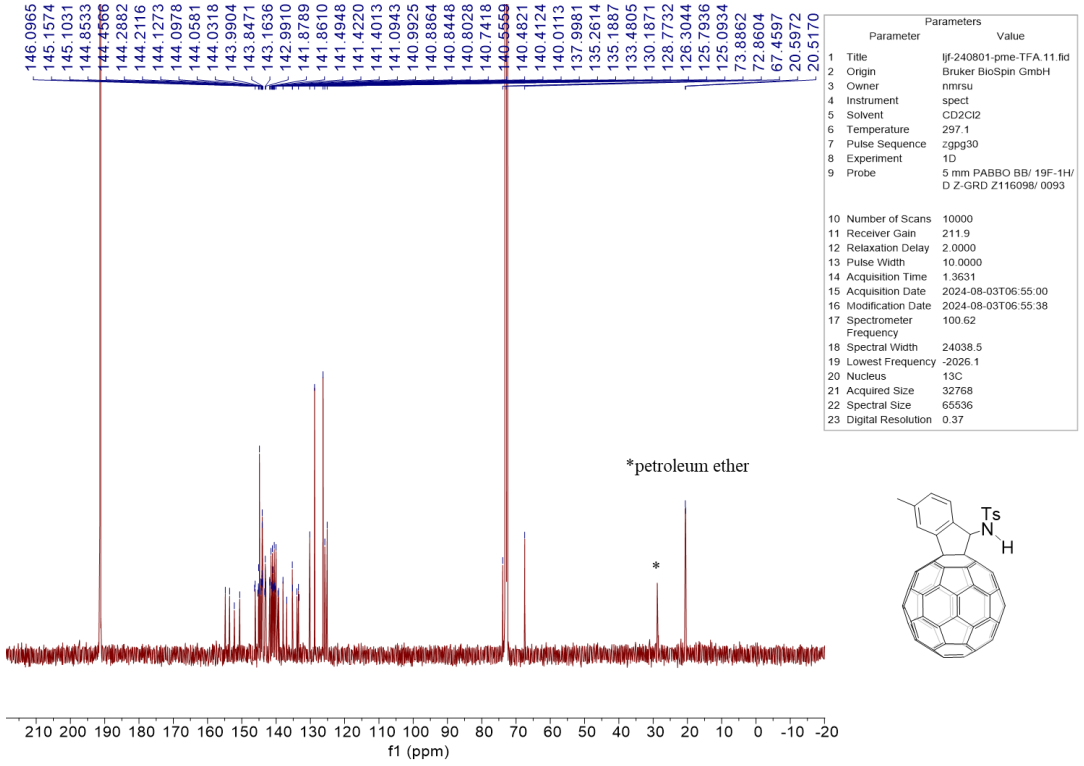

Fig. S11 ^{13}C NMR (101 MHz, 1:1 CS_2/$CDCl_2CDCl_2$) of compound **3aa**.

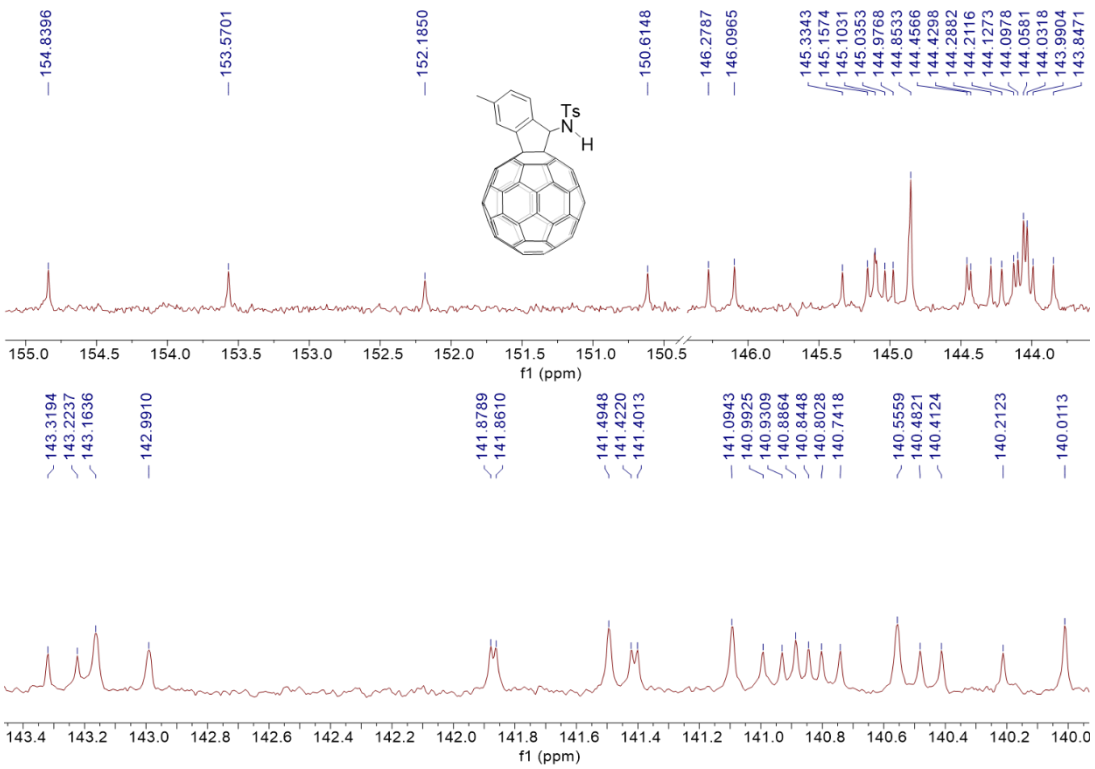

Fig. S12 Expanded ^{13}C NMR (101 MHz, 1:1 $CS_2/CDCl_2CDCl_2$) of compound **3aa**.

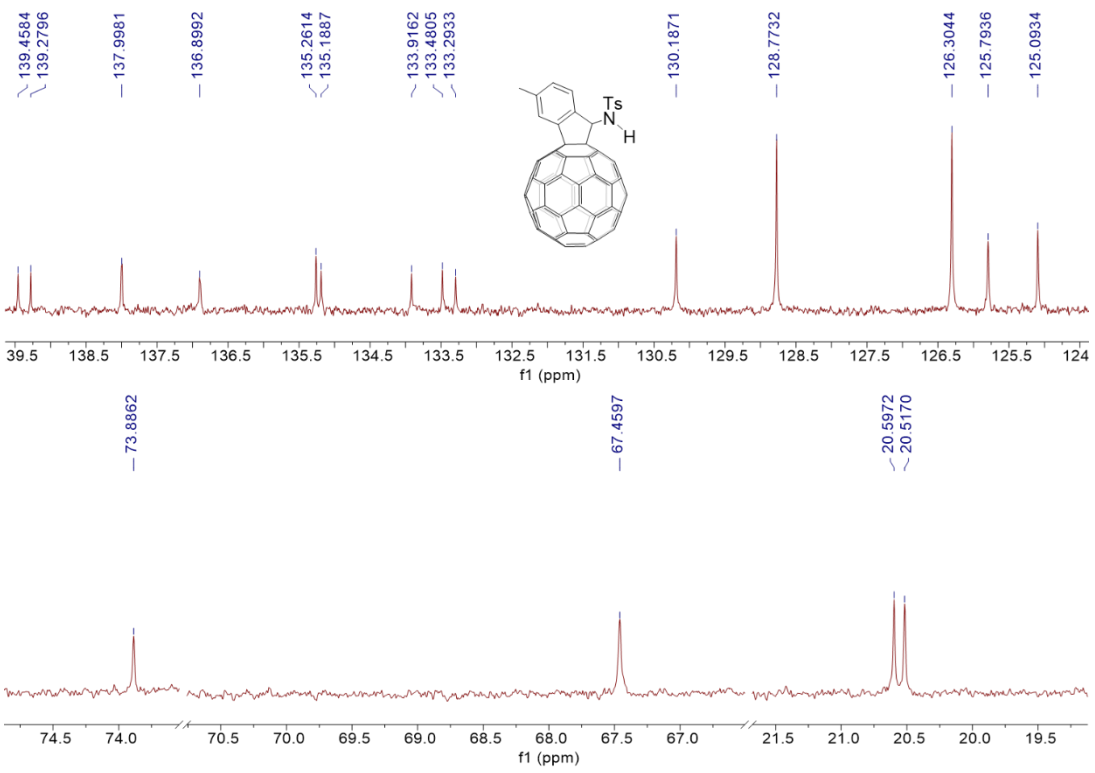

Fig. S13 Expanded ^{13}C NMR (101 MHz, 1:1 $CS_2/CDCl_2CDCl_2$) of compound **3aa**.

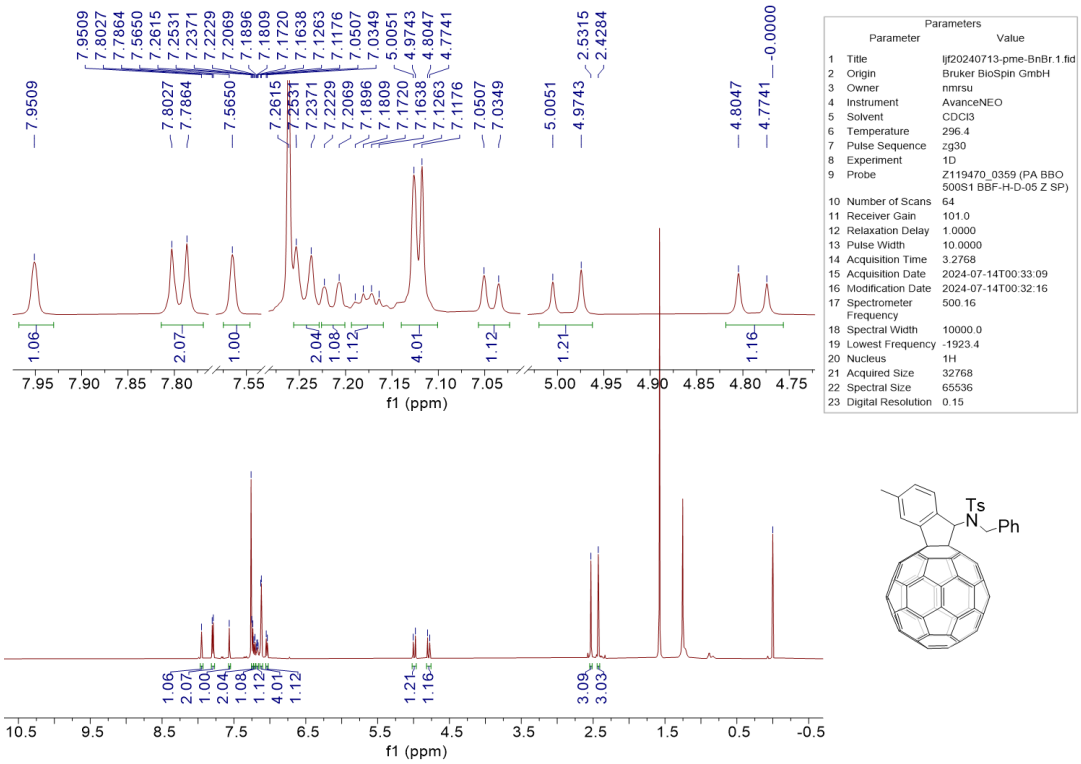

Fig. S14 ^{1}H NMR (500 MHz, $CDCl_3$) of compound **3ab**.

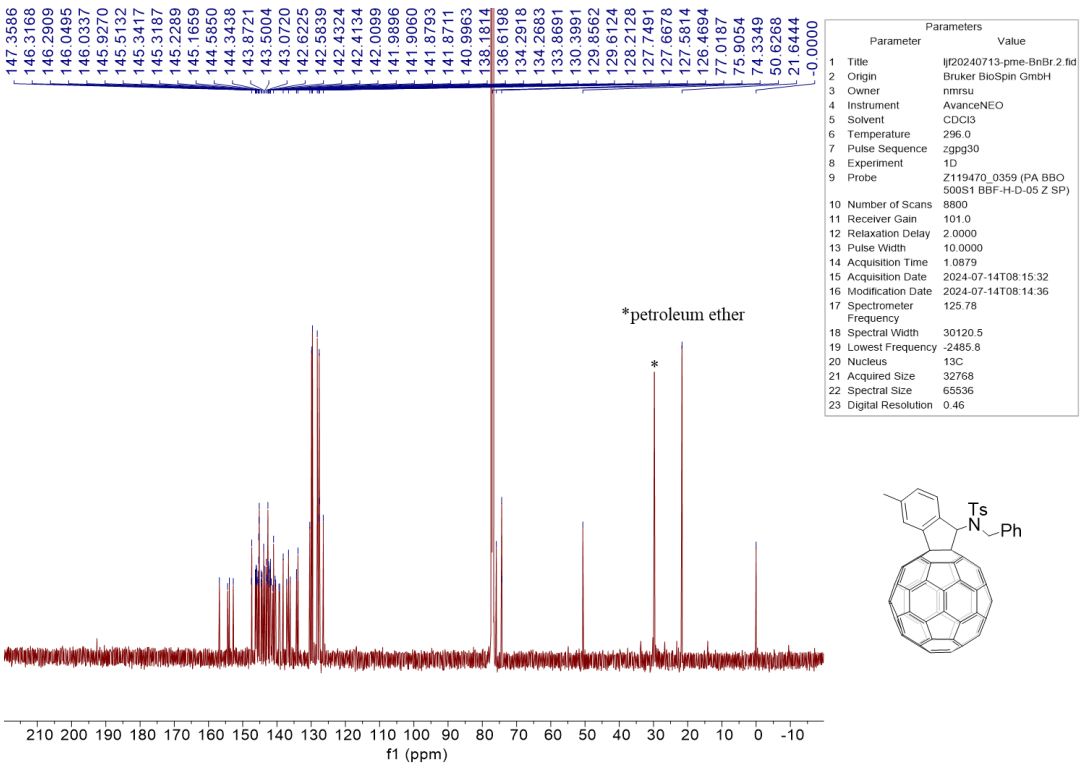

Fig. S15 ^{13}C NMR (126 MHz, $CDCl_3$) of compound **3ab**.

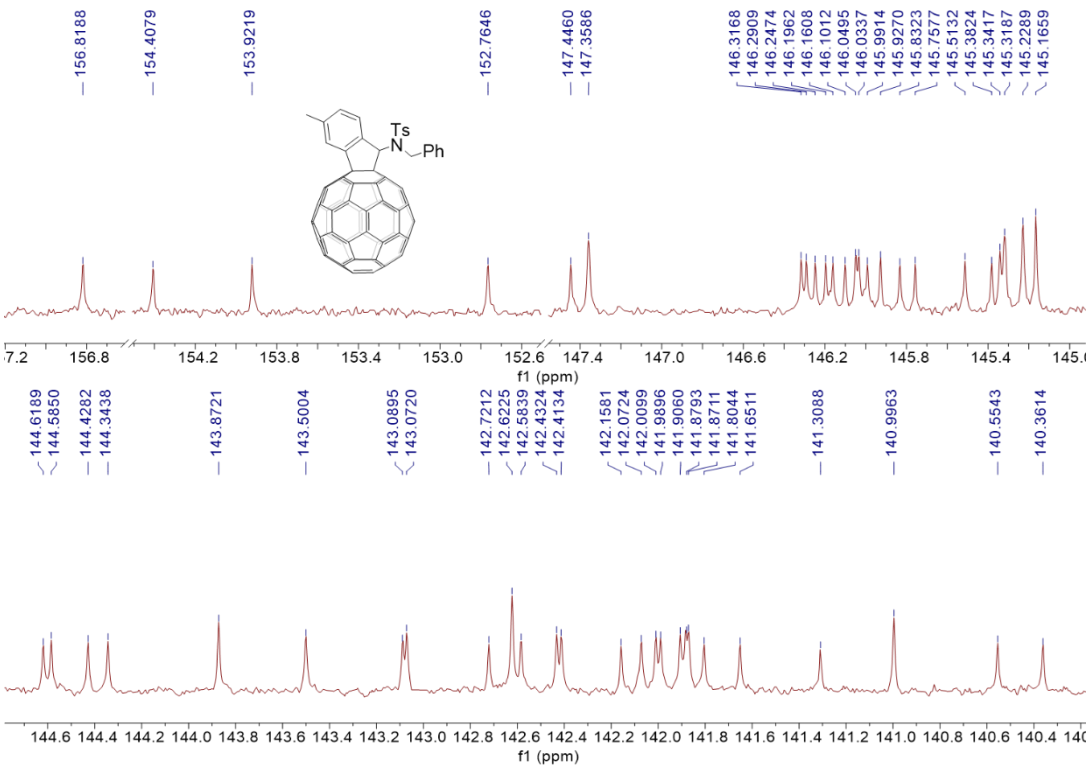

Fig. S16 Expanded ^{13}C NMR (126 MHz, $CDCl_3$) of compound **3ab**.

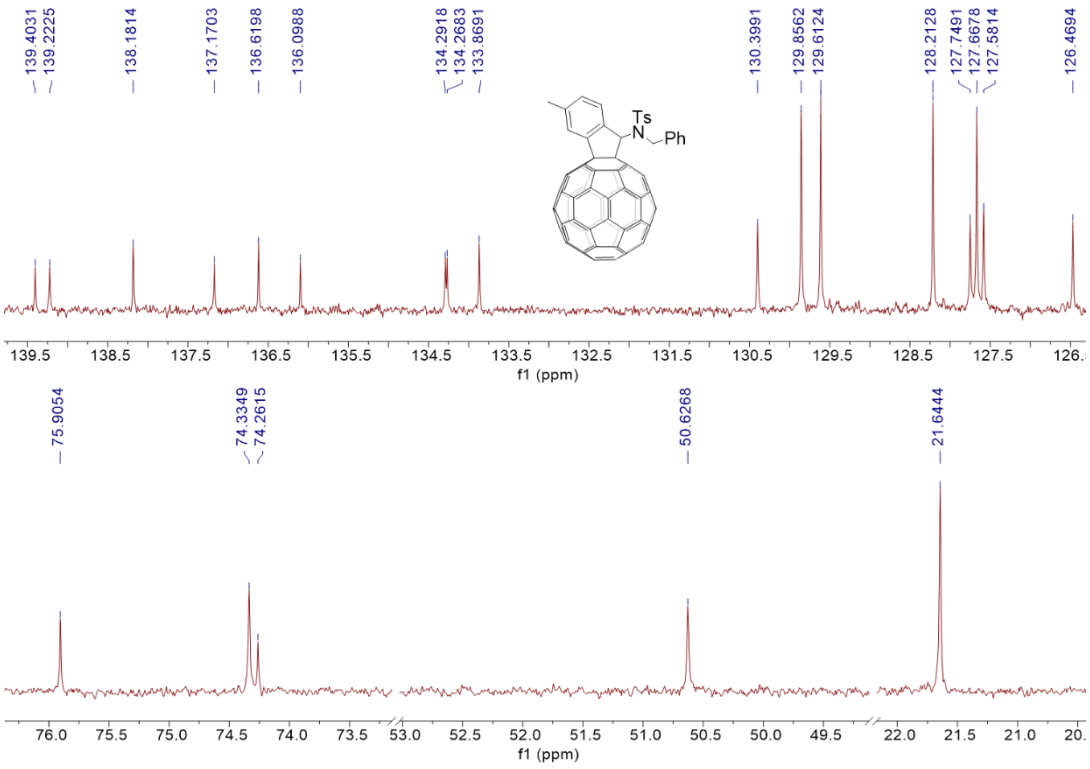

Fig. S17 Expanded ^{13}C NMR (126 MHz, $CDCl_3$) of compound **3ab**.

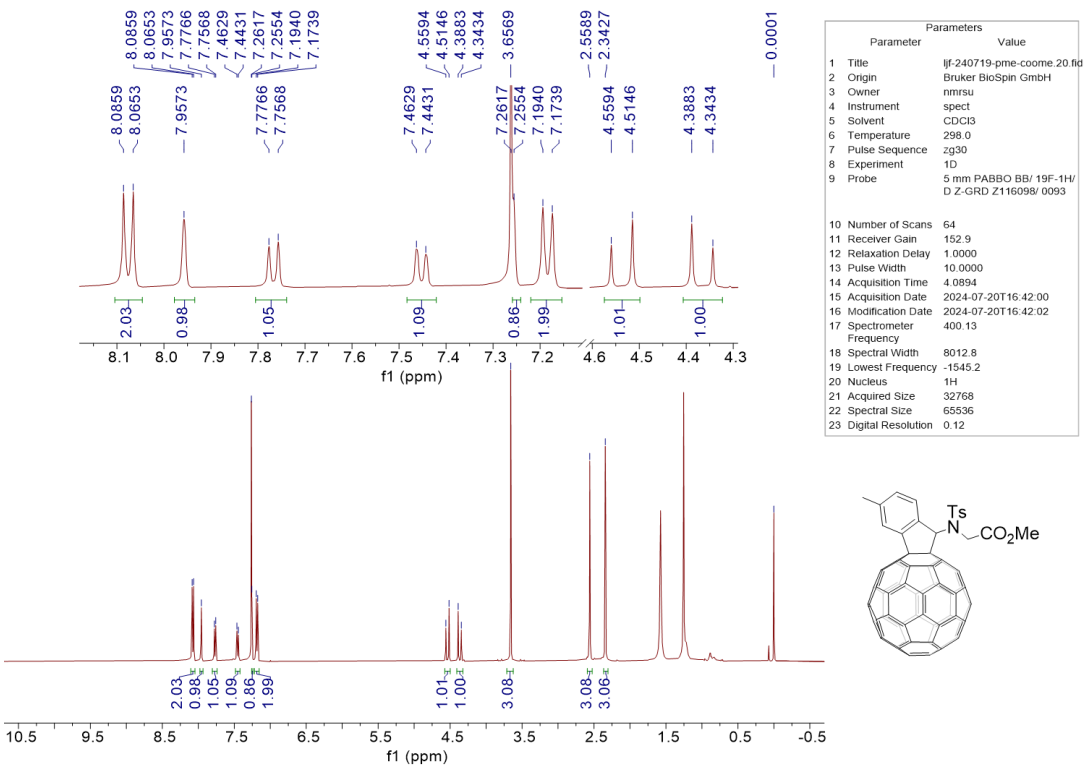

Fig. S18 ^{1}H NMR (400 MHz, $CDCl_3$) of compound **3ac**.

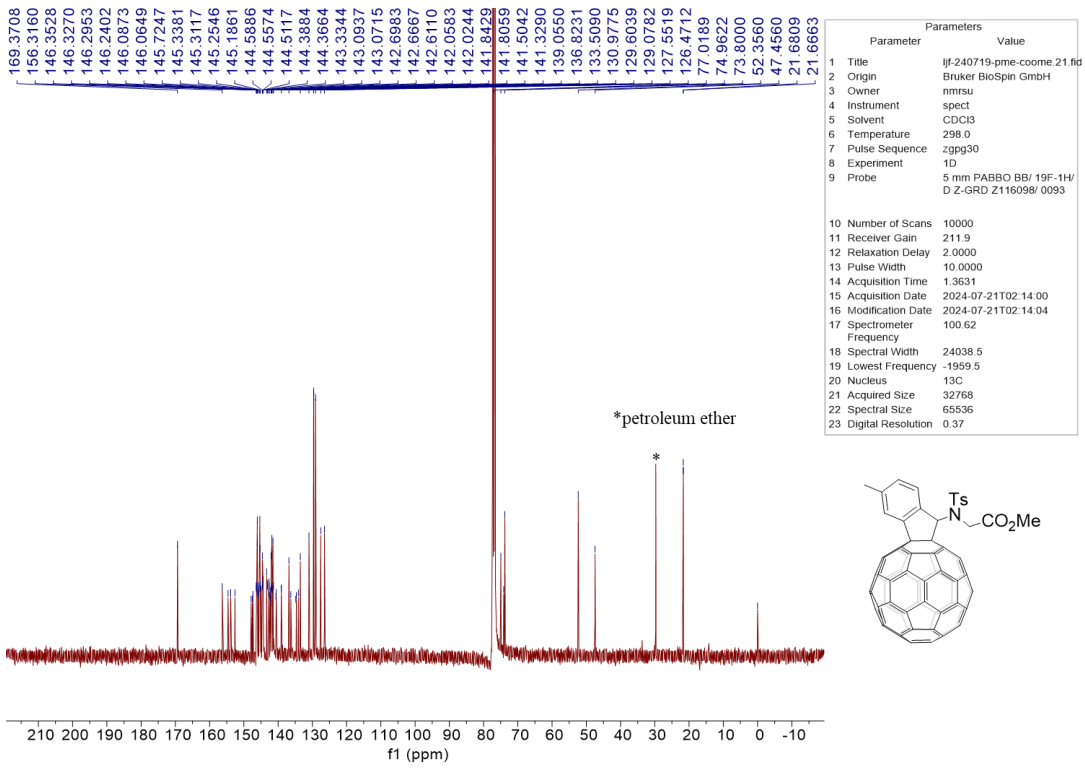

Fig. S19 ^{13}C NMR (101 MHz, $CDCl_3$) of compound **3ac**.

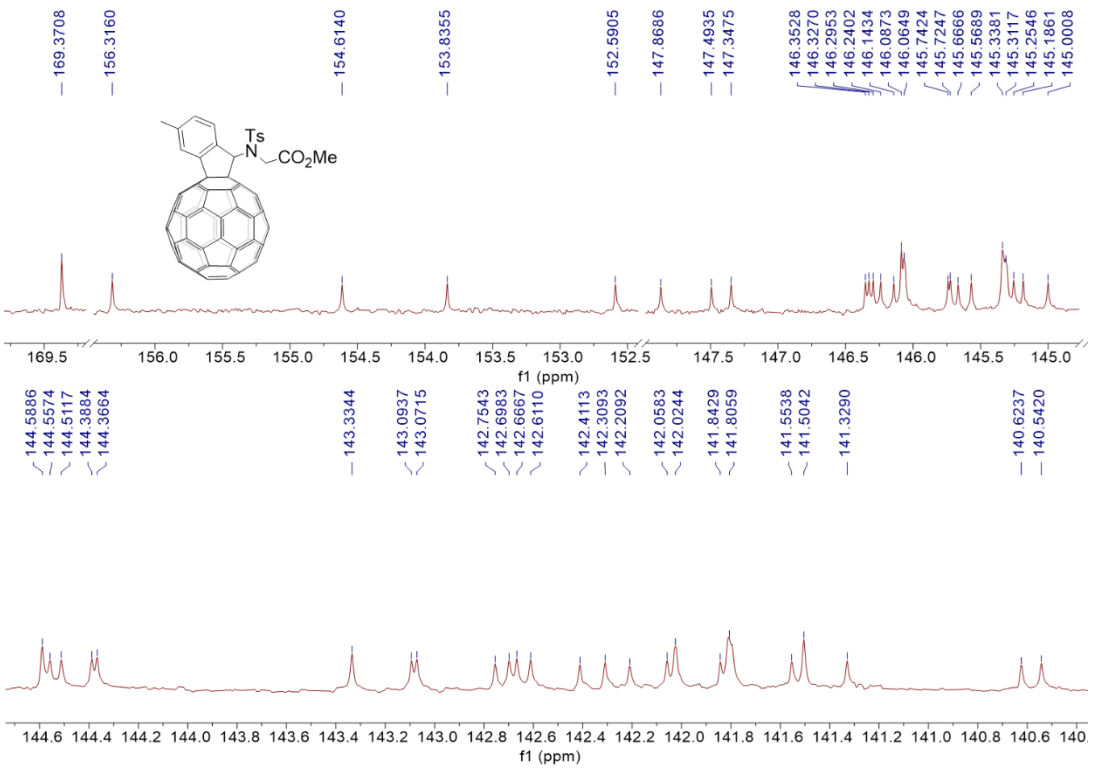

Fig. S20 Expanded ^{13}C NMR (101 MHz, $CDCl_3$) of compound **3ac**.

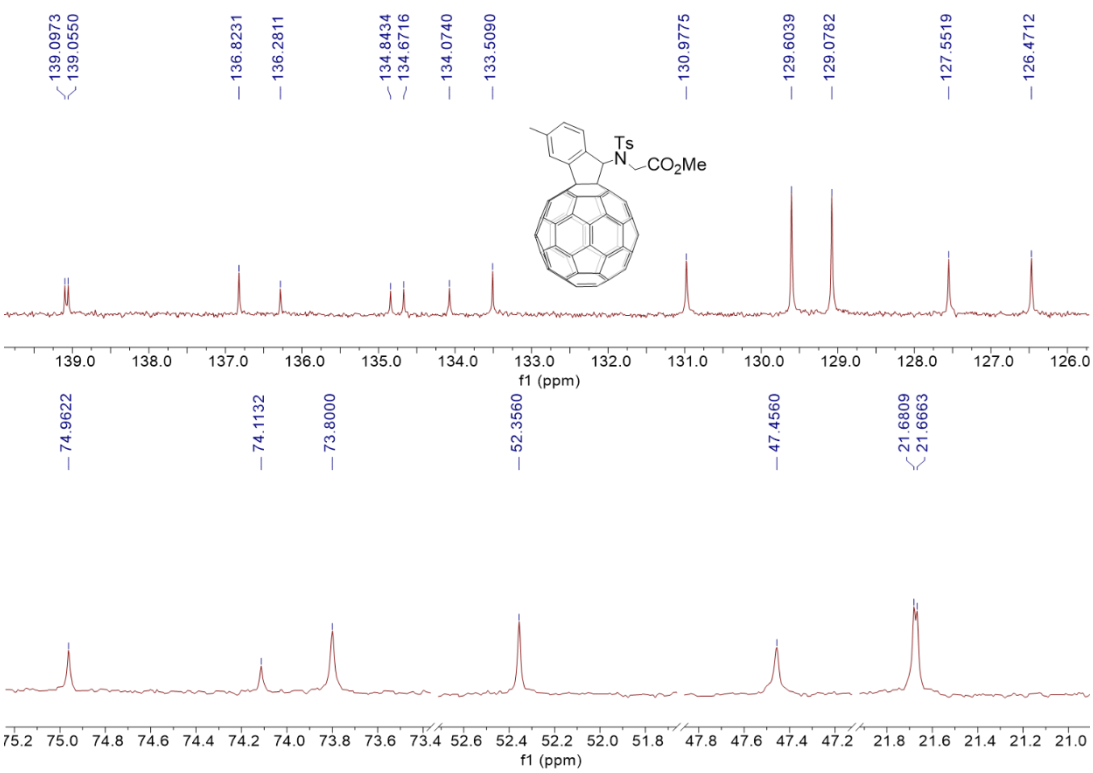

Fig. S21 Expanded ^{13}C NMR (101 MHz, $CDCl_3$) of compound **3ac**.

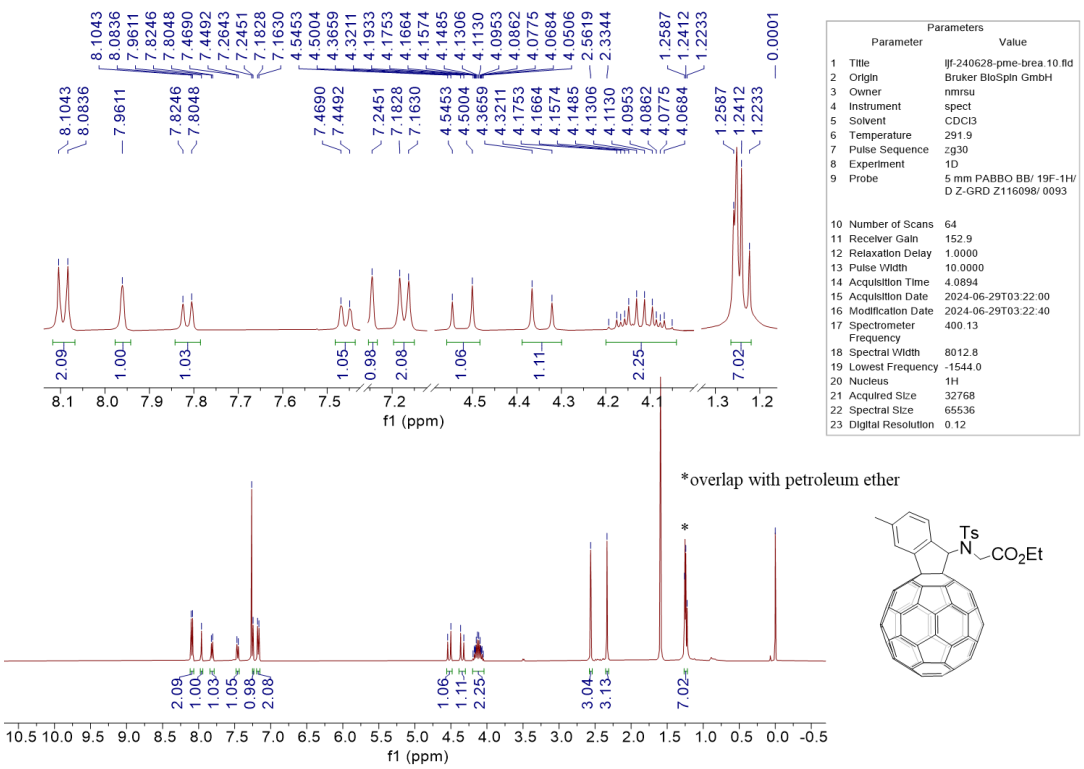

Fig. S22 ^{1}H NMR (400 MHz, $CDCl_3$) of compound **3ad**.

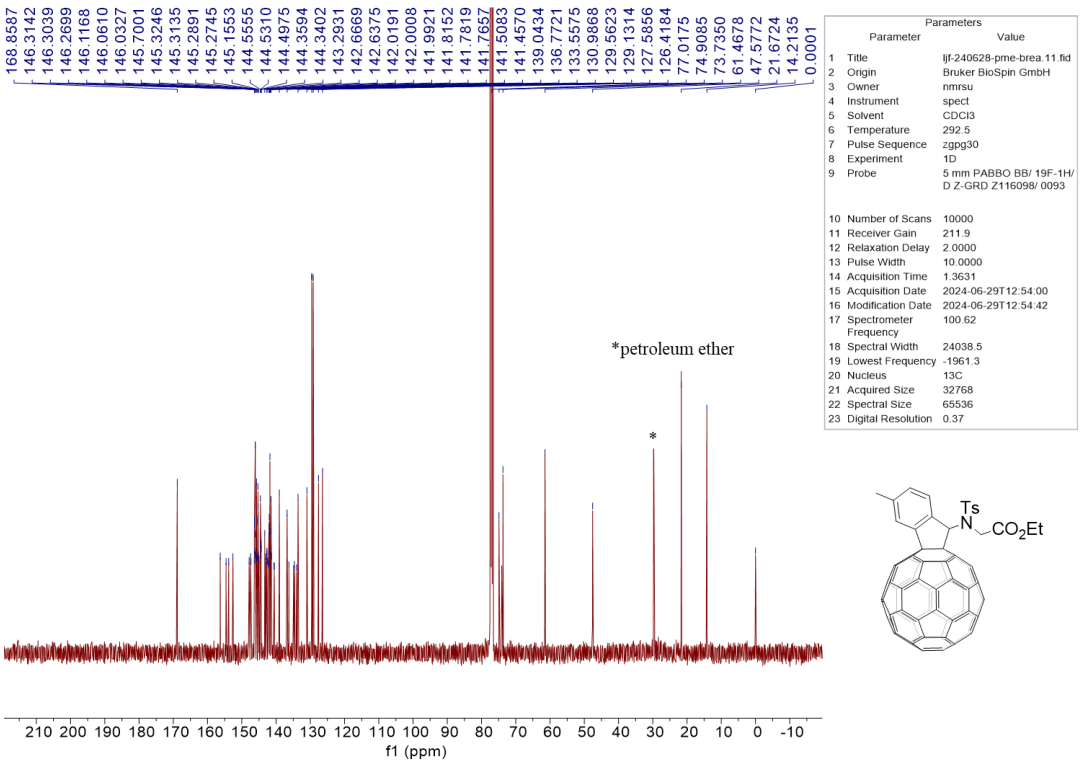

Fig. S23 ^{13}C NMR (101 MHz, $CDCl_3$) of compound **3ad**.

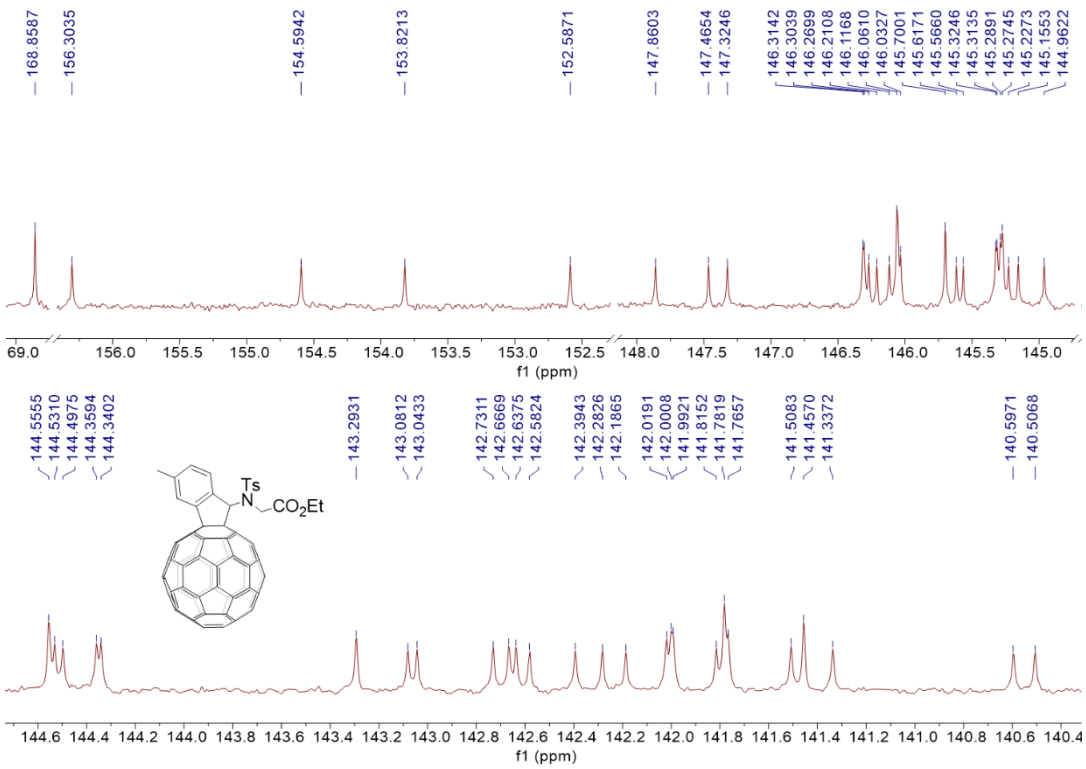

Fig. S24 Expanded ^{13}C NMR (101 MHz, $CDCl_3$) of compound **3ad**.

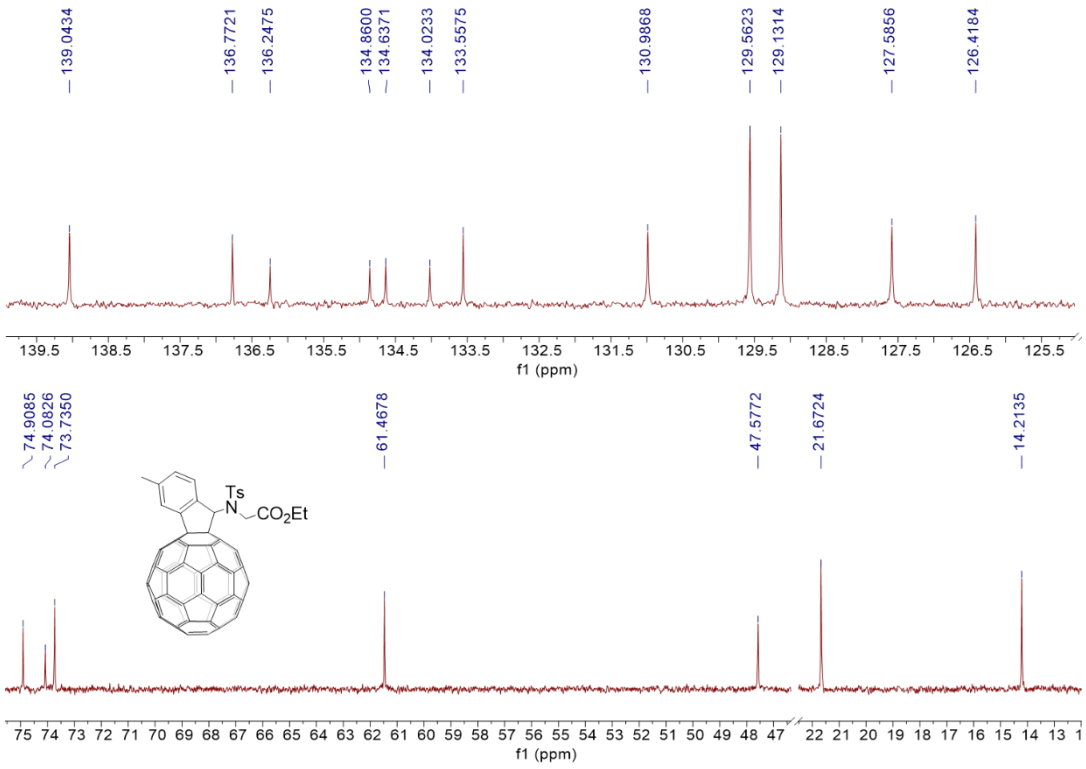

Fig. S25 Expanded ^{13}C NMR (101 MHz, $CDCl_3$) of compound **3ad**.

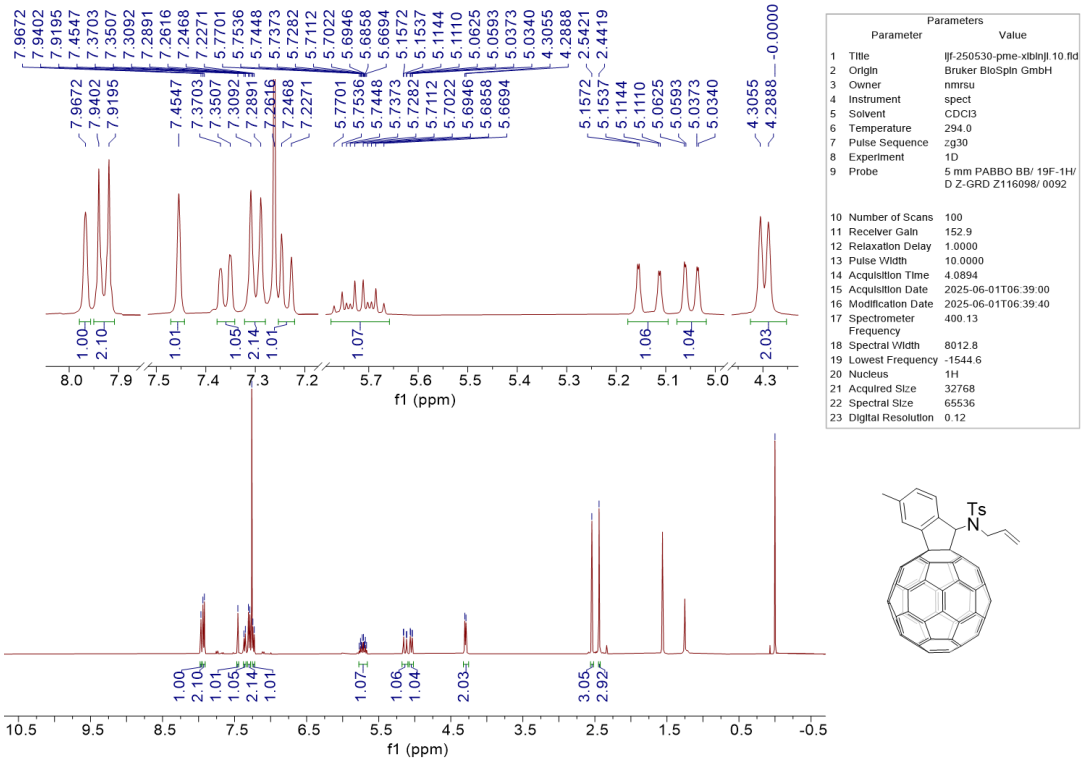

Fig. S26 ^{1}H NMR (400 MHz, $CDCl_3$) of compound **3ae**.

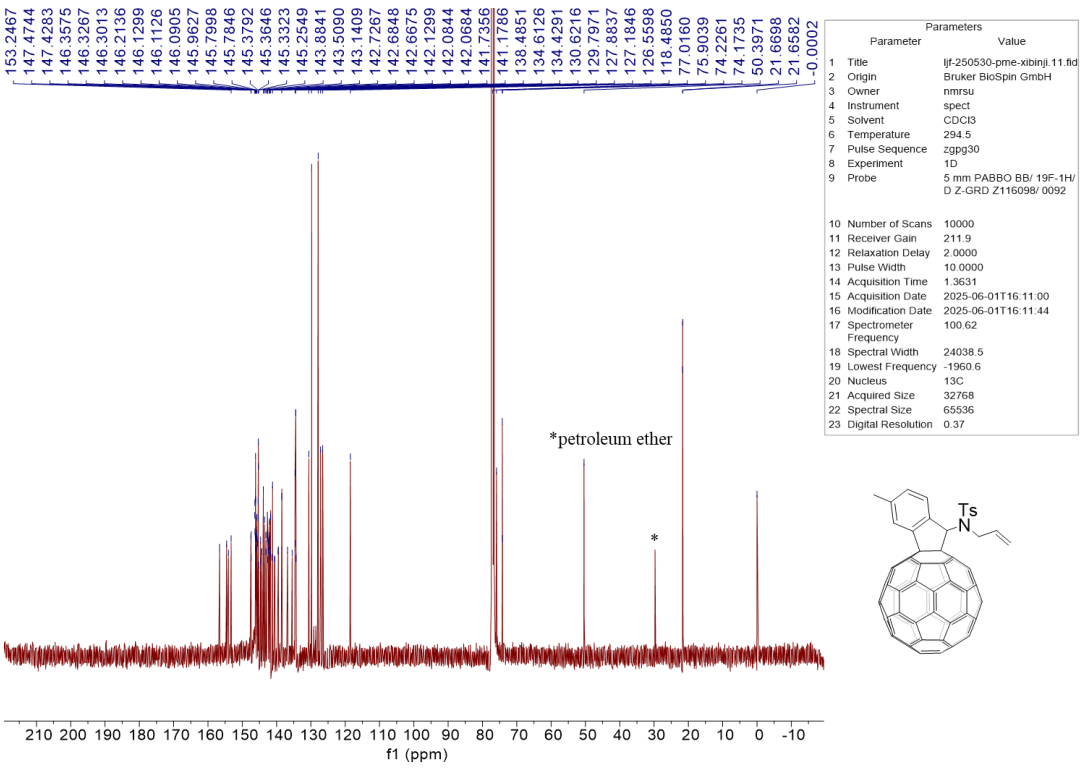

Fig. S27 ^{13}C NMR (101 MHz, $CDCl_3$) of compound **3ae**.

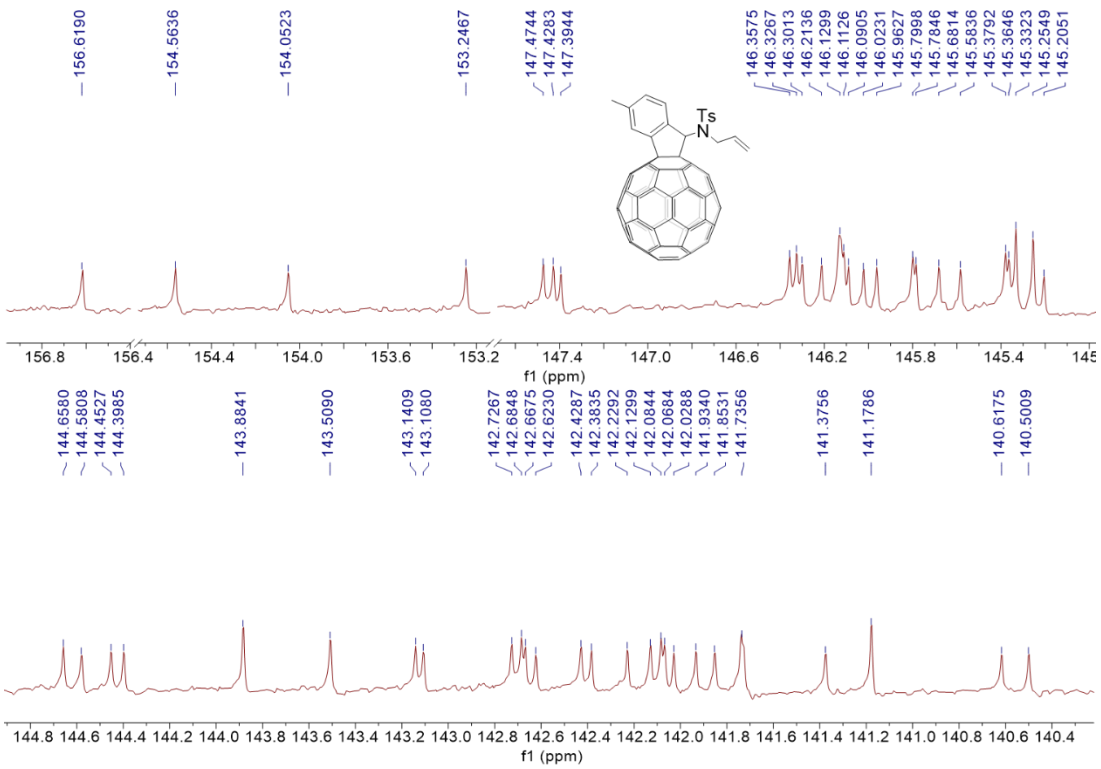

Fig. S28 Expanded ^{13}C NMR (101 MHz, $CDCl_3$) of compound **3ae**.

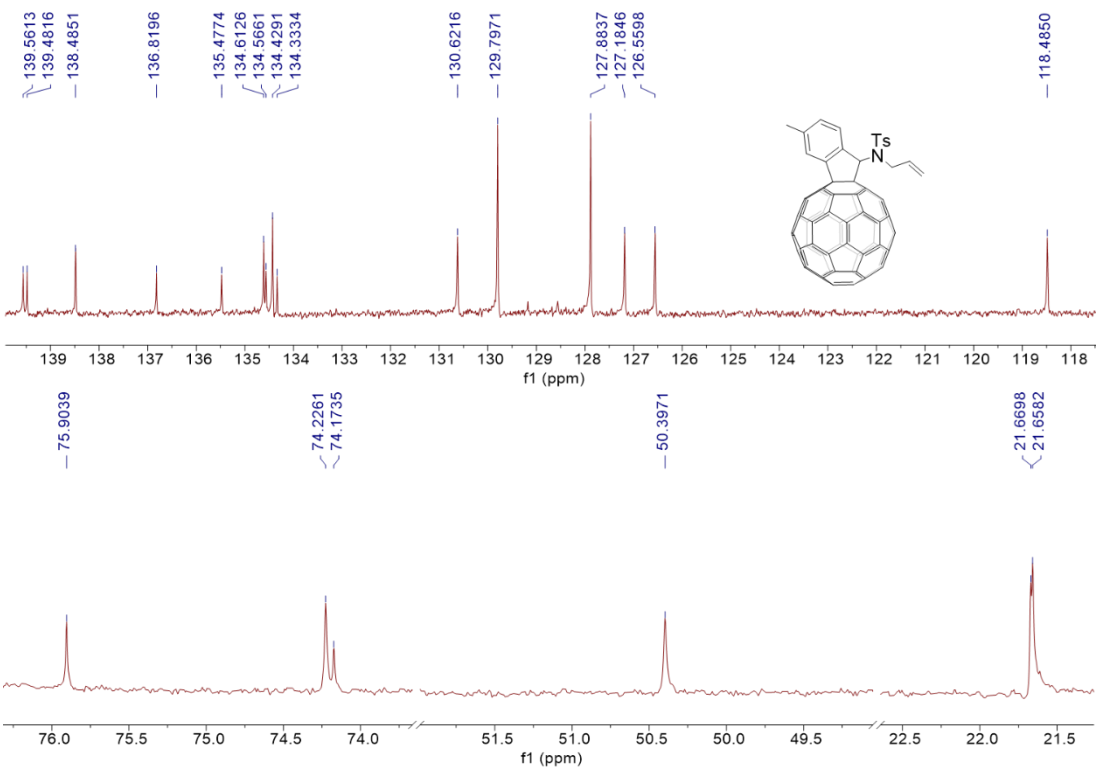

Fig. S29 Expanded ^{13}C NMR (101 MHz, $CDCl_3$) of compound **3ae**.

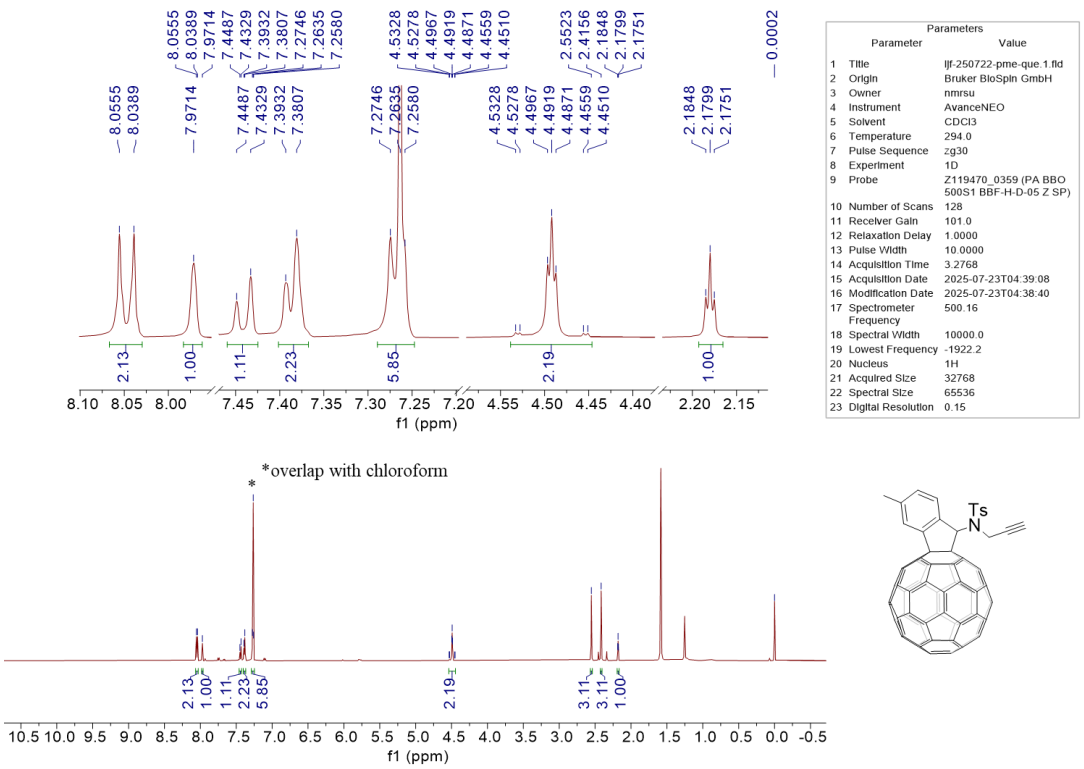

Fig. S30 ^{1}H NMR (500 MHz, $CDCl_3$) of compound **3af**.

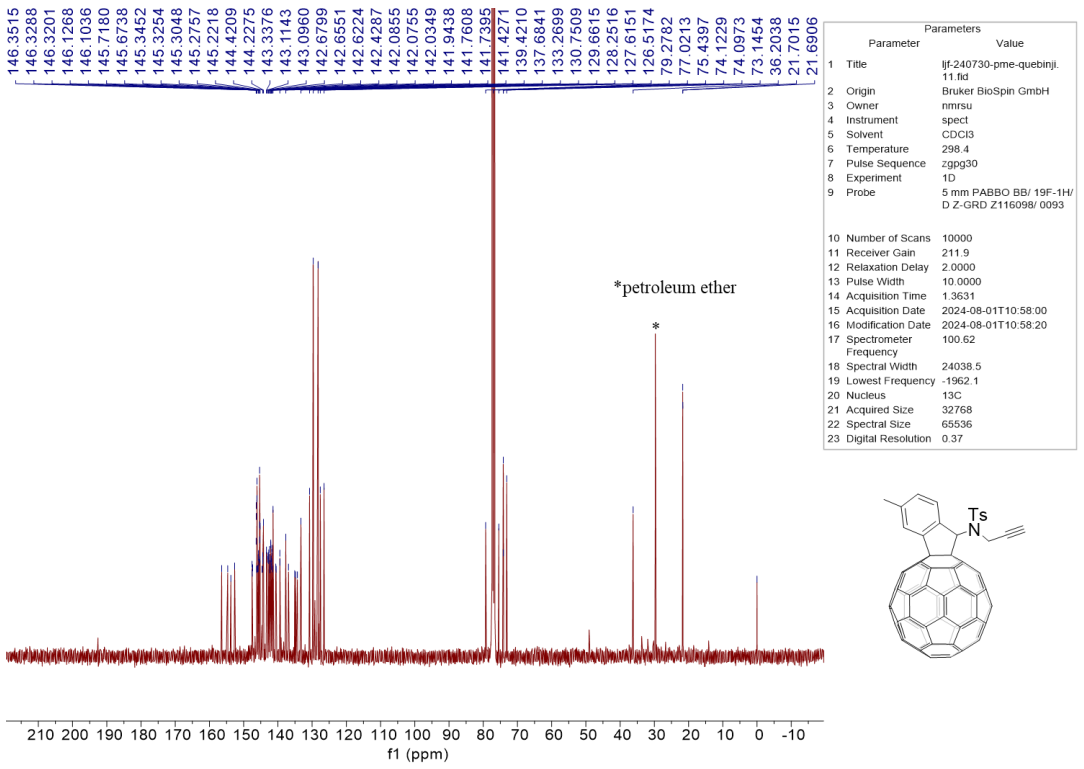

Fig. S31 ^{13}C NMR (101 MHz, $CDCl_3$) of compound **3af**.

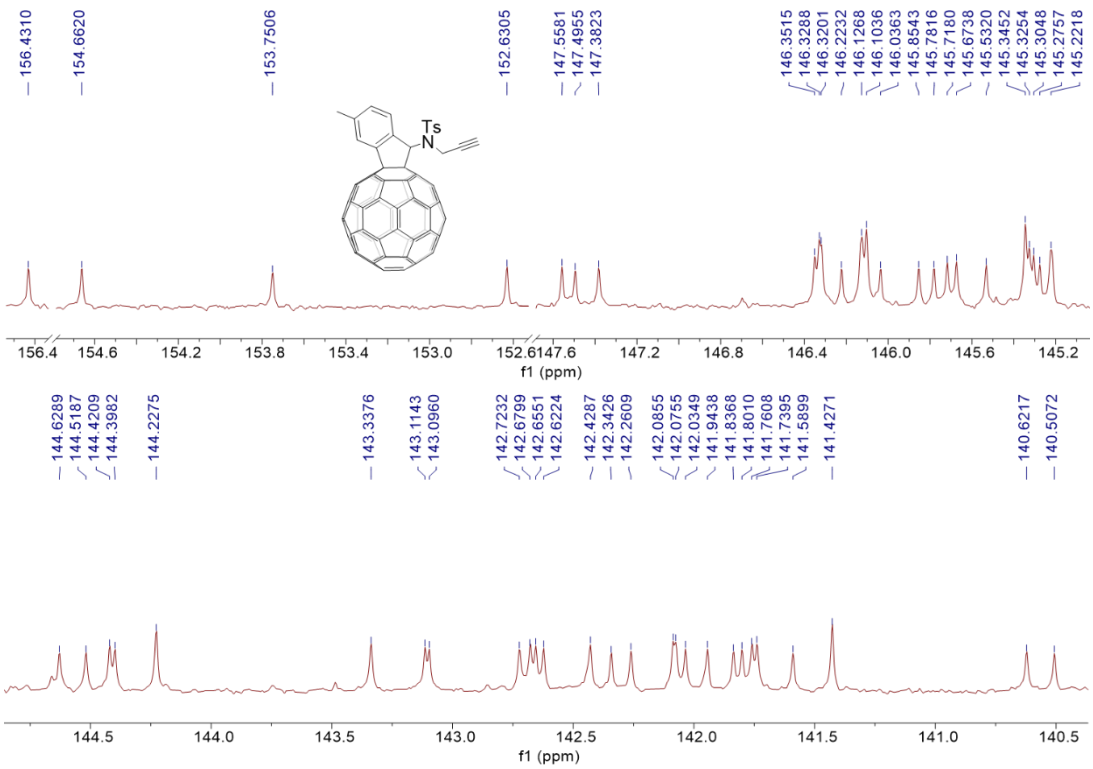

Fig. S32 Expanded ^{13}C NMR (101 MHz, $CDCl_3$) of compound **3af**.

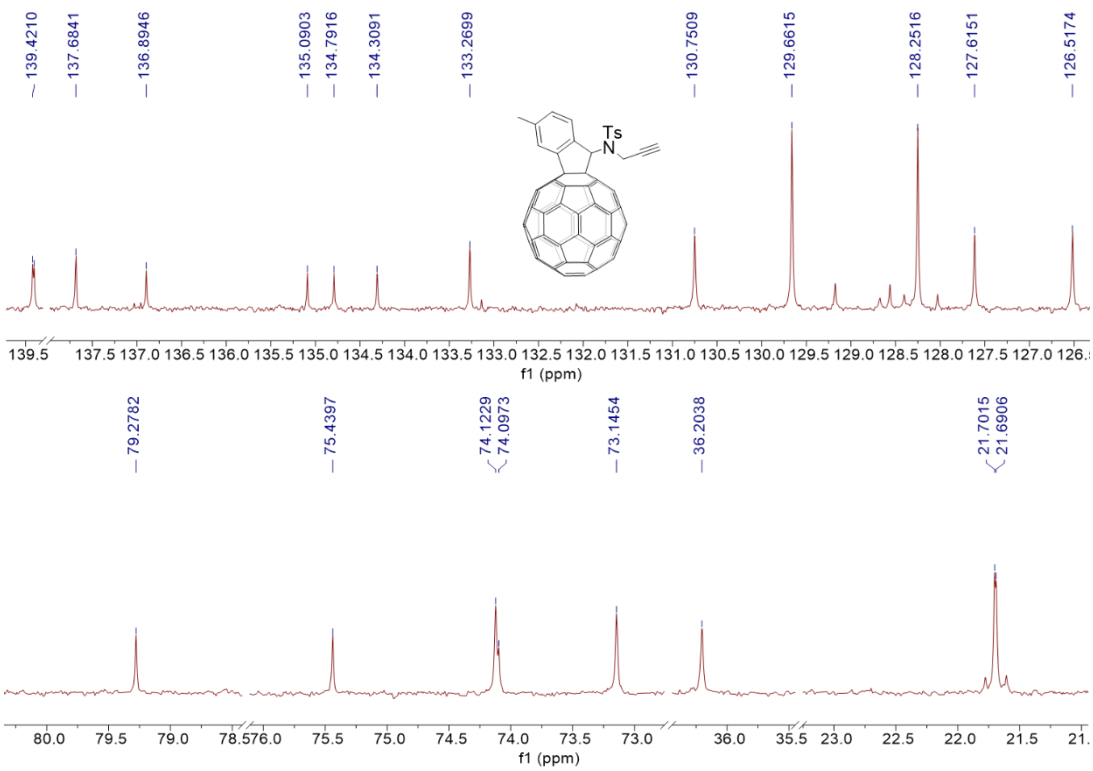

Fig. S33 Expanded ^{13}C NMR (101 MHz, $CDCl_3$) of compound **3af**.

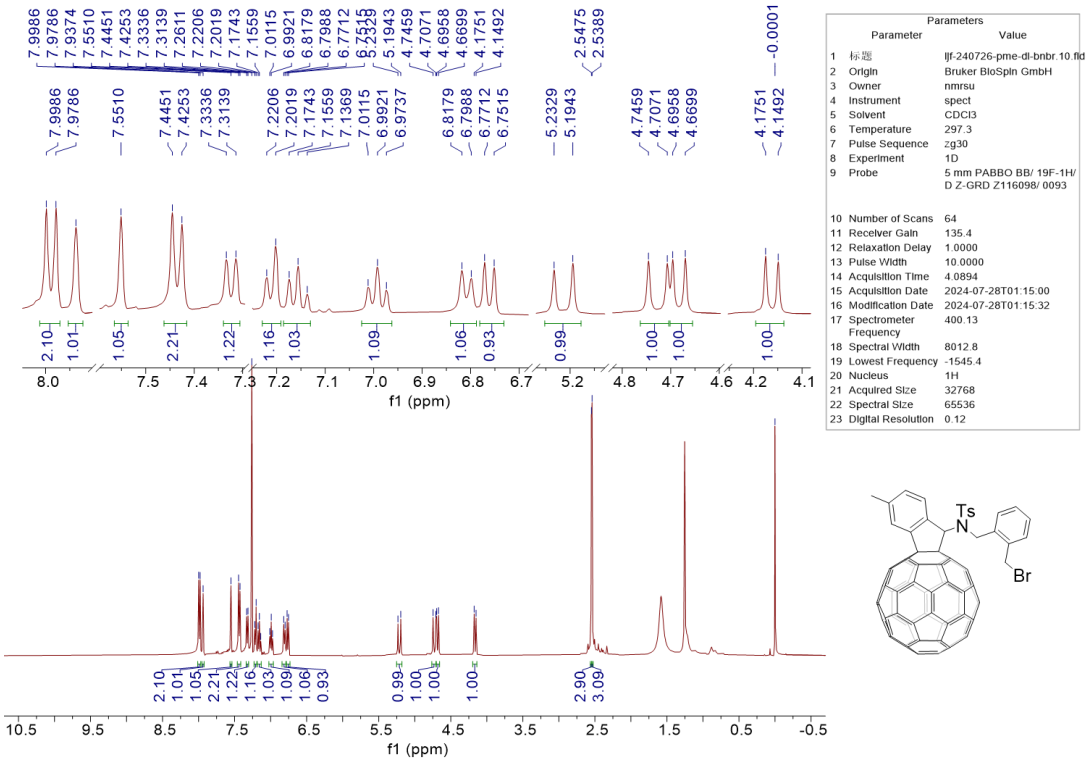

Fig. S34 ^{1}H NMR (400 MHz, $CDCl_3$) of compound **3ag**.

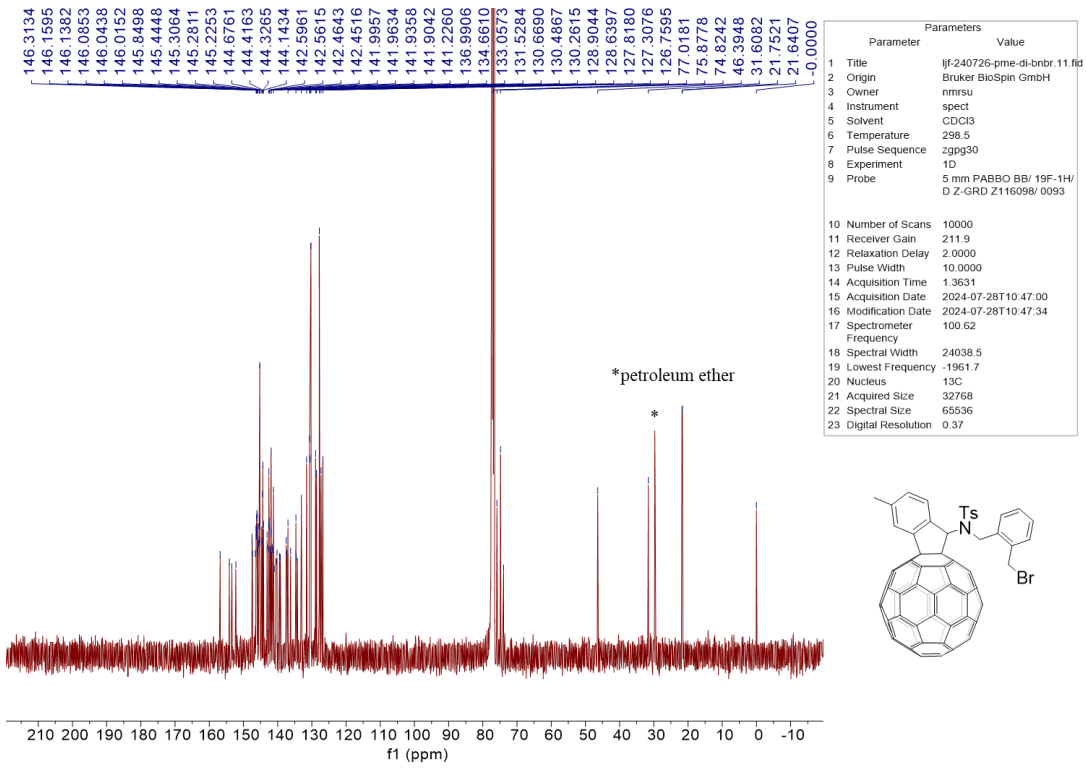

Fig. S35 ^{13}C NMR (101 MHz, $CDCl_3$) of compound **3ag**.

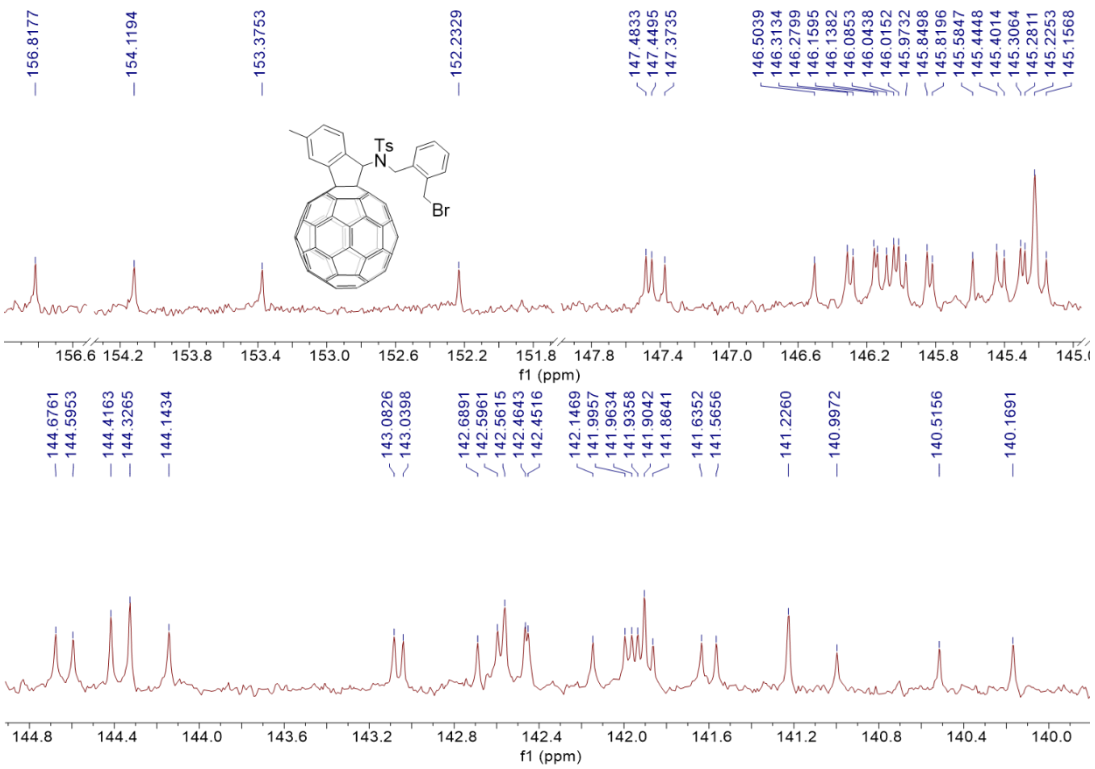

Fig. S36 Expanded ^{13}C NMR (101 MHz, $CDCl_3$) of compound **3ag**.

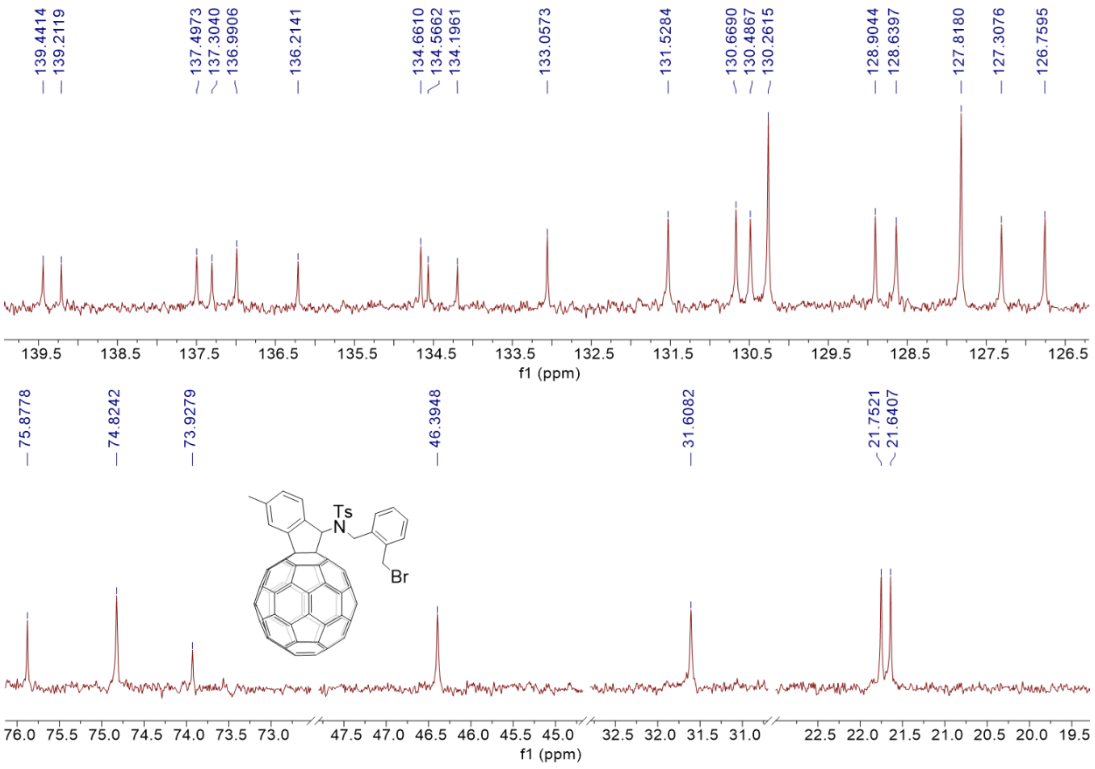

Fig. S37 Expanded ^{13}C NMR (101 MHz, $CDCl_3$) of compound **3ag**.

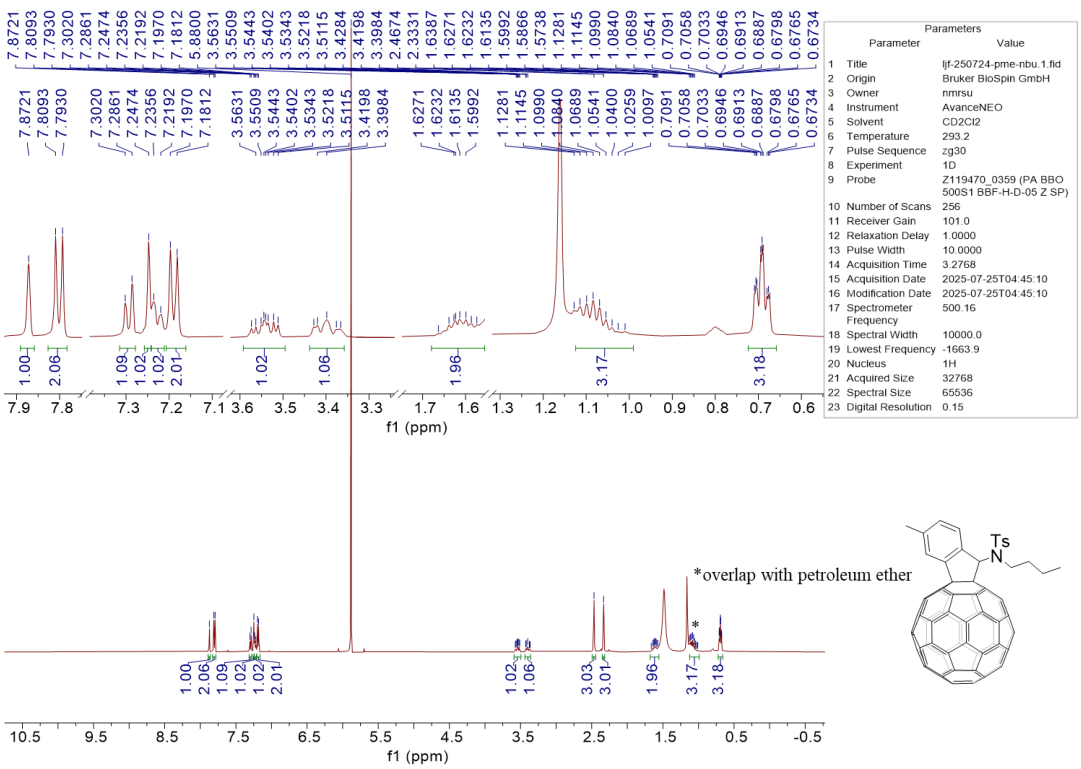

Fig. S38 ^{1}H NMR (500 MHz, 1:1 CS_2/$CDCl_2CDCl_2$) of compound **3ah**.

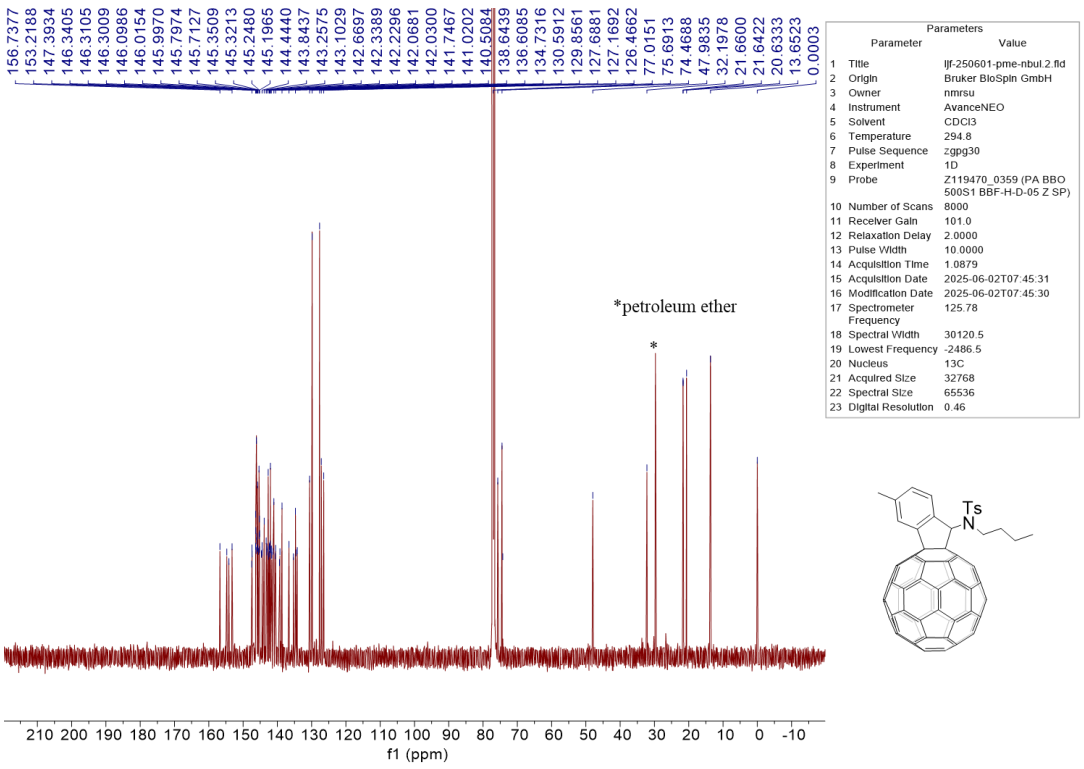

Fig. S39 ^{13}C NMR (126 MHz, $CDCl_3$) of compound **3ah**.

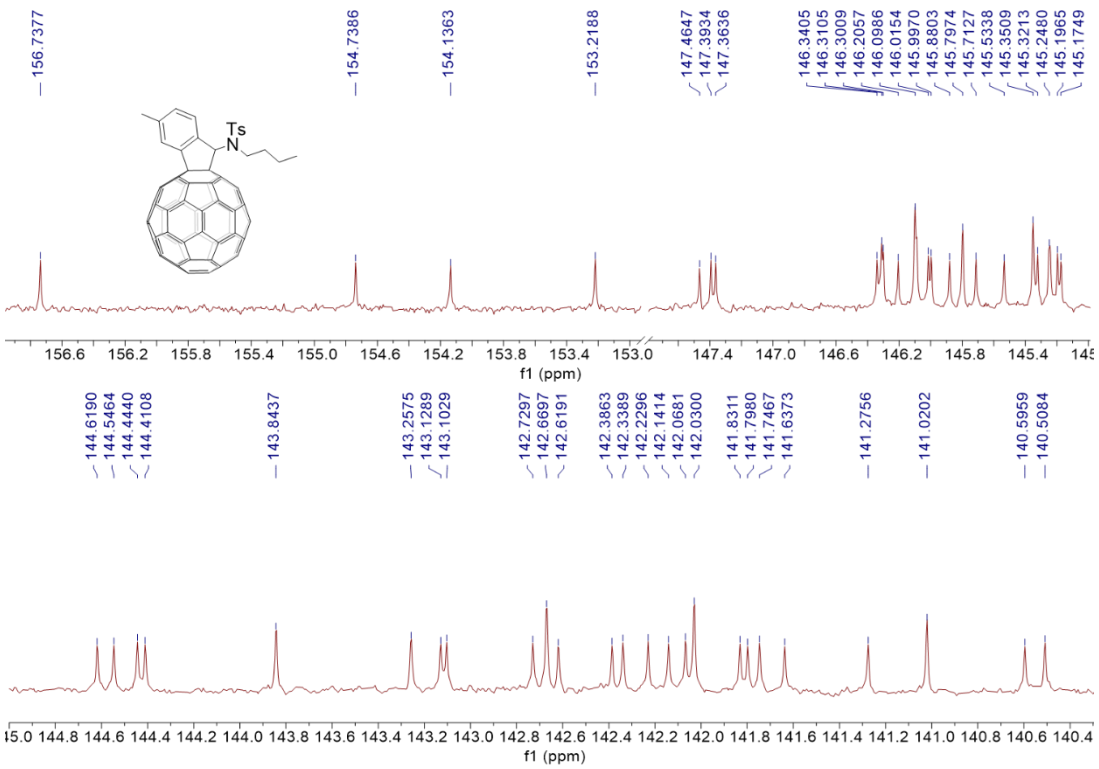

Fig. S40 Expanded ^{13}C NMR (126 MHz, $CDCl_3$) of compound **3ah**.

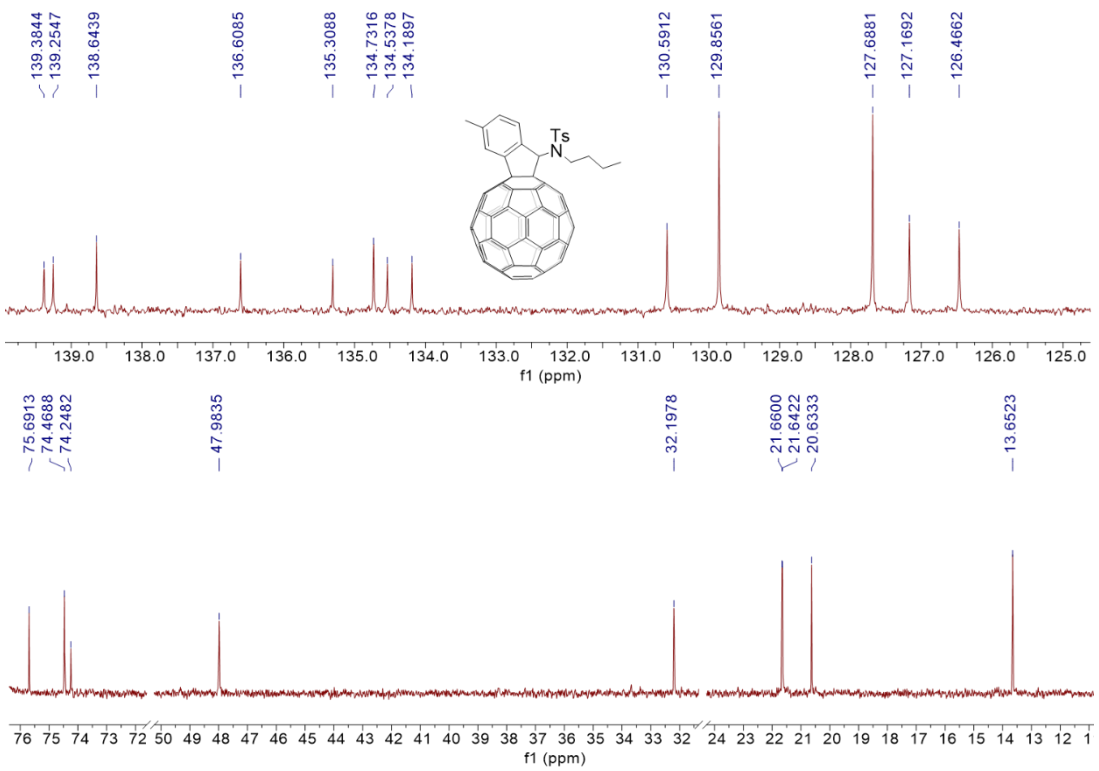

Fig. S41 Expanded ^{13}C NMR (126 MHz, $CDCl_3$) of compound **3ah**.

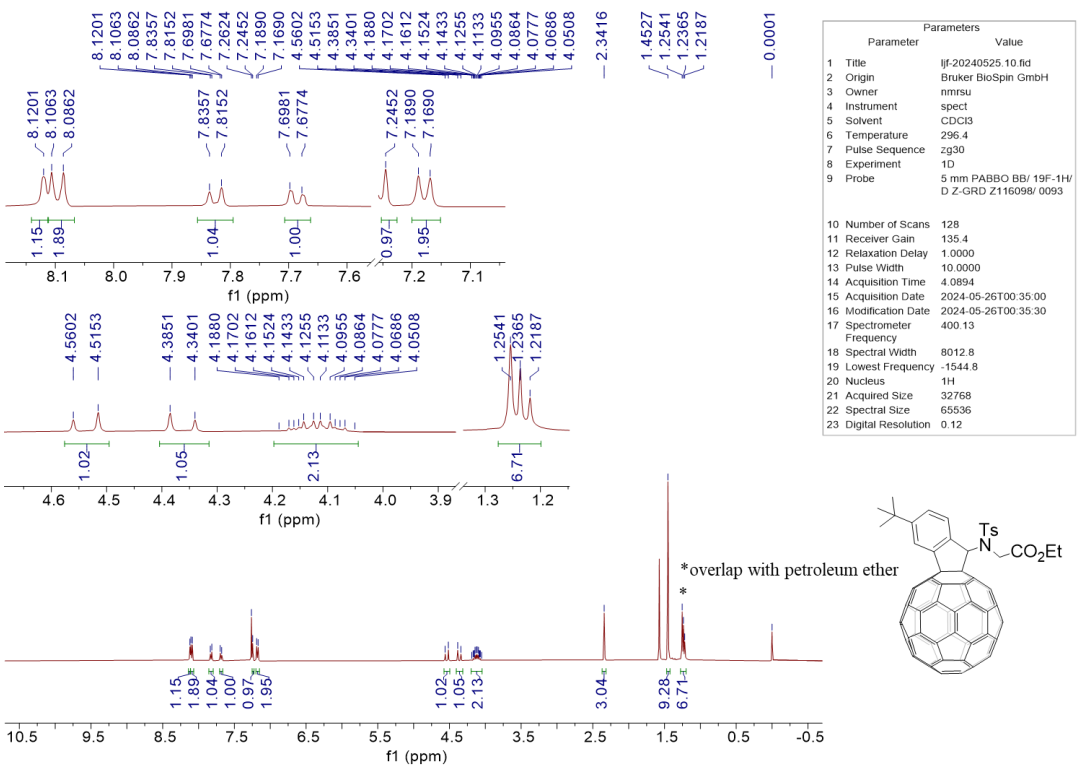

Fig. S42 ^{1}H NMR (400 MHz, $CDCl_3$) of compound **3bd**.

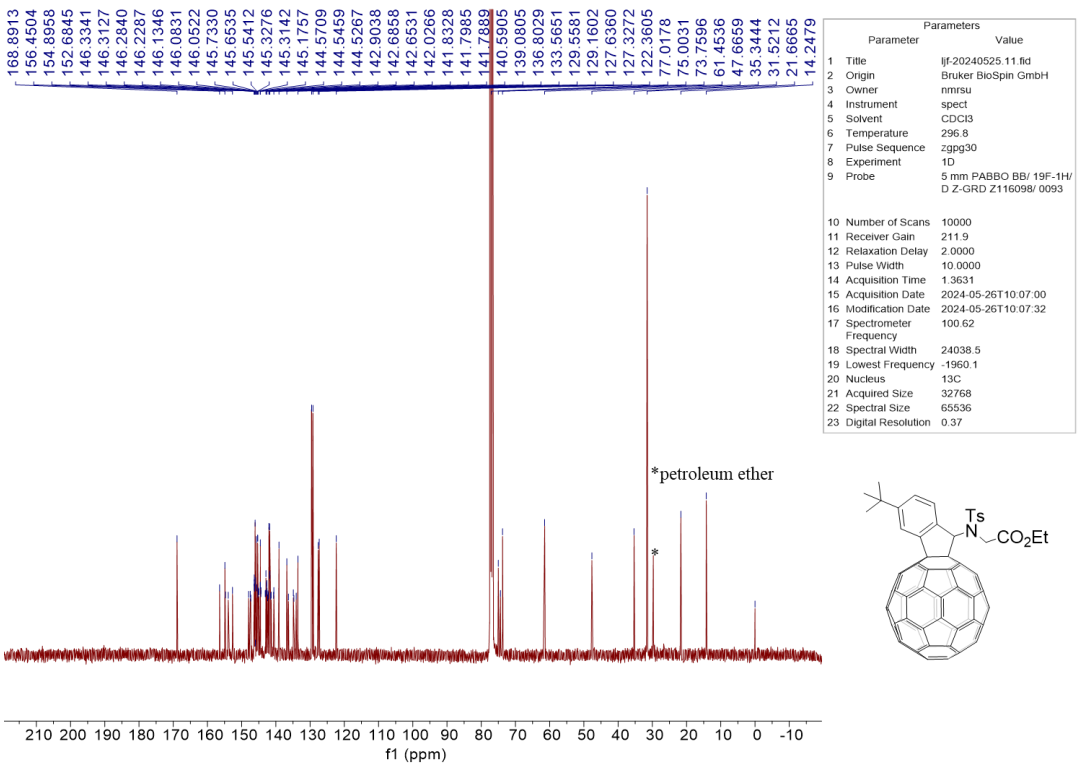

Fig. S43 ^{13}C NMR (101 MHz, $CDCl_3$) of compound **3bd**.

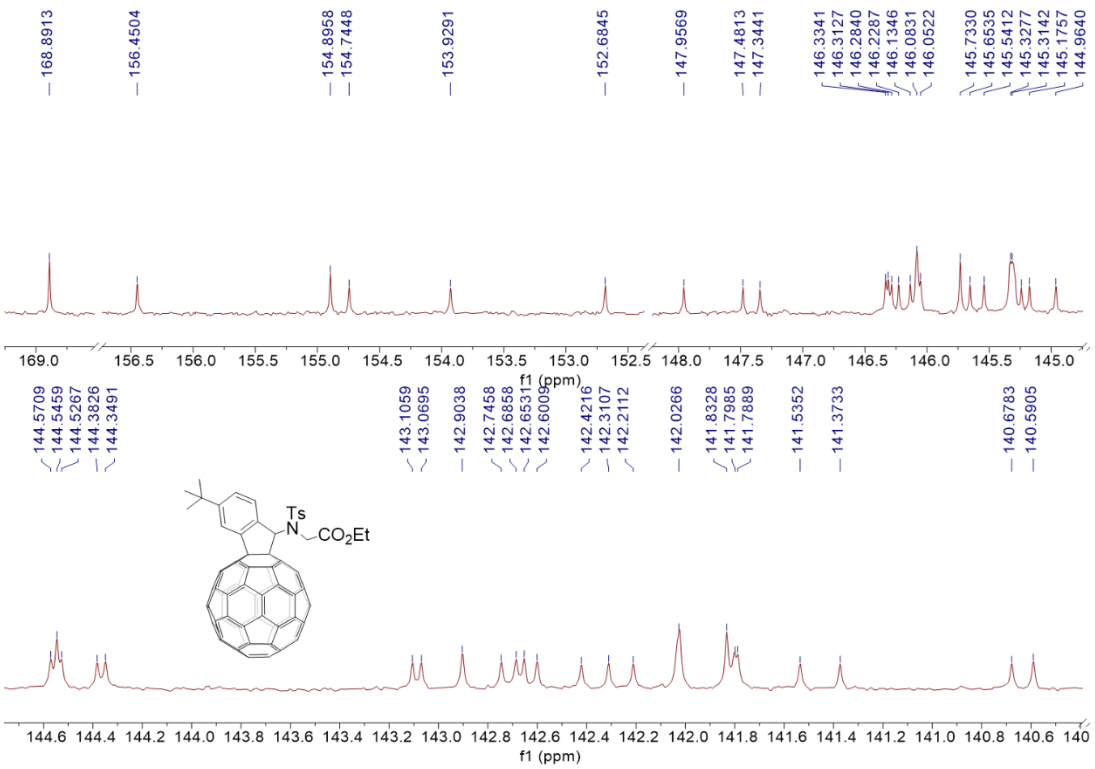

Fig. S44 Expanded ^{13}C NMR (101 MHz, $CDCl_3$) of compound **3bd**.

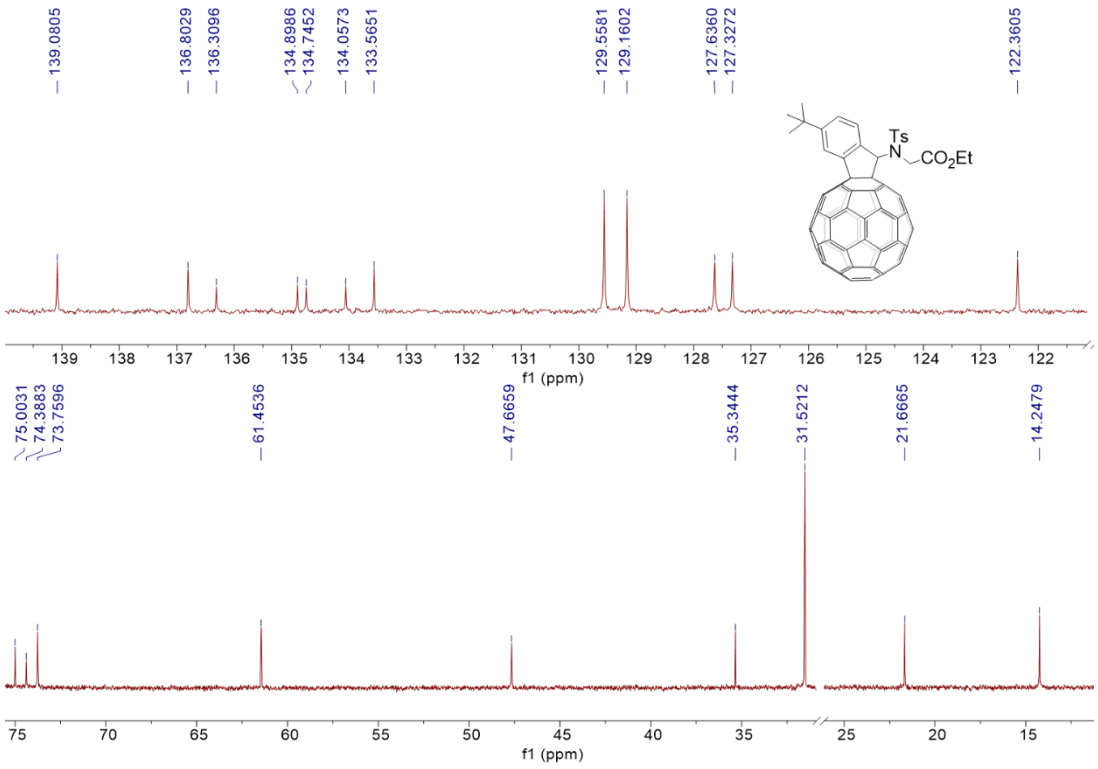

Fig. S45 Expanded ^{13}C NMR (101 MHz, $CDCl_3$) of compound **3bd**.

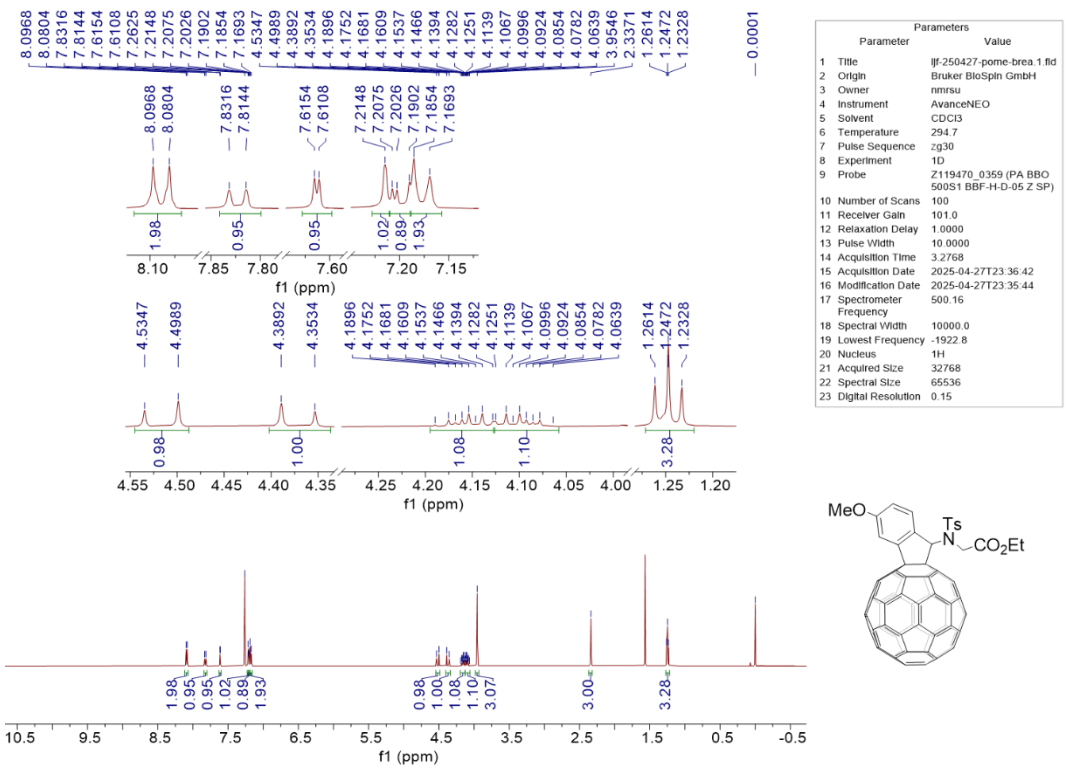

Fig. S46 ^{1}H NMR (500 MHz, $CDCl_3$) of compound **3cd**.

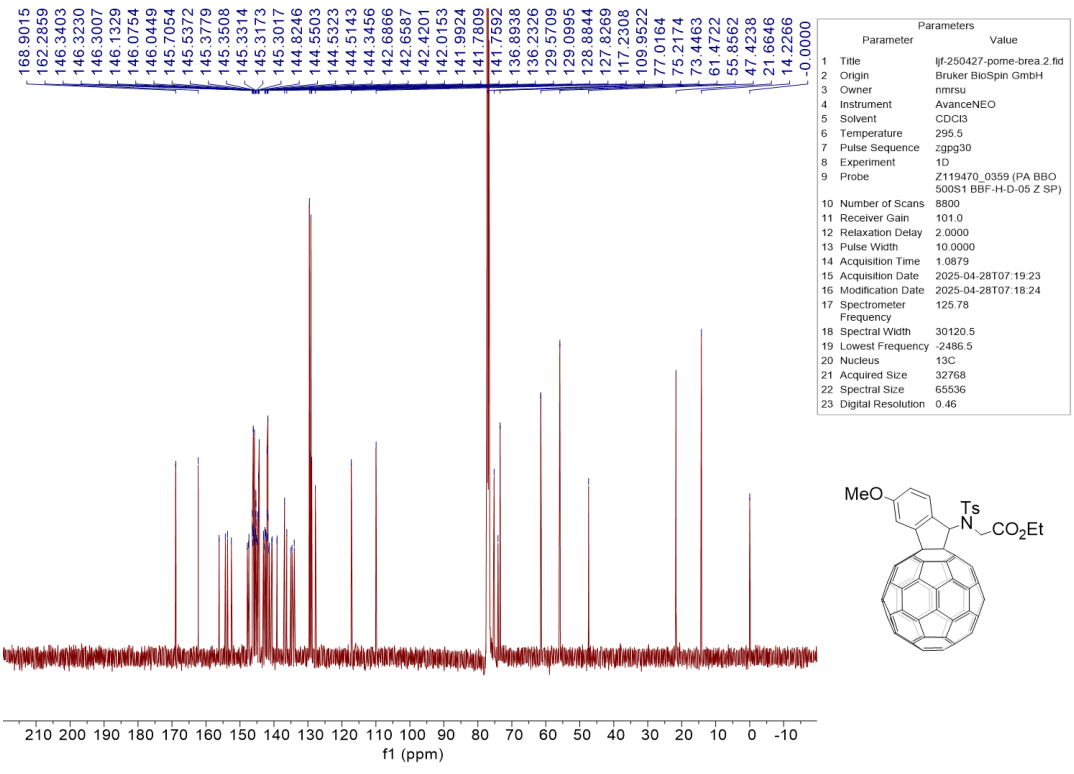

Fig. S47 ^{13}C NMR (126 MHz, $CDCl_3$) of compound **3cd**.

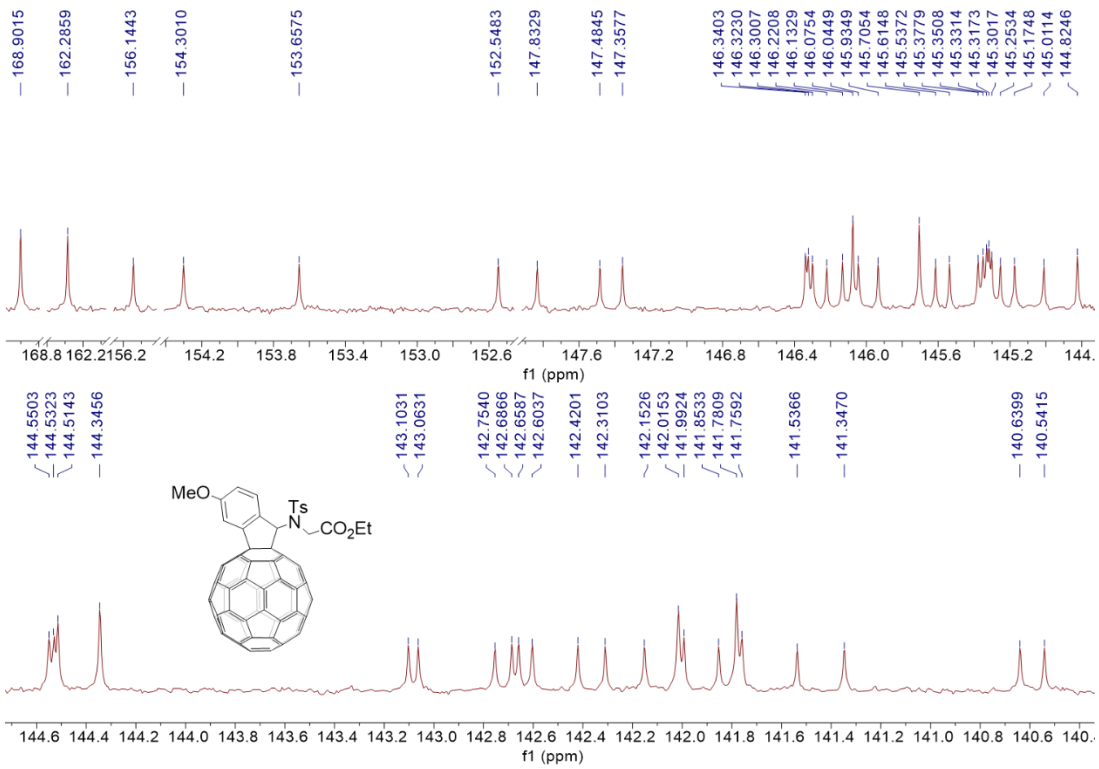

Fig. S48 Expanded ^{13}C NMR (126 MHz, $CDCl_3$) of compound **3cd**.

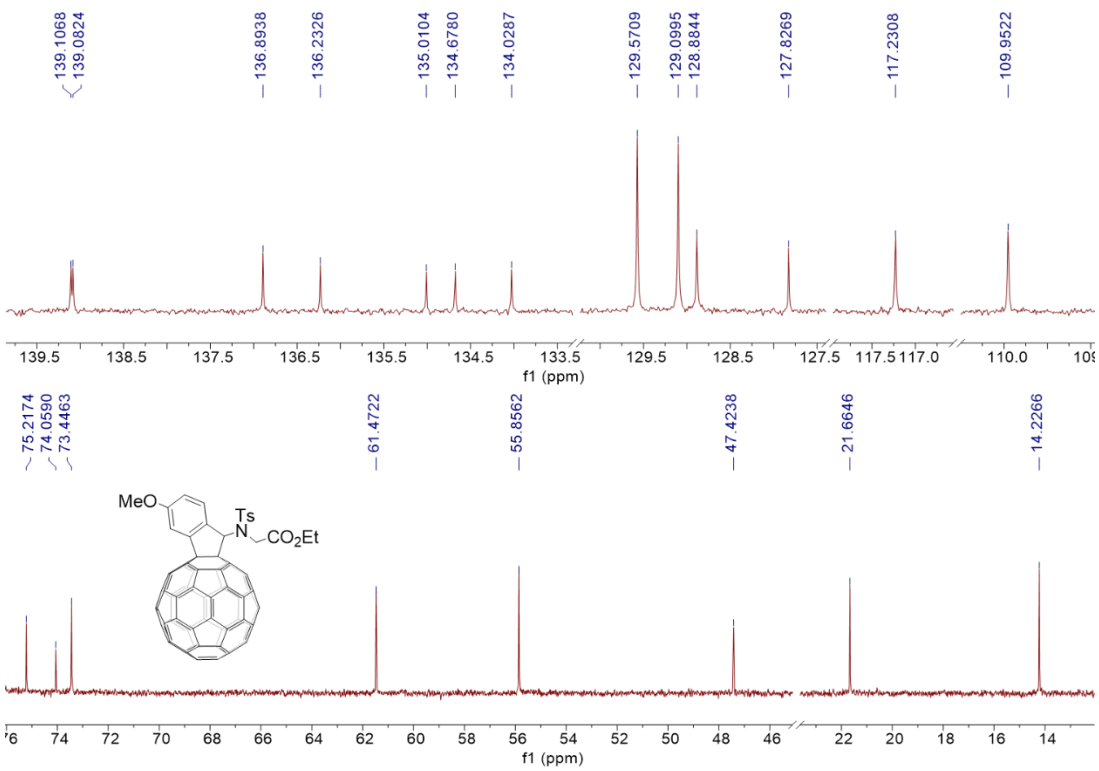

Fig. S49 Expanded ^{13}C NMR (126 MHz, $CDCl_3$) of compound **3cd**.

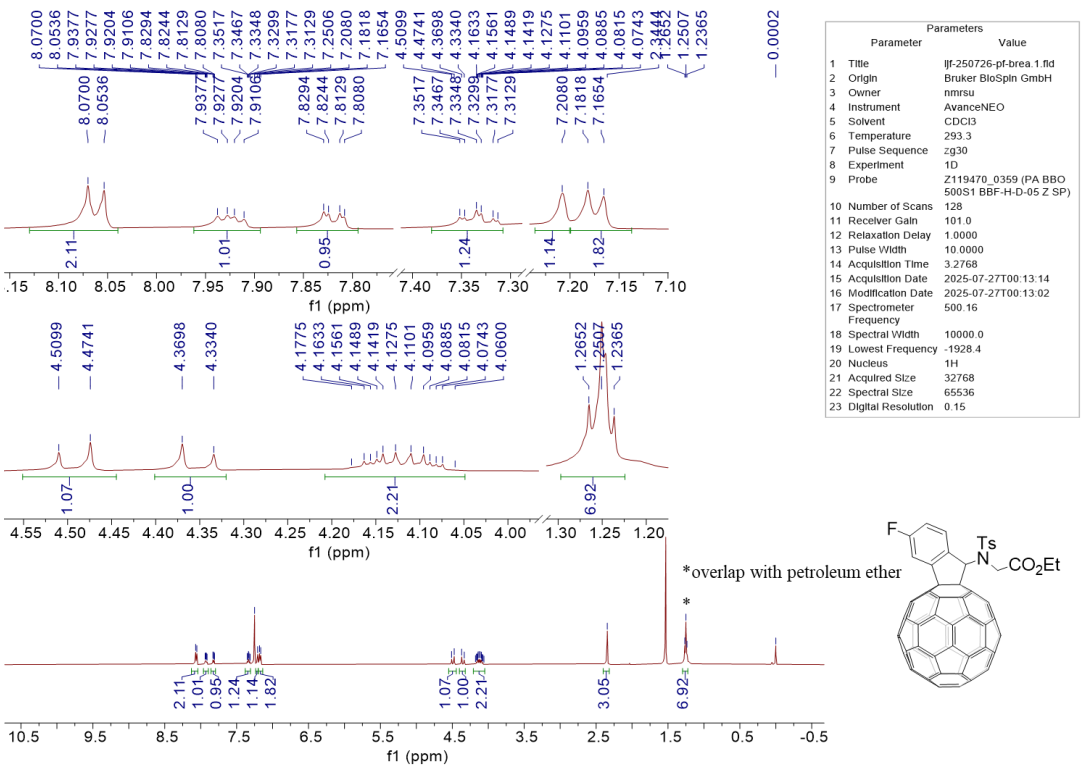

Fig. S50 ^{1}H NMR (500 MHz, $CDCl_3$) of compound **3dd**.

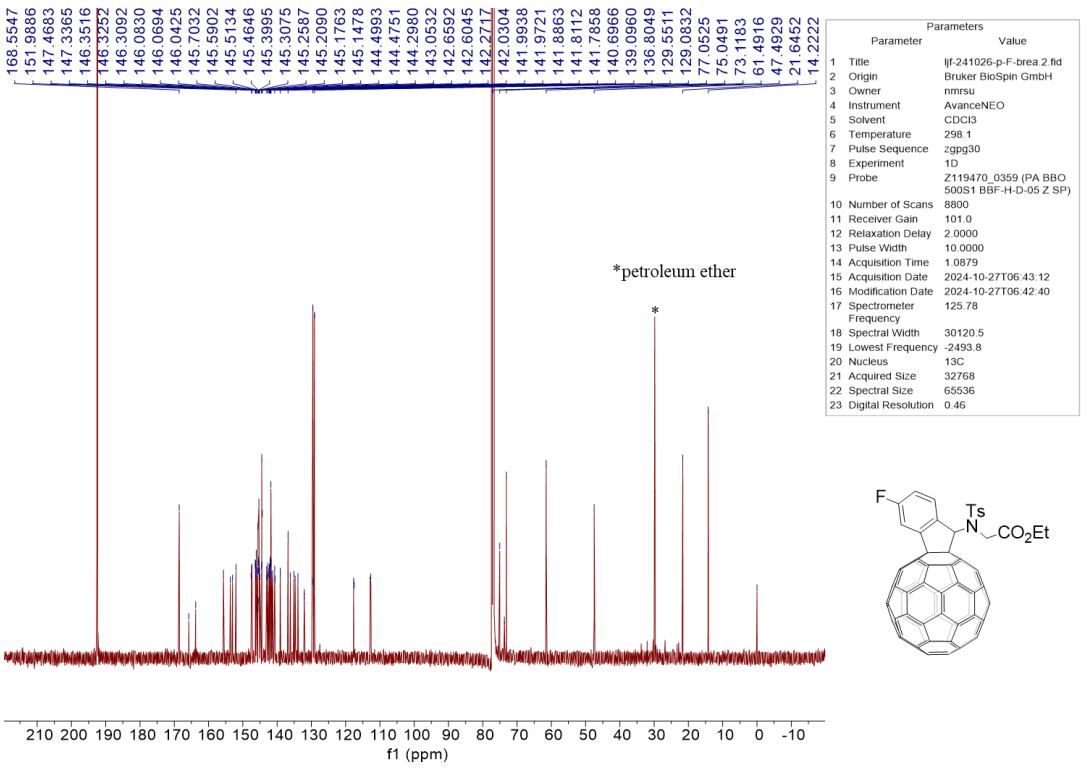

Fig. S51 ^{13}C NMR (126 MHz, 1:1 CS_2/$CDCl_3$) of compound **3dd**.

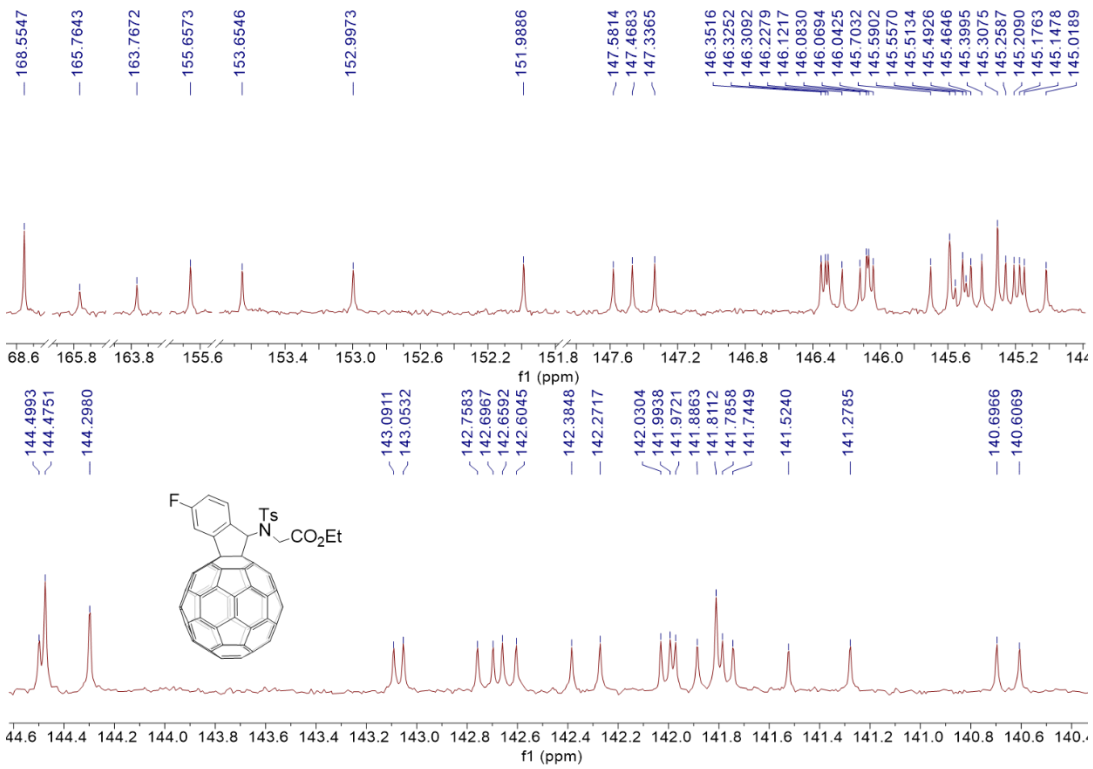

Fig. S52 Expanded ^{13}C NMR (126 MHz, 1:1 $CS_2/CDCl_3$) of compound **3dd**.

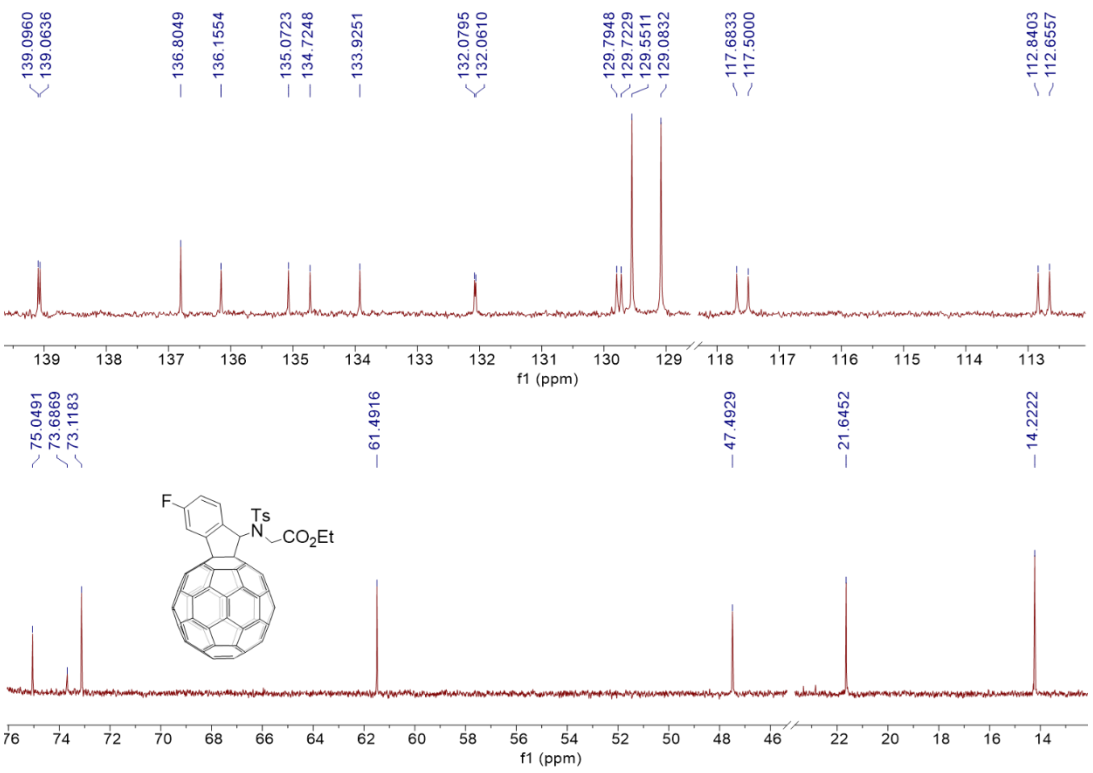

Fig. S53 Expanded ^{13}C NMR (126 MHz, 1:1 $CS_2/CDCl_3$) of compound **3dd**.

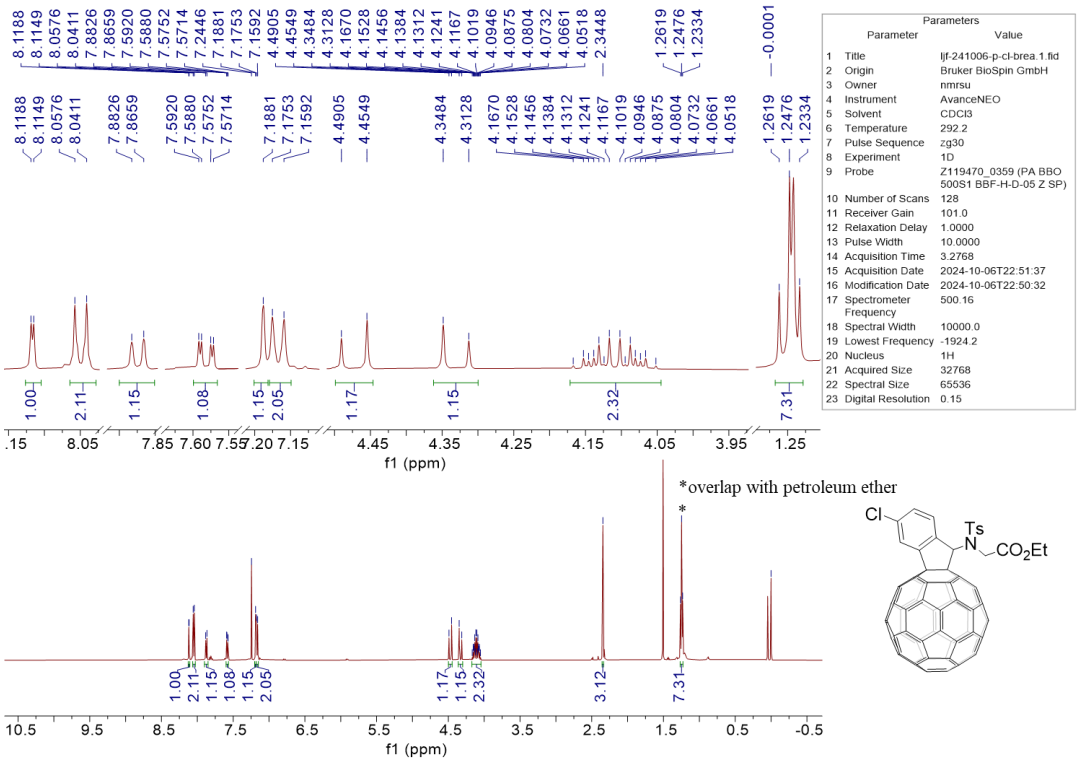

Fig. S54 ^{1}H NMR (500 MHz, 1:1 CS_2/$CDCl_3$) of compound **3ed**.

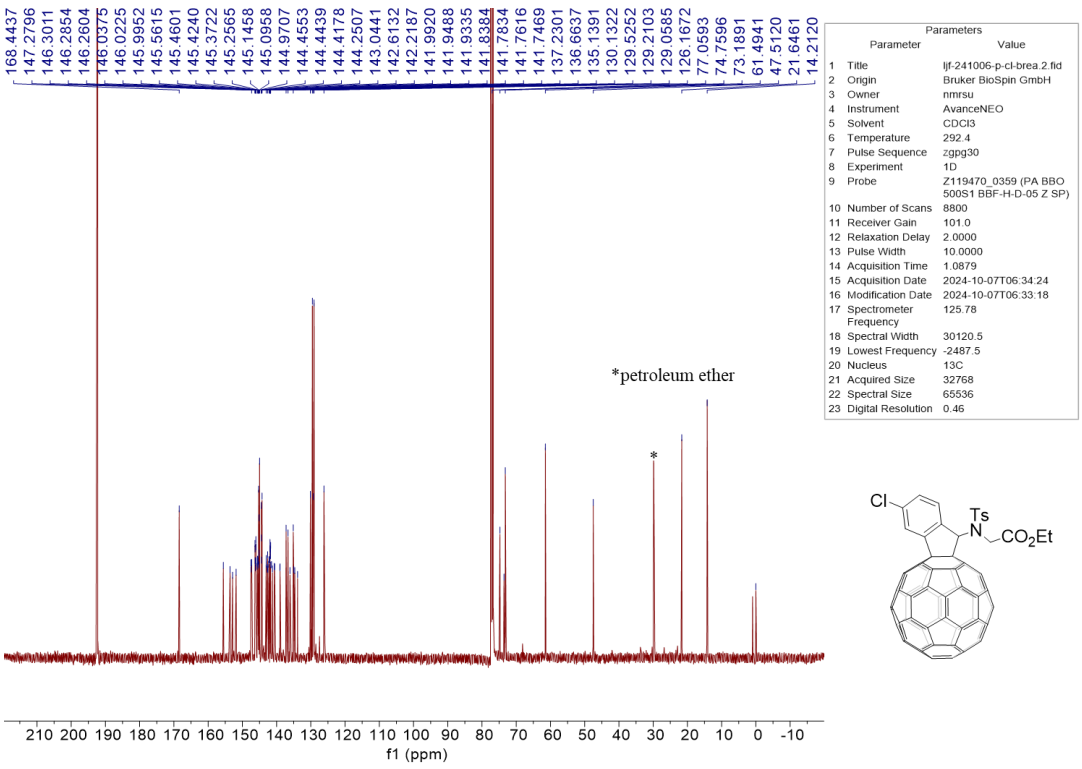

Fig. S55 ^{13}C NMR (126 MHz, 1:1 CS_2/$CDCl_3$) of compound **3ed**.

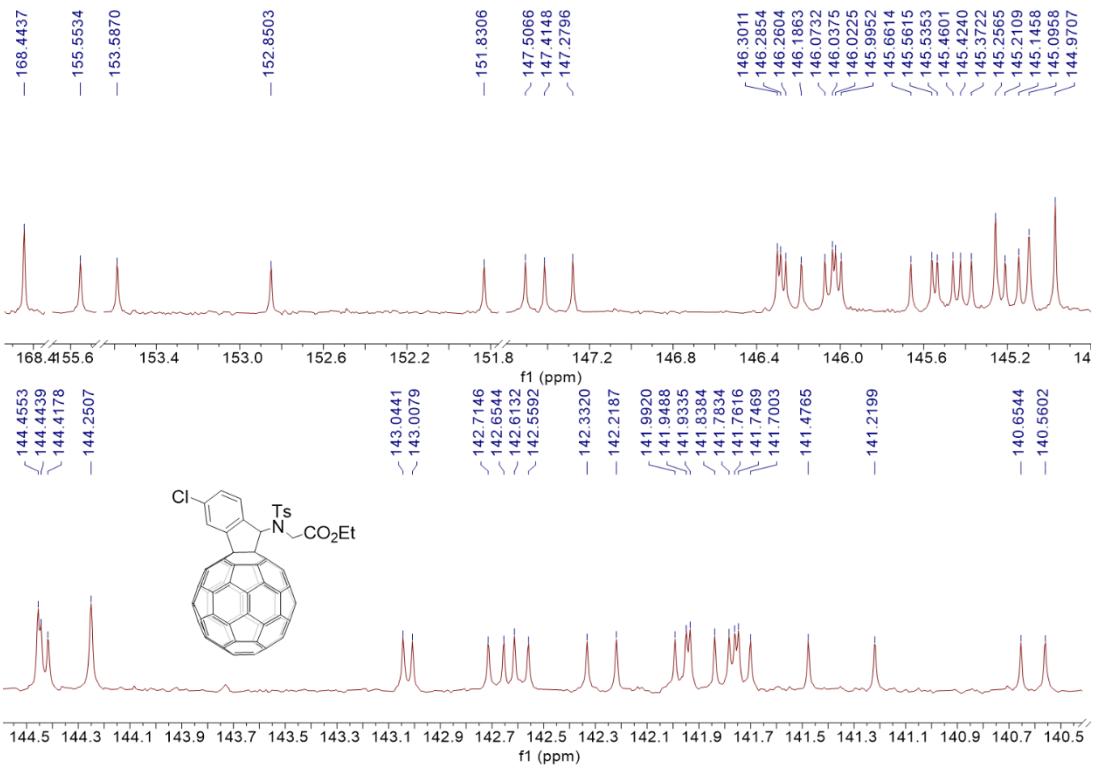

Fig. S56 Expanded ^{13}C NMR (126 MHz, 1:1 $CS_2/CDCl_3$) of compound **3ed**.

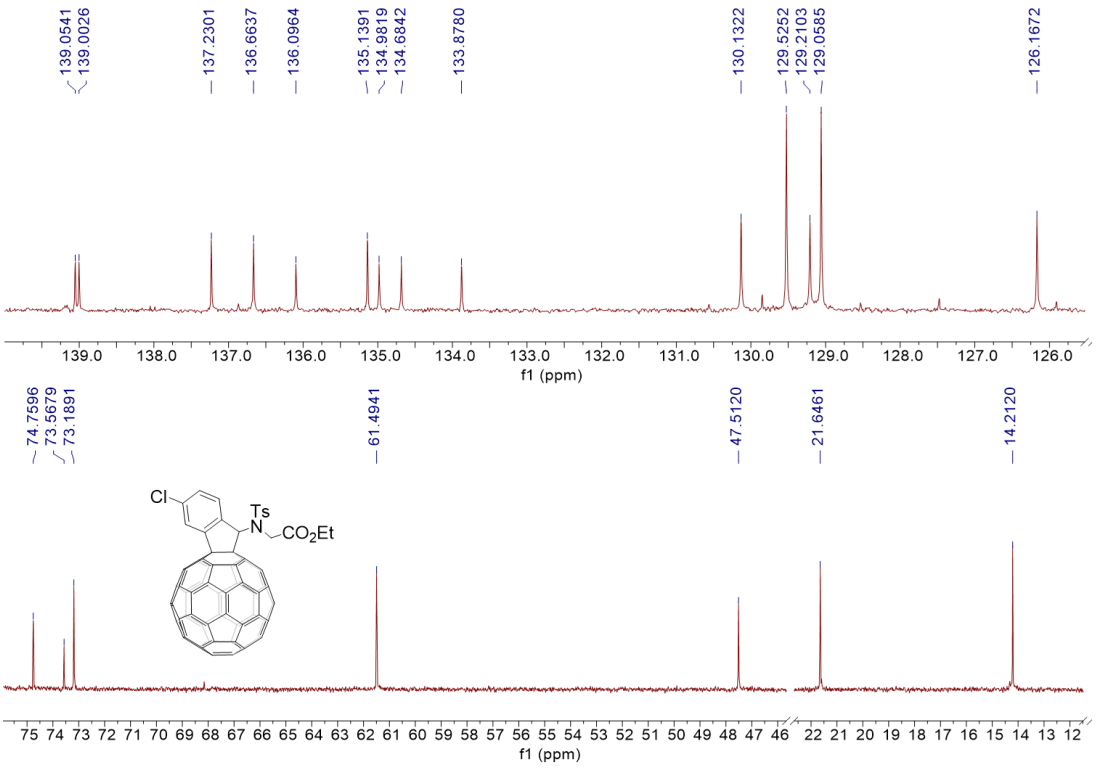

Fig. S57 Expanded ^{13}C NMR (126 MHz, 1:1 $CS_2/CDCl_3$) of compound **3ed**.

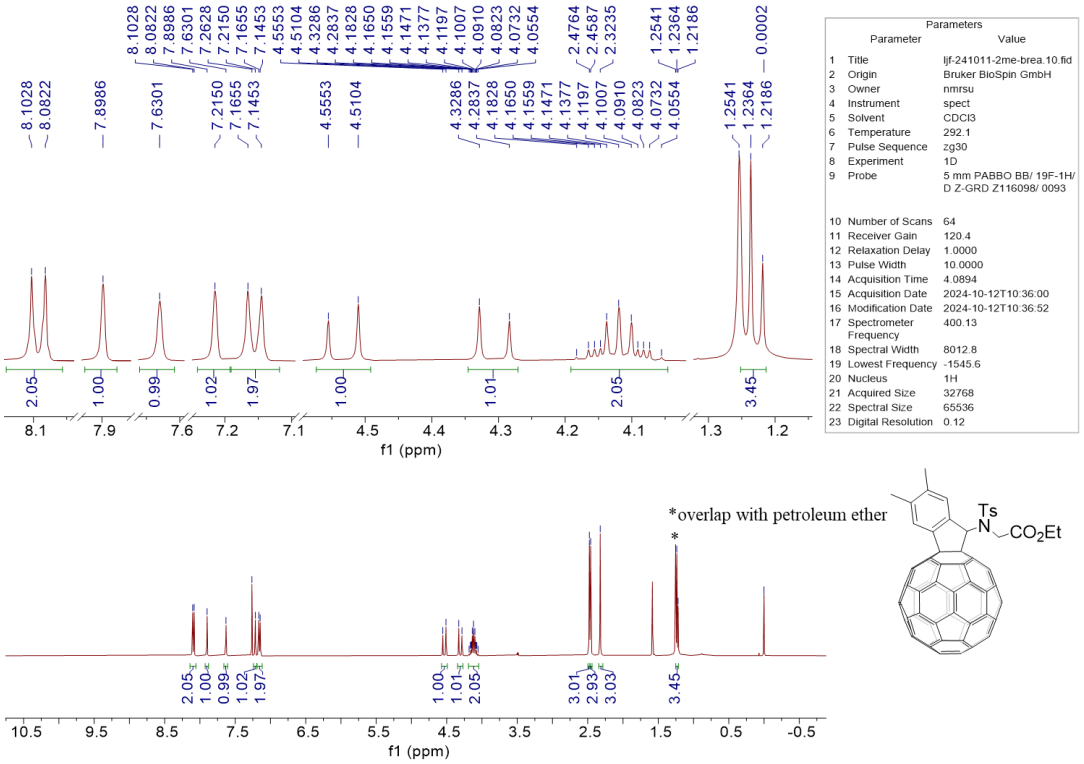

Fig. S58 ^{1}H NMR (400 MHz, $CDCl_3$) of compound **3fd**.

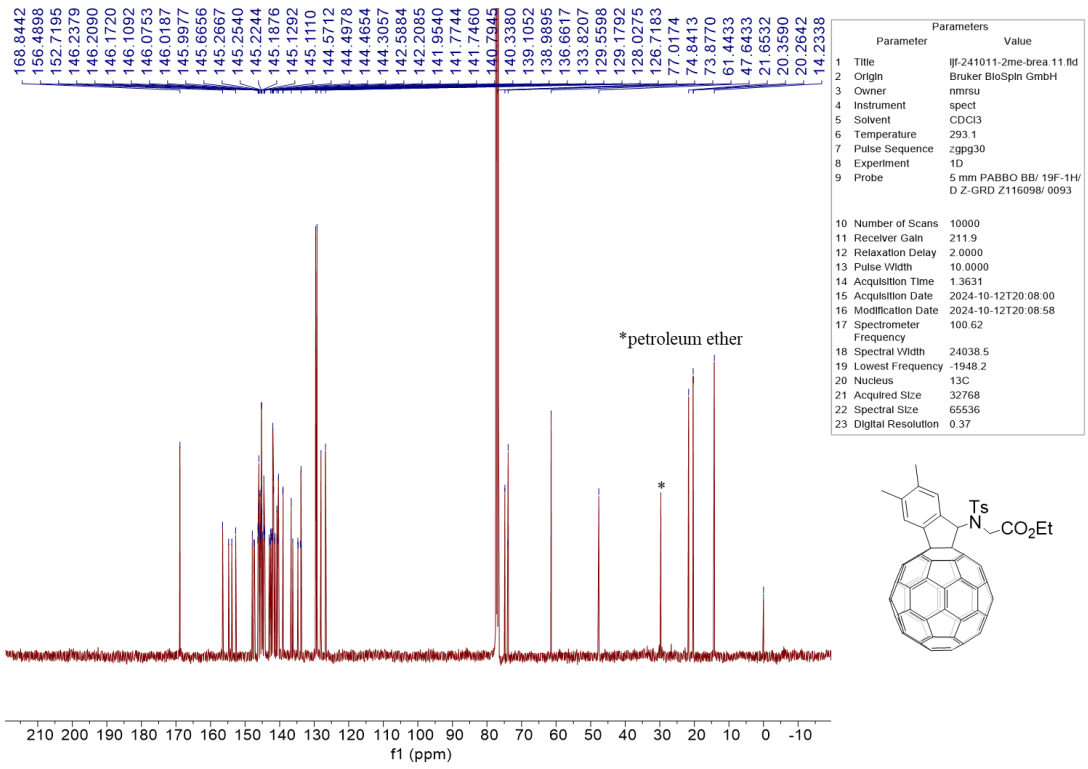

Fig. S59 ^{13}C NMR (101 MHz, $CDCl_3$) of compound **3fd**.

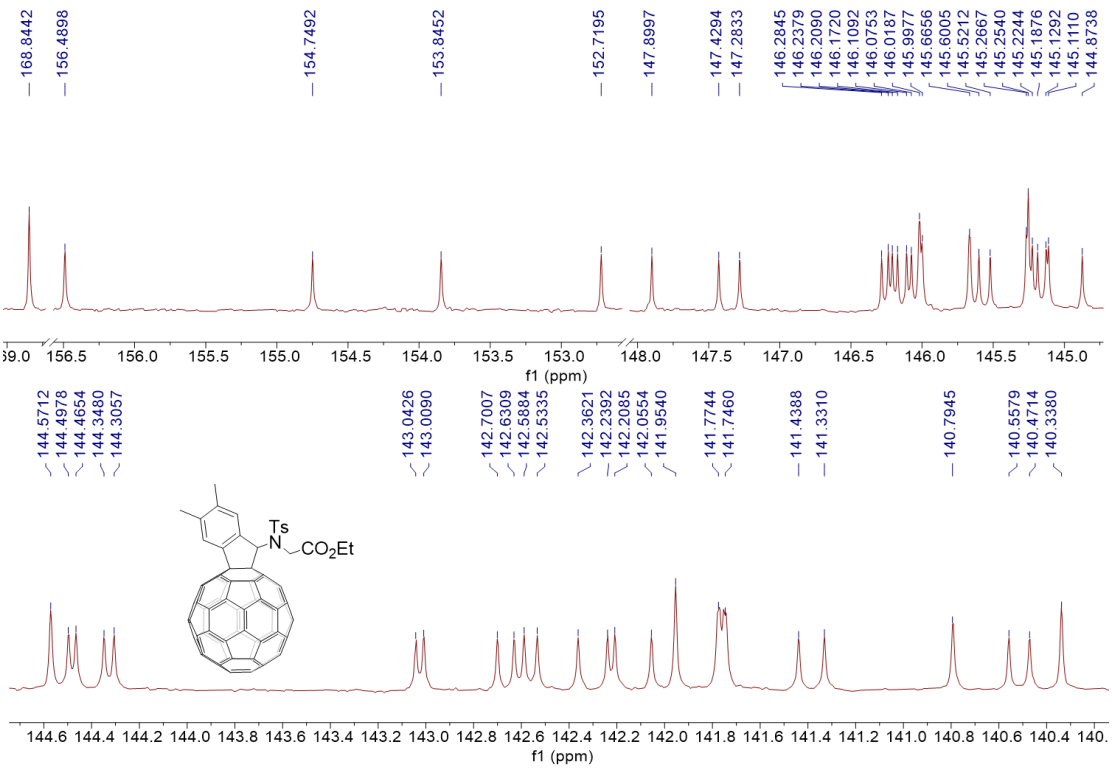

Fig. S60 Expanded ^{13}C NMR (101 MHz, $CDCl_3$) of compound **3fd**.

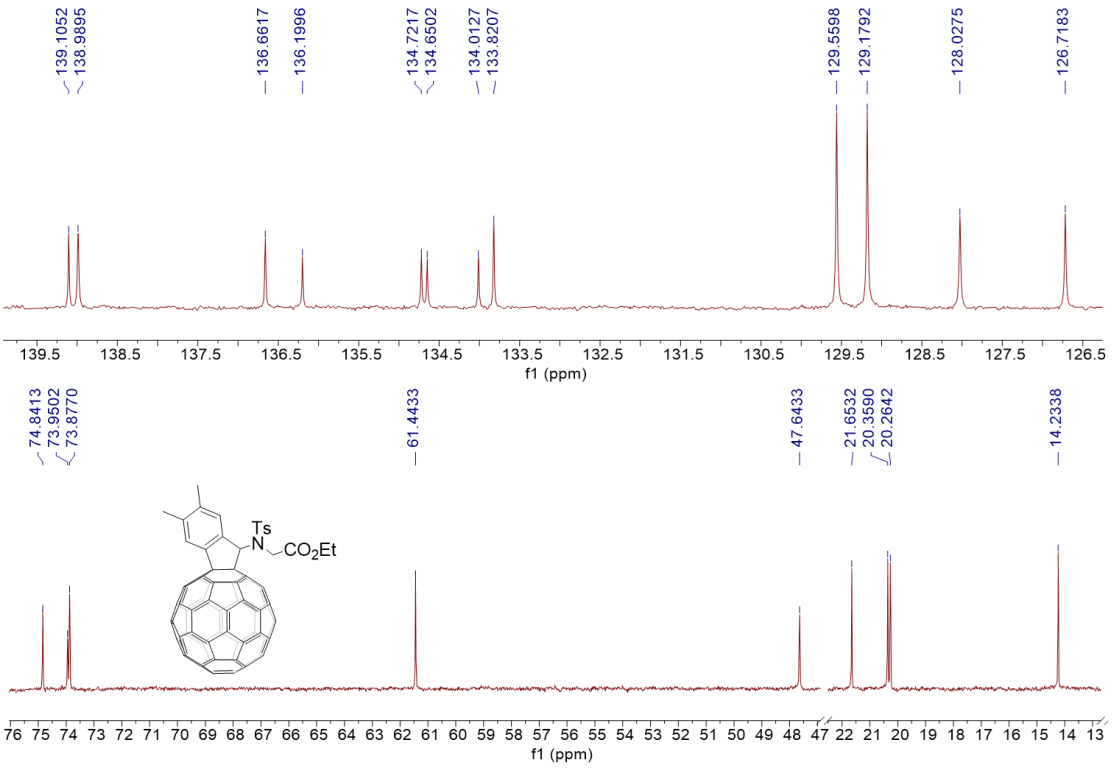

Fig. S61 Expanded ^{13}C NMR (101 MHz, $CDCl_3$) of compound **3fd**.

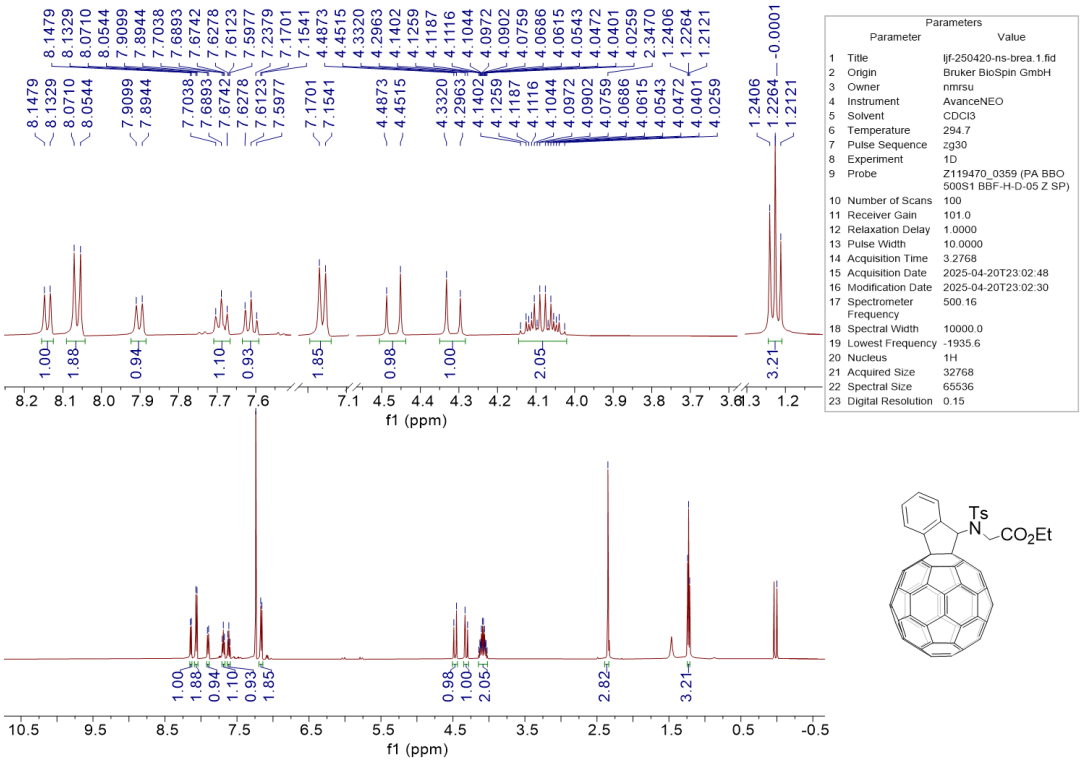

Fig. S62 ^{1}H NMR (500 MHz, 1:1 CS_2/$CDCl_3$) of compound **3gd**.

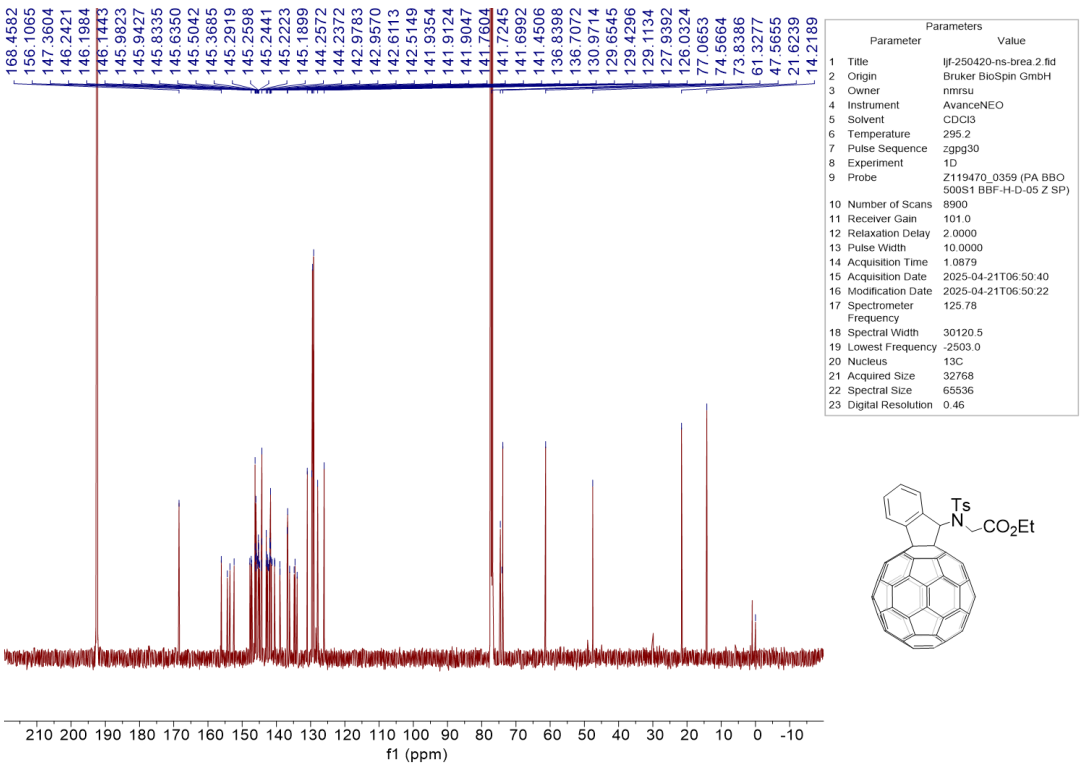

Fig. S63 ^{13}C NMR (126 MHz, 1:1 CS_2/$CDCl_3$) of compound **3gd**.

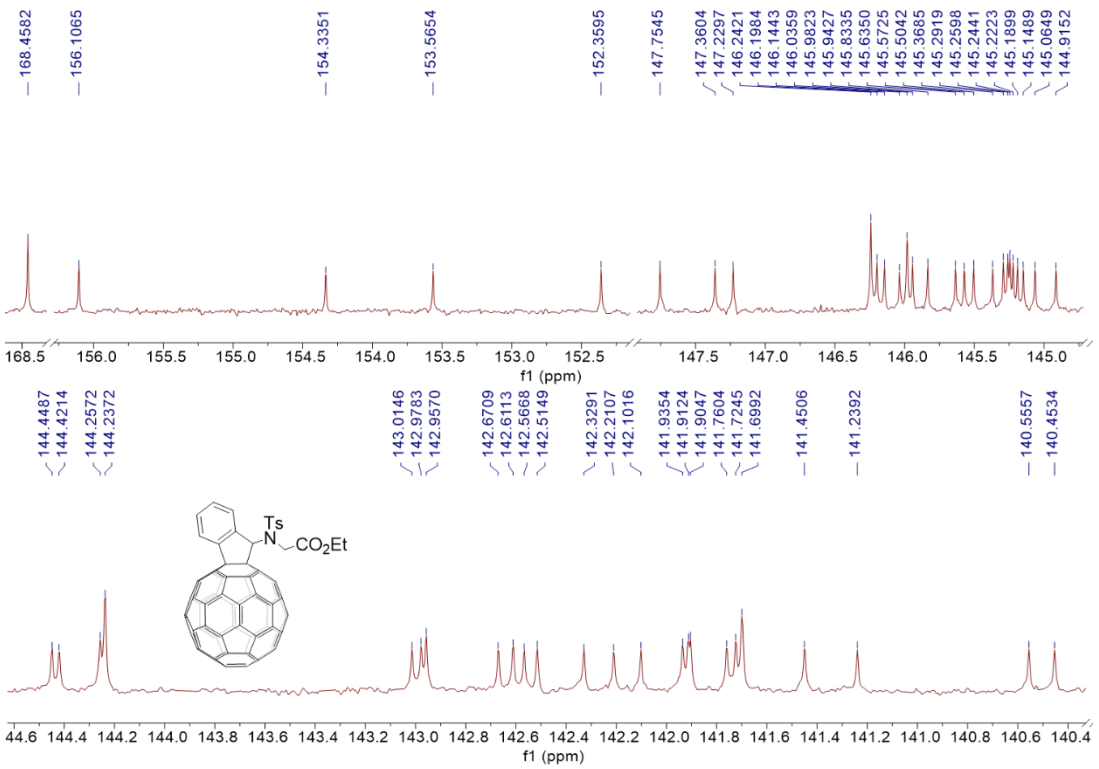

Fig. S64 Expanded ^{13}C NMR (126 MHz, 1:1 $CS_2/CDCl_3$) of compound **3gd**.

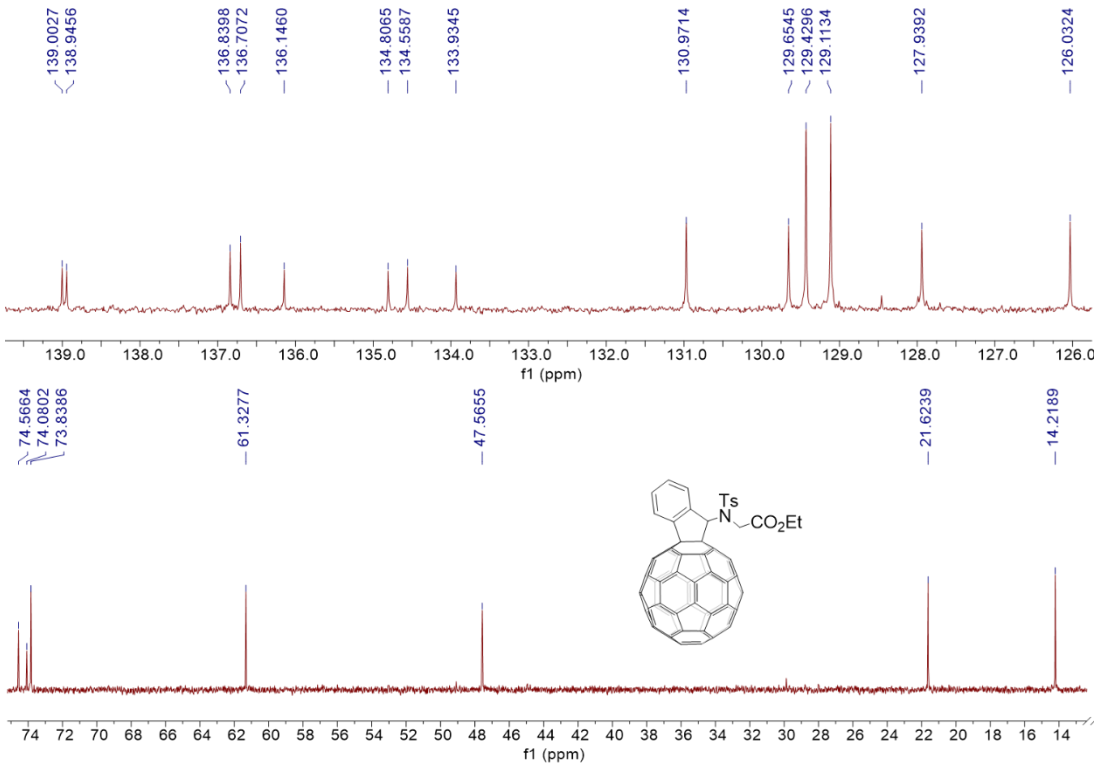

Fig. S65 Expanded ^{13}C NMR (126 MHz, 1:1 $CS_2/CDCl_3$) of compound **3gd**.

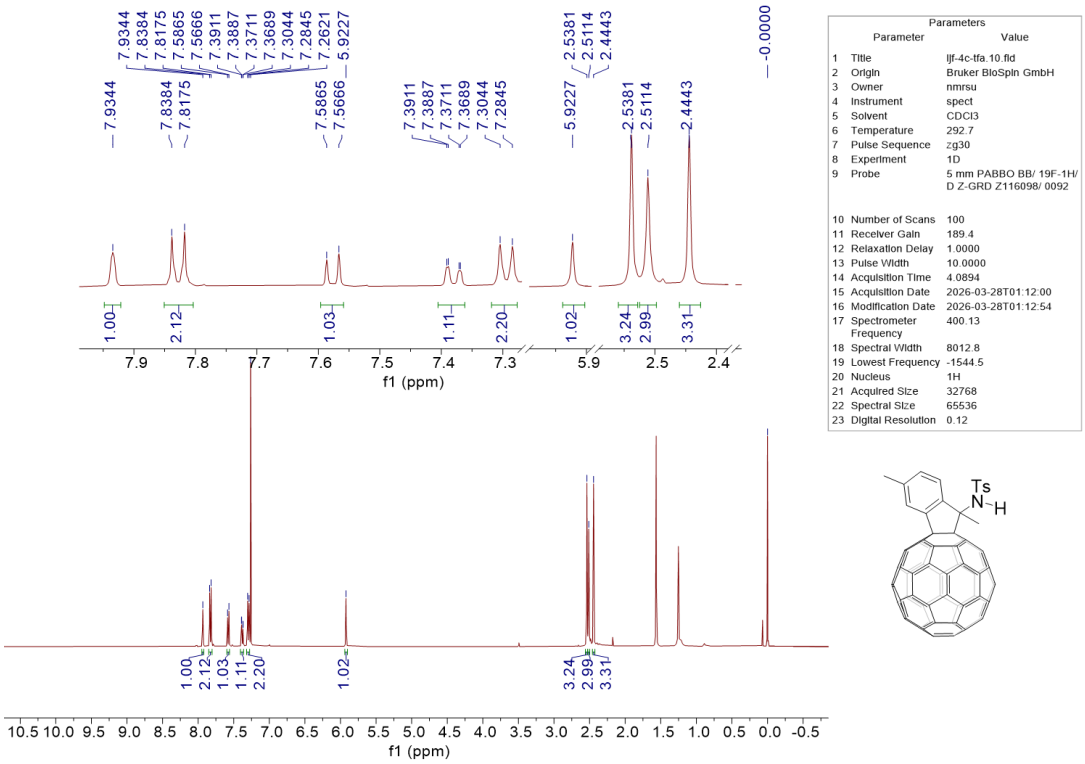

Fig. S66 ^{1}H NMR (400 MHz, $CDCl_3$) of compound **3ha**.

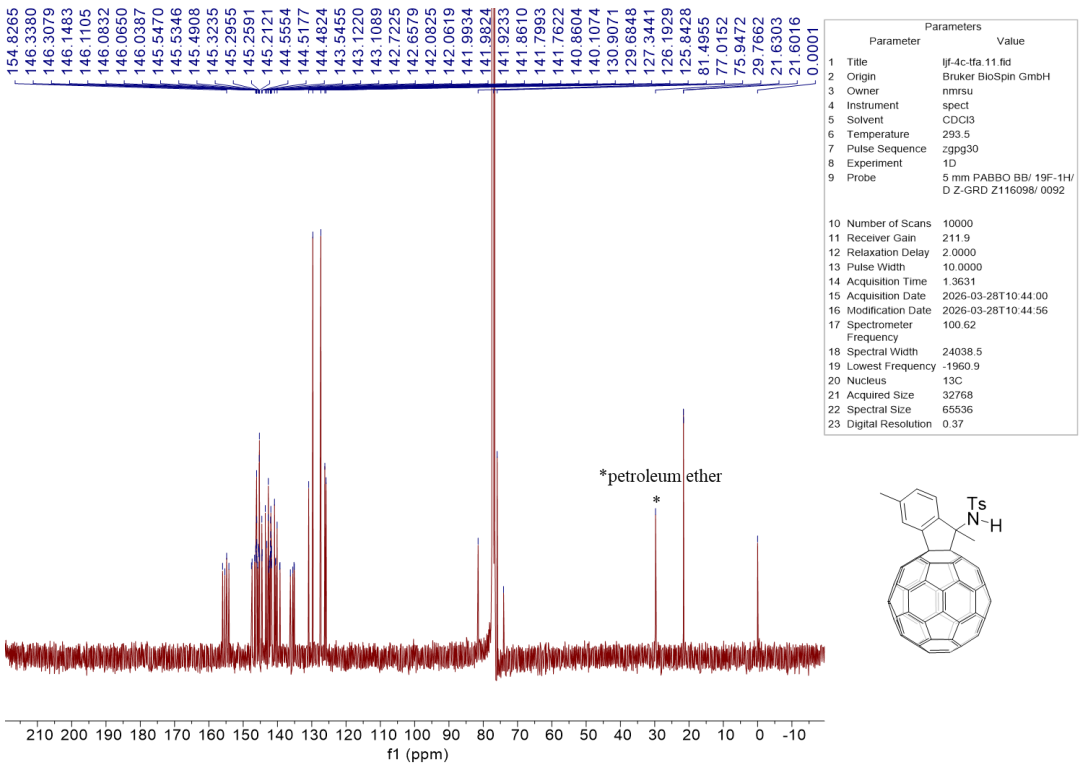

Fig. S67 ^{13}C NMR (101 MHz, $CDCl_3$) of compound **3ha**.

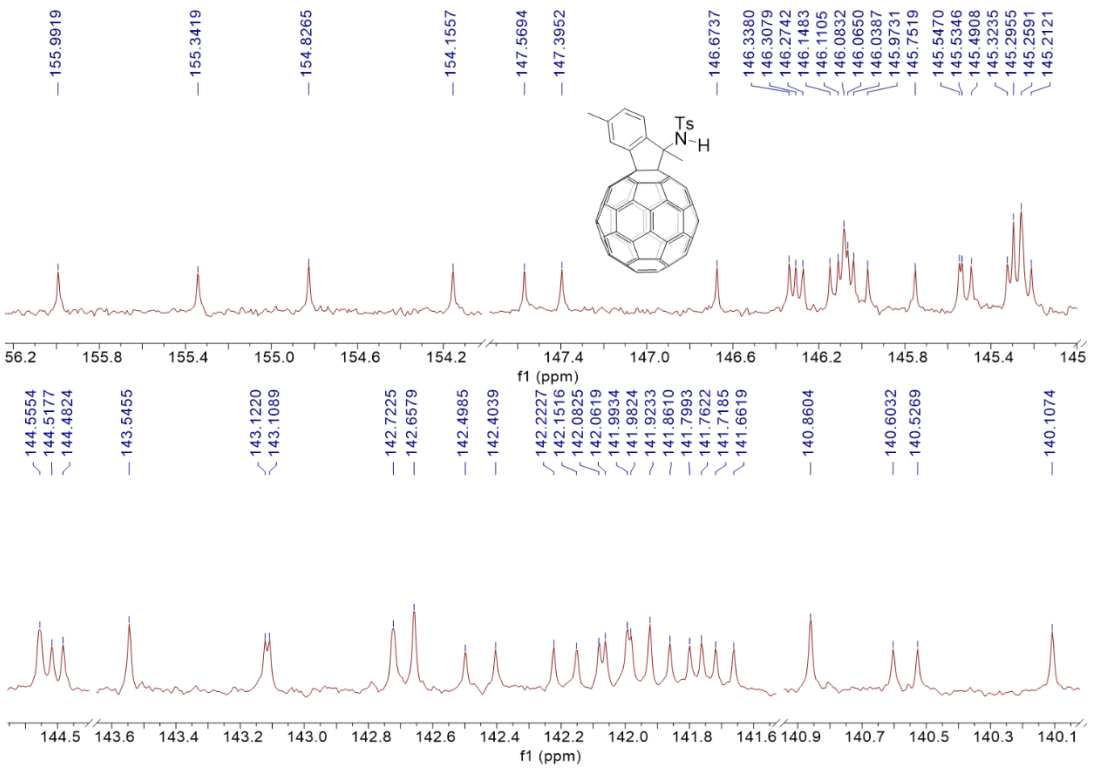

Fig. S68 Expanded ^{13}C NMR (101 MHz, $CDCl_3$) of compound **3ha**.

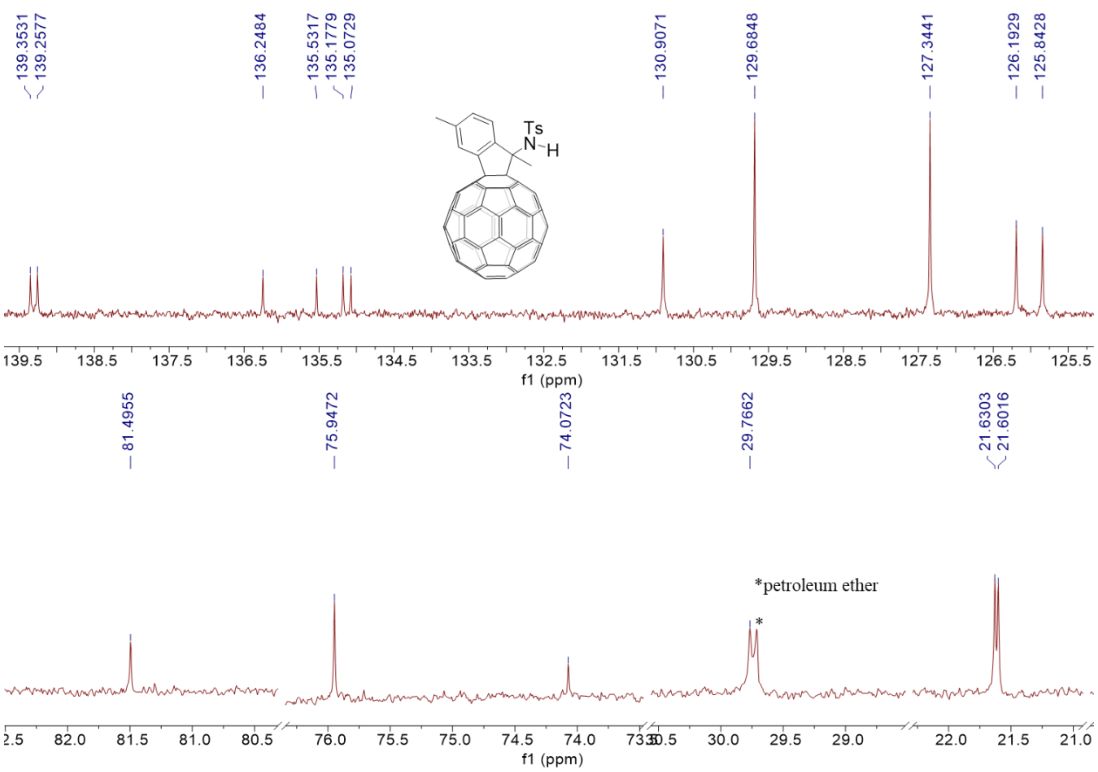

Fig. S69 Expanded ^{13}C NMR (101 MHz, $CDCl_3$) of compound **3ha**.

7. UV-vis spectra of compounds 3aa–ha

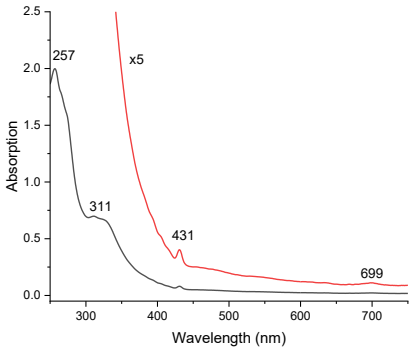

Fig. S70 UV-vis absorption of **3aa**

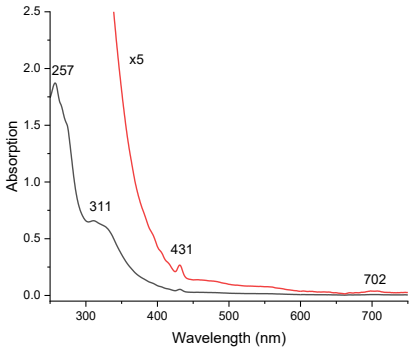

Fig. S71 UV-vis absorption of **3ab**

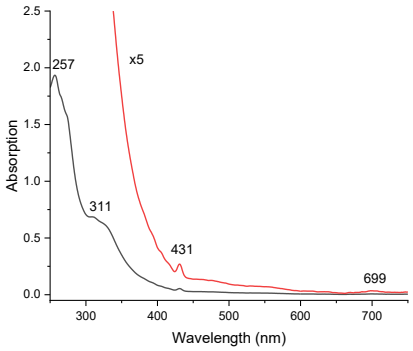

Fig. S72 UV-vis absorption of **3ac**

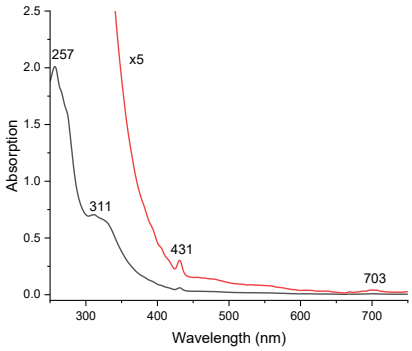

Fig. S73 UV-vis absorption of **3ad**

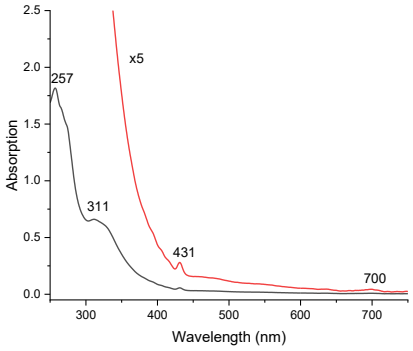

Fig. S74 UV-vis absorption of **3ae**

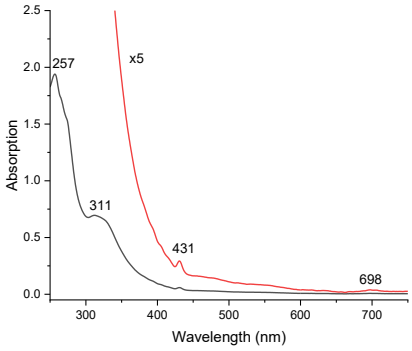

Fig. S75 UV-vis absorption of **3af**

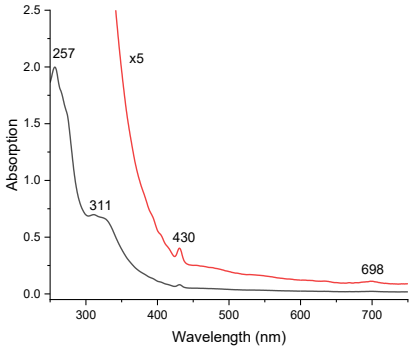

Fig. S76 UV-vis absorption of **3ag**

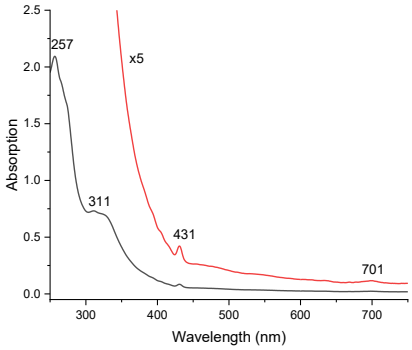

Fig. S77 UV-vis absorption of **3ah**

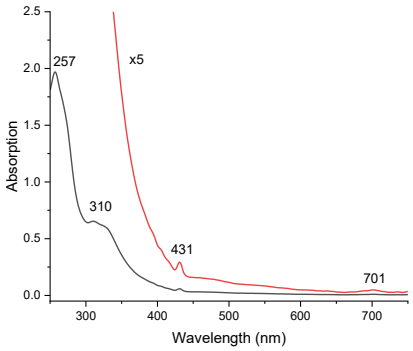

Fig. S78 UV-vis absorption of **3bd**

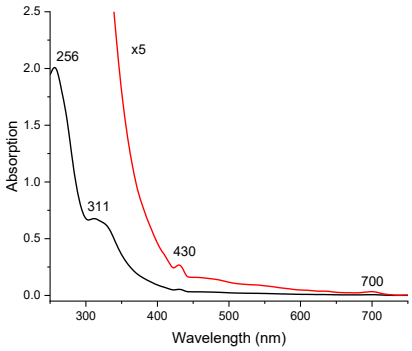

Fig. S79 UV-vis absorption of **3cd**

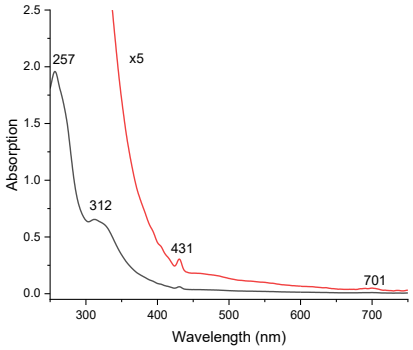

Fig. S80 UV-vis absorption of **3dd**

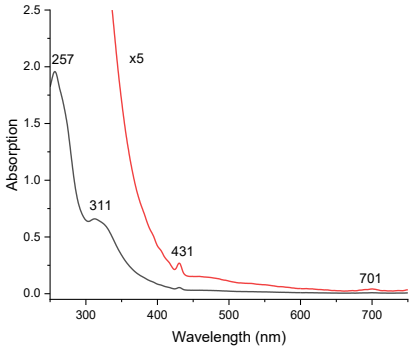

Fig. S81 UV-vis absorption of **3ed**

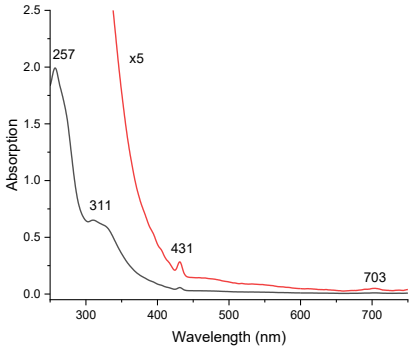

Fig. S82 UV-vis absorption of **3fd**

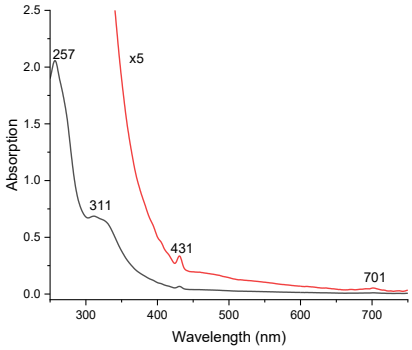

Fig. S83 UV-vis absorption of **3gd**

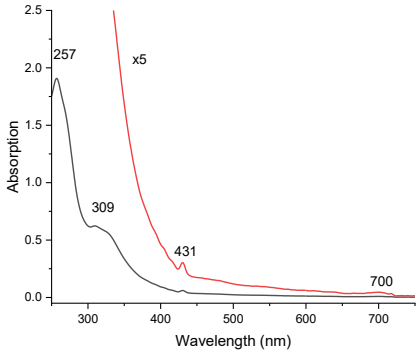

Fig. S84 UV-vis absorption of **3ha**

8. Cyclic voltammograms and differential pulse voltammograms of compounds 3aa–ha

Table S2 Half-Wave reduction potentials (V) of compounds **3aa**–**ha** determined by DPV[a]

Compound	E_1	E_2	E_3
3aa	-1.152	/	/
3ab	-1.148	-1.536	-2.060
3ac	-1.136	-1.520	-2.040
3ad	-1.140	-1.524	-2.044
3ae	-1.144	-1.532	-2.060
3af	-1.148	-1.532	-2.060
3ag	-1.180	-1.552	-2.080
3ah	-1.140	-1.532	-2.068
3bd	-1.144	-1.540	-2.064
3cd	-1.148	-1.532	-2.056
3dd	-1.128	-1.524	-2.036
3ed	-1.120	-1.516	-2.032
3fd	-1.180	-1.600	-2.144
3gd	-1.128	-1.532	-2.036
3ha	-1.144	-1.508	-1.896

[a]Versus ferrocene/ferrocenium. Experimental conditions: 1.0 mM compound and 0.1 M TBAP in anhydrous 1,2-$C_6H_4Cl_2$; reference electrode: SCE; working electrode: Pt disc; auxiliary electrode: Pt wire; pulse amplitude: 50 mV.

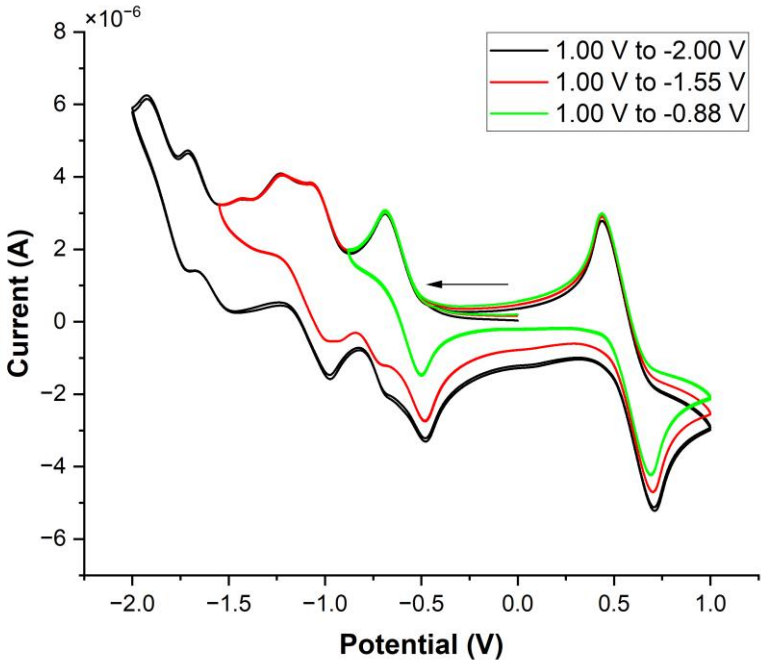

Fig. S85 CV of compound **3aa**. (scanning rate: 50 mV s^{-1})

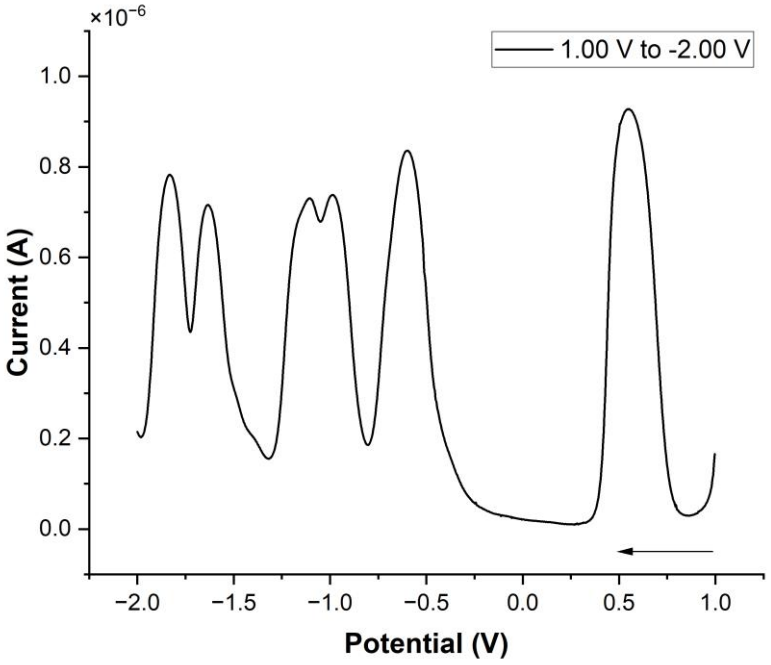

Fig. S86 DPV of compound **3aa**. (pulse amplitude: 50 mV; pulse width: 0.05 s; pulse period: 0.5 s)

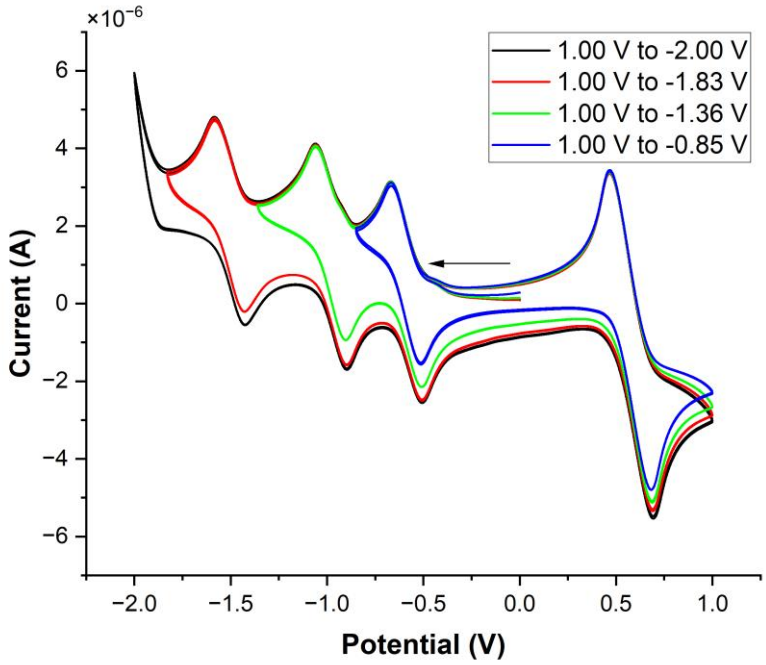

Fig. S87 CV of compound **3ab**. (scanning rate: 50 mV s^{-1})

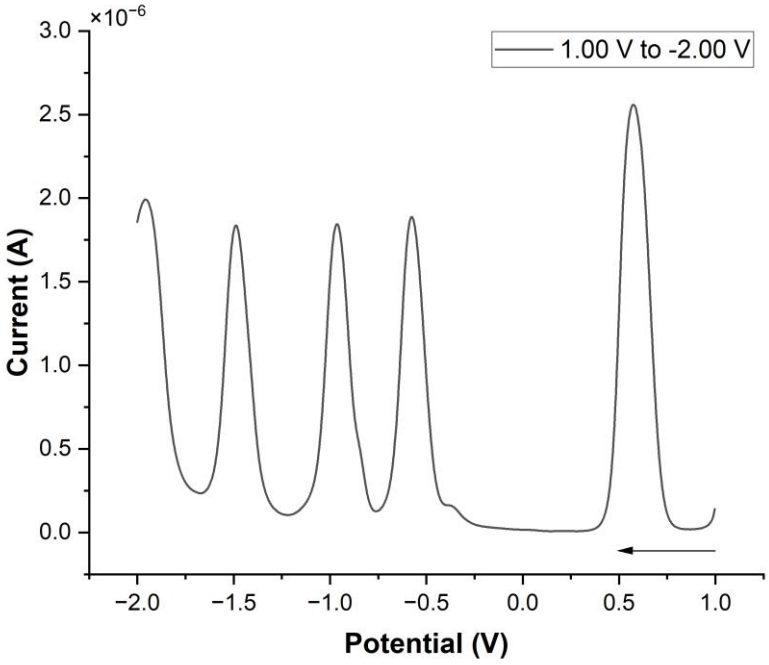

Fig. S88 DPV of compound **3ab**. (pulse amplitude: 50 mV; pulse width: 0.05 s; pulse period: 0.5 s)

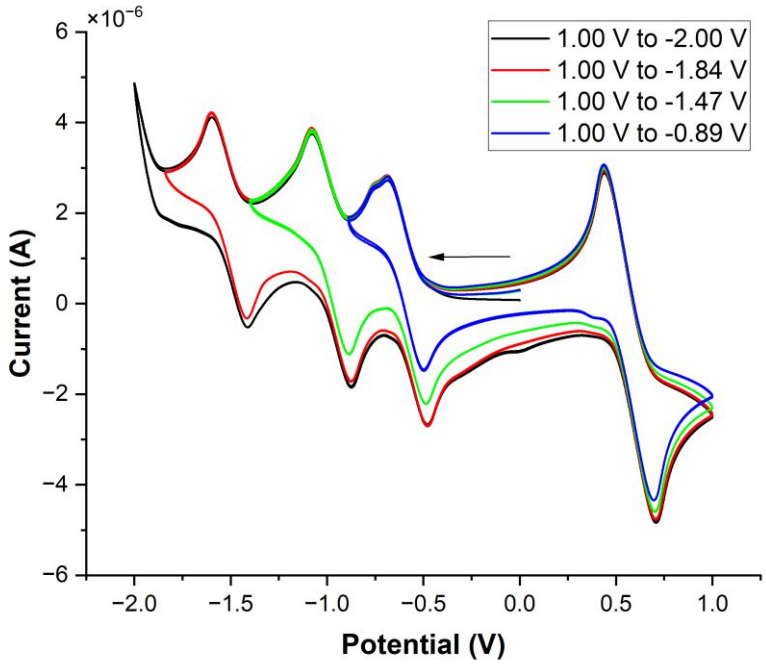

Fig. S89 CV of compound **3ac**. (scanning rate: 50 mV s^{-1})

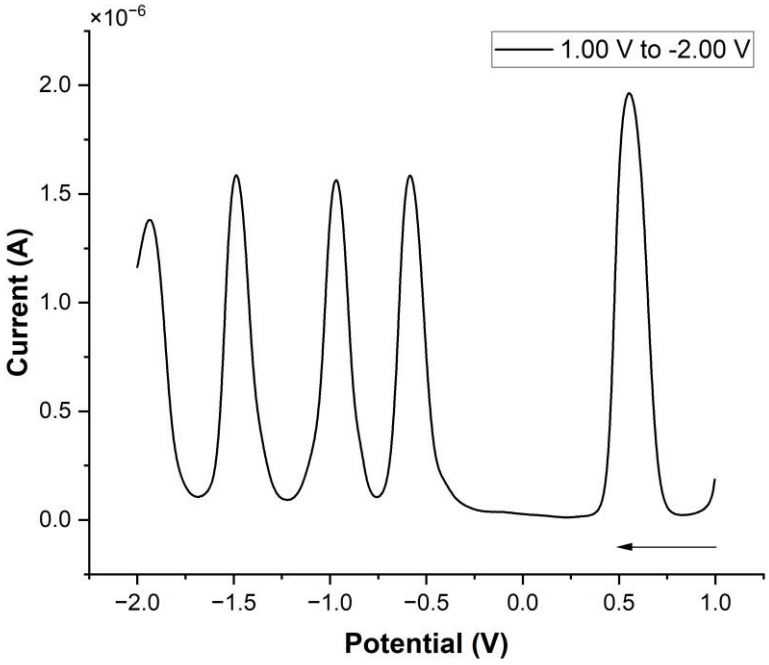

Fig. S90 DPV of compound **3ac**. (pulse amplitude: 50 mV; pulse width: 0.05 s; pulse period: 0.5 s)

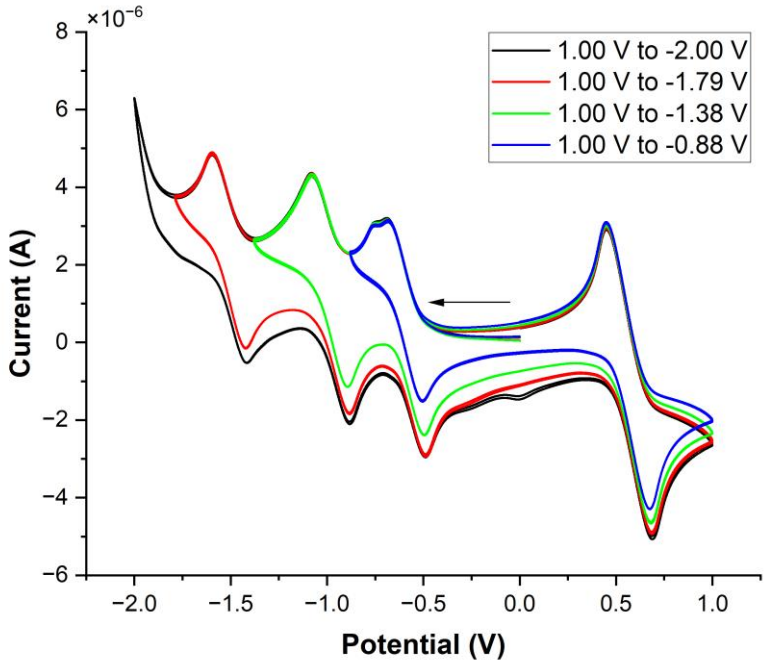

Fig. S91 CV of compound **3ad**. (scanning rate: 50 mV s^{-1})

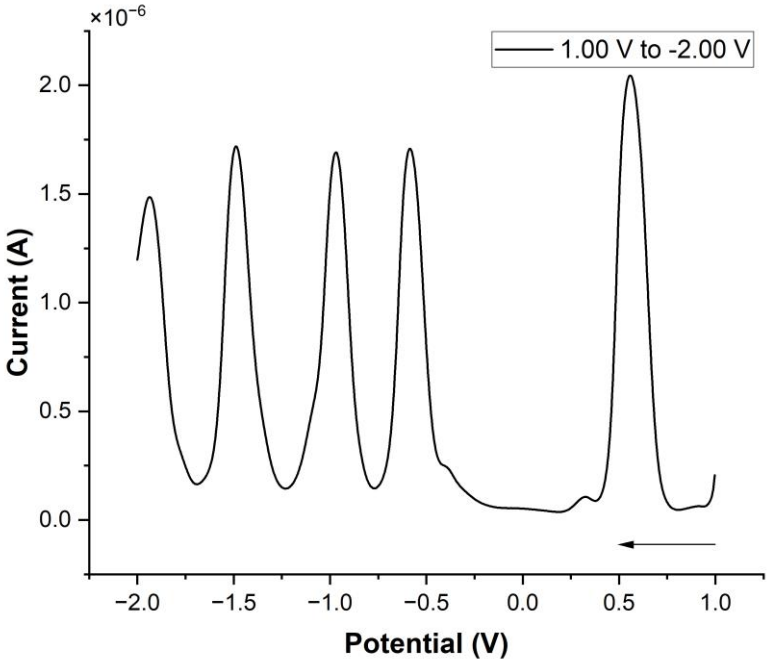

Fig. S92 DPV of compound **3ad**. (pulse amplitude: 50 mV; pulse width: 0.05 s; pulse period: 0.5 s)

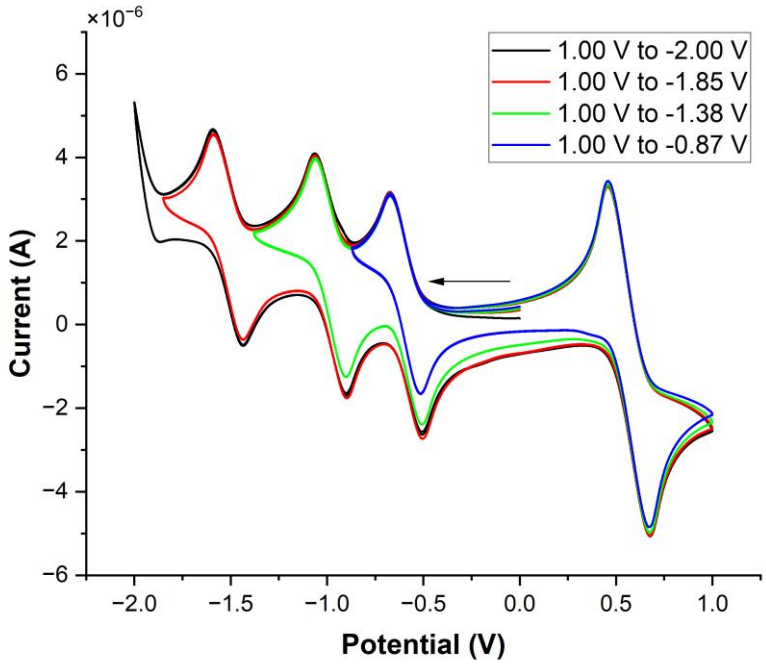

Fig. S93 CV of compound **3ae**. (scanning rate: 50 mV s^{-1})

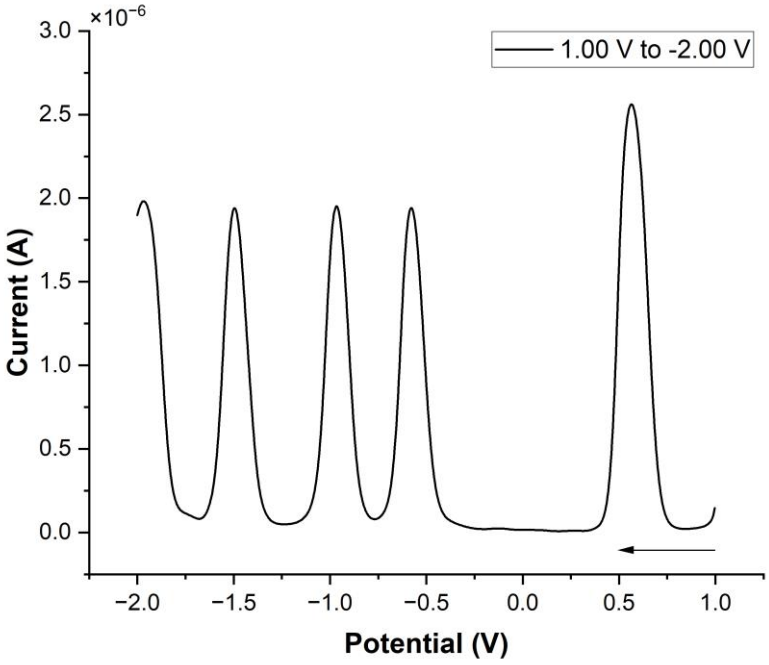

Fig. S94 DPV of compound **3ae**. (pulse amplitude: 50 mV; pulse width: 0.05 s; pulse period: 0.5 s)

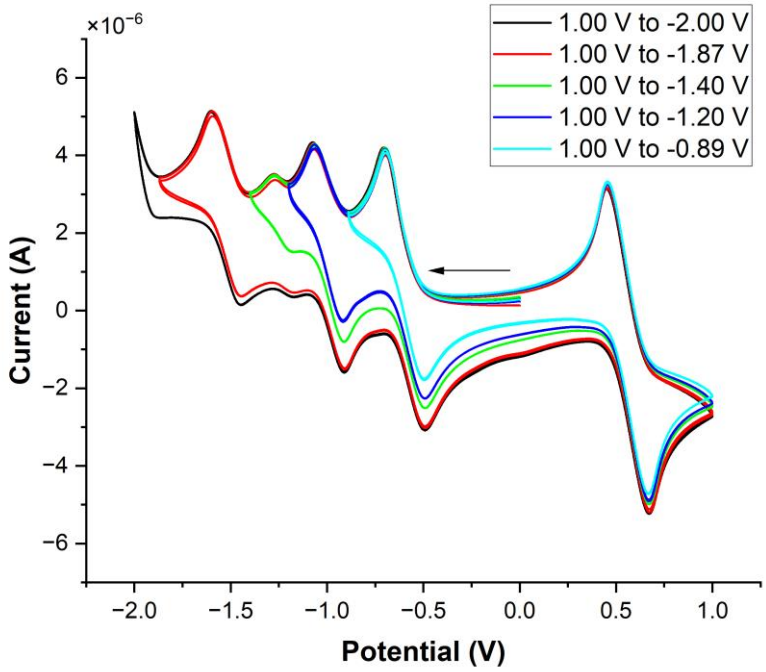

Fig. S95 CV of compound **3af**. (scanning rate: 50 mV s^{-1})

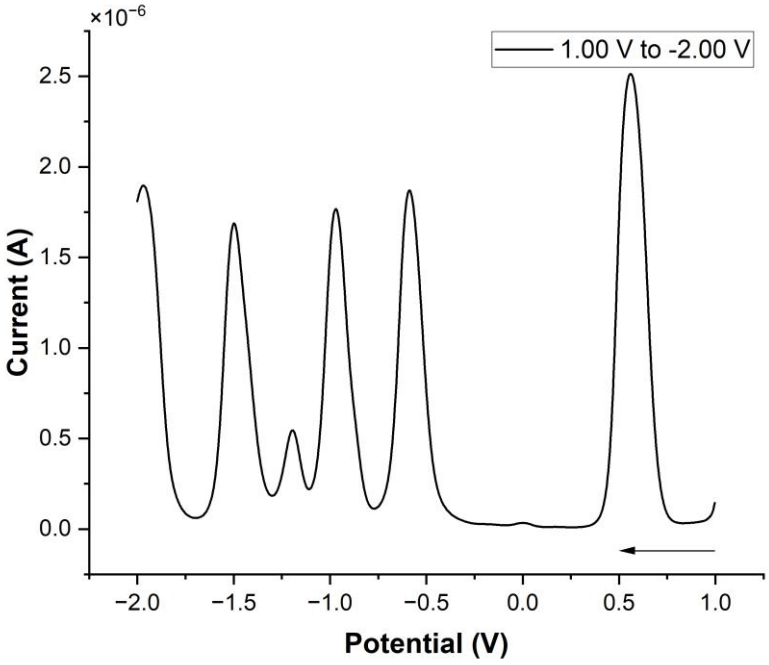

Fig. S96 DPV of compound **3af**. (pulse amplitude: 50 mV; pulse width: 0.05 s; pulse period: 0.5 s)

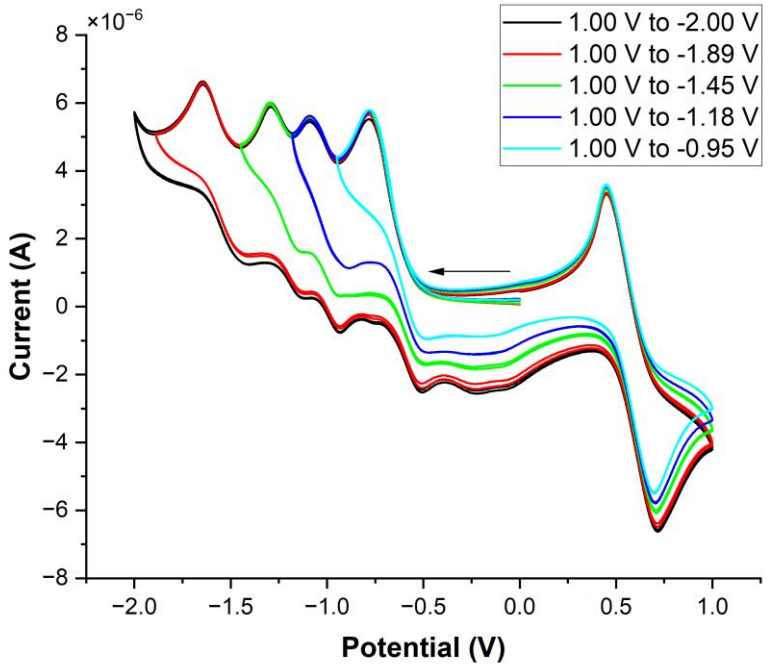

Fig. S97 CV of compound **3ag**. (scanning rate: 50 mV s^{-1})

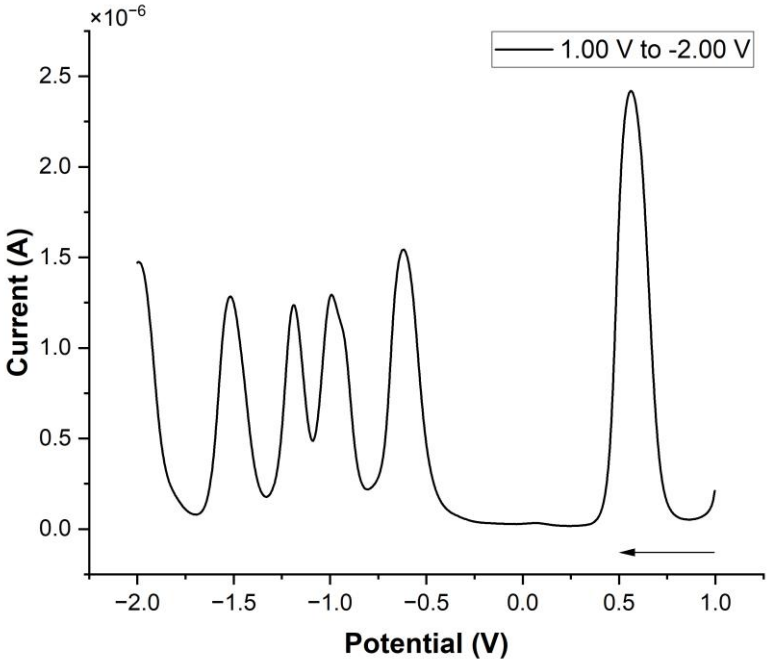

Fig. S98 DPV of compound **3ag**. (pulse amplitude: 50 mV; pulse width: 0.05 s; pulse period: 0.5 s)

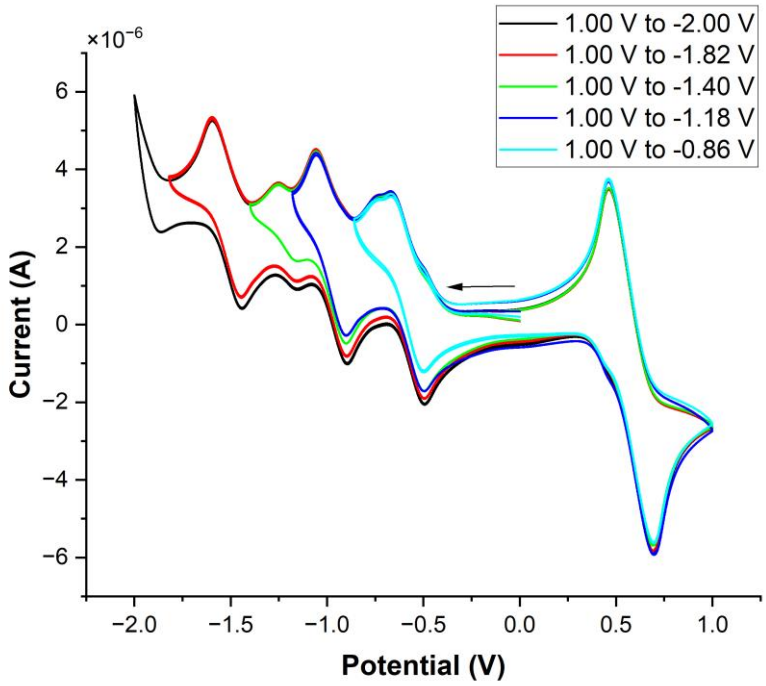

Fig. S99 CV of compound **3ah**. (scanning rate: 50 mV s^{-1})

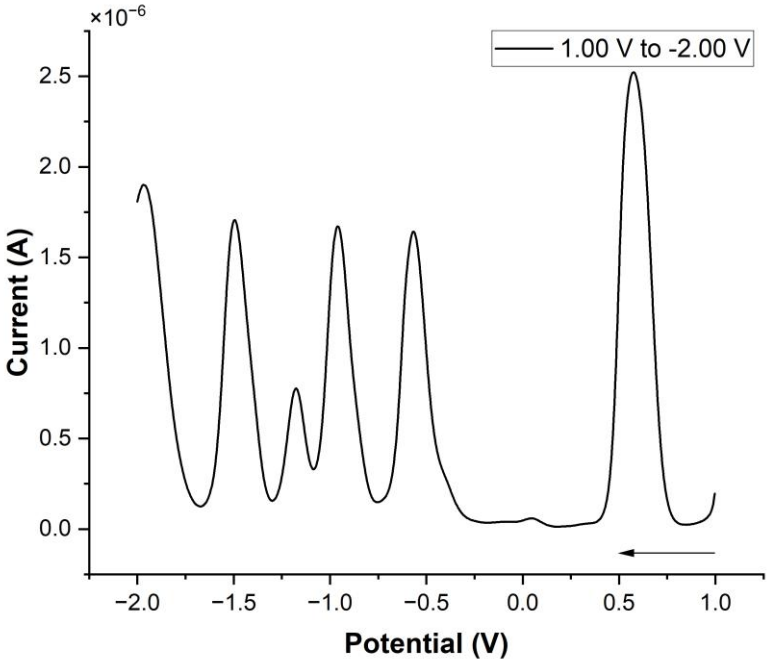

Fig. S100 DPV of compound **3ah**. (pulse amplitude: 50 mV; pulse width: 0.05 s; pulse period: 0.5 s)

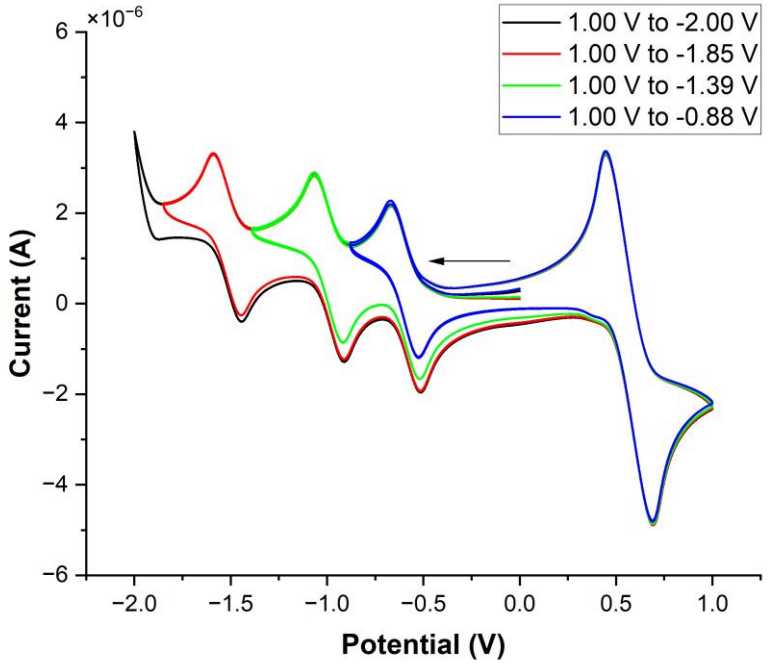

Fig. S101 CV of compound **3bd**. (scanning rate: 50 mV s^{-1})

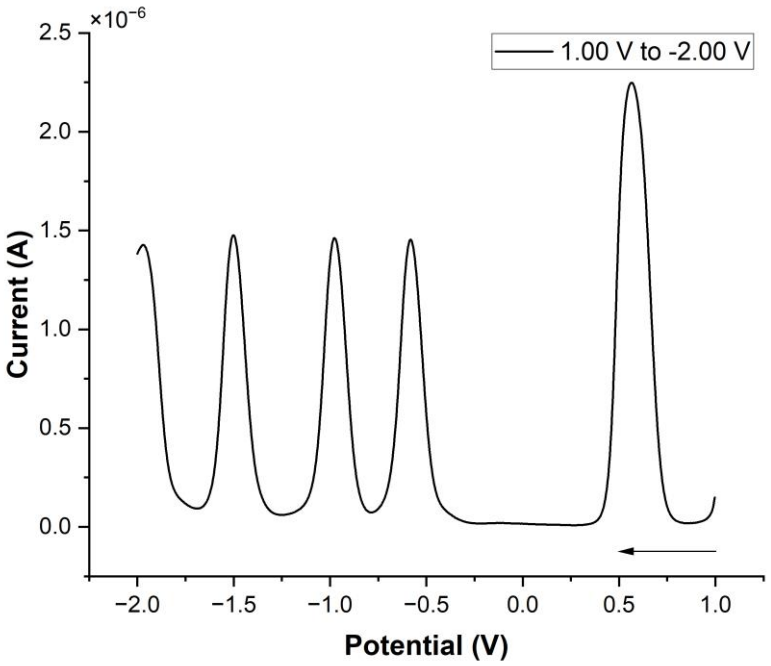

Fig. S102 DPV of compound **3bd**. (pulse amplitude: 50 mV; pulse width: 0.05 s; pulse period: 0.5 s)

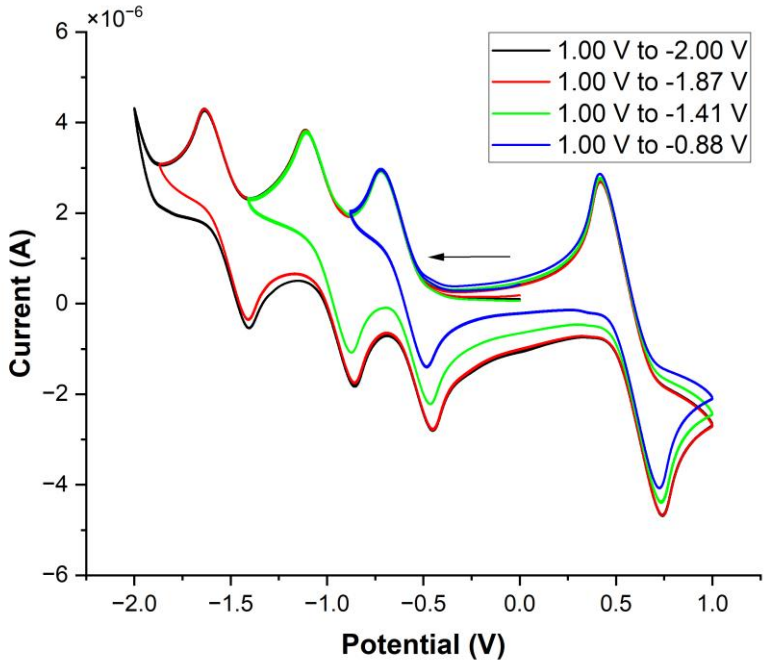

Fig. S103 CV of compound **3cd**. (scanning rate: 50 mV s^{-1})

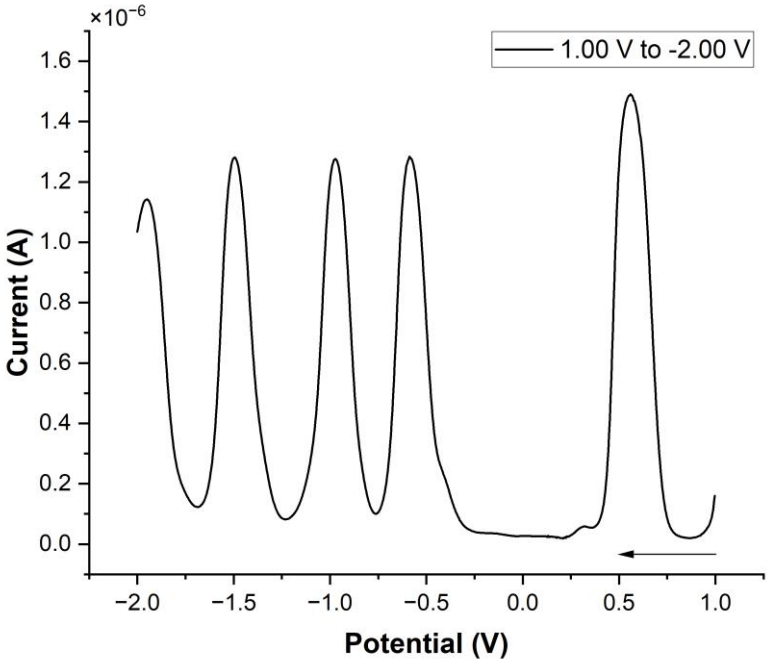

Fig. S104 DPV of compound **3cd**. (pulse amplitude: 50 mV; pulse width: 0.05 s; pulse period: 0.5 s)

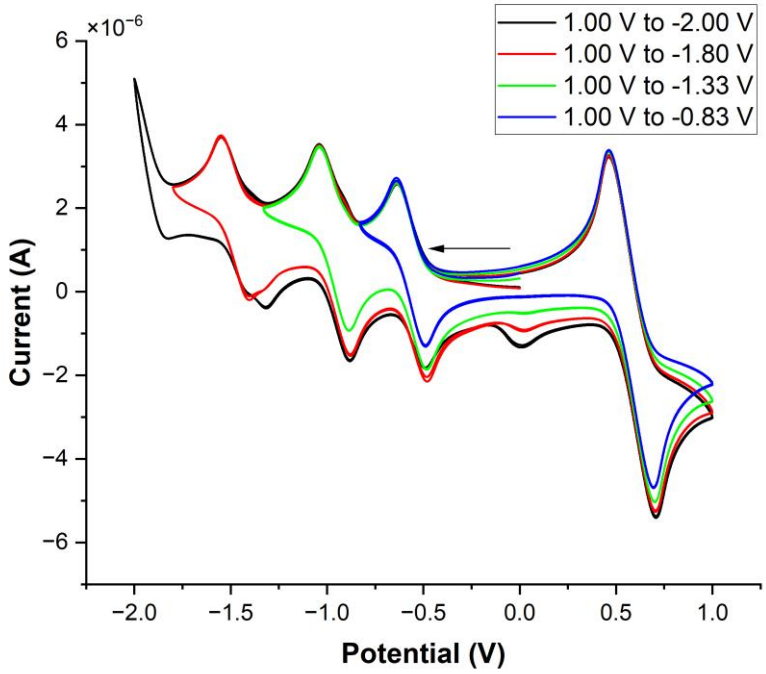

Fig. S105 CV of compound **3dd**. (scanning rate: 50 mV s^{-1})

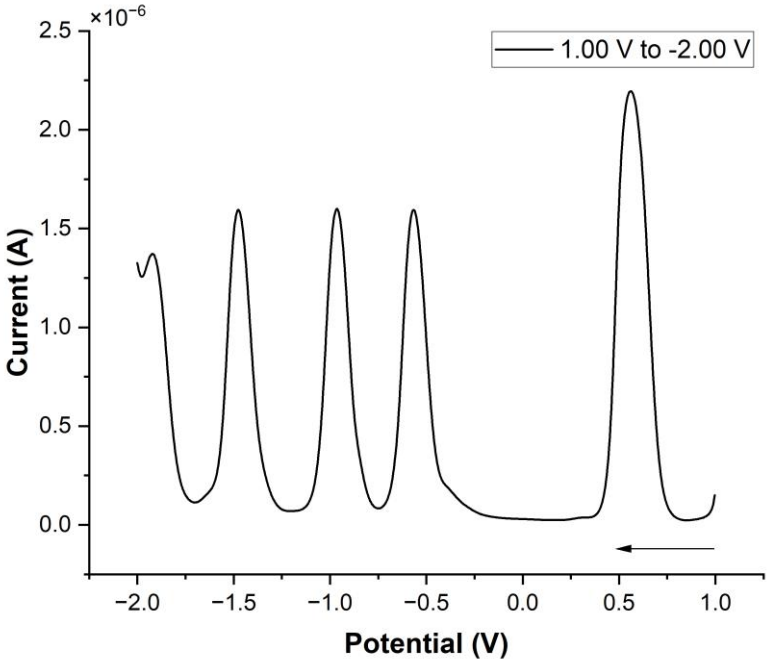

Fig. S106 DPV of compound **3dd**. (pulse amplitude: 50 mV; pulse width: 0.05 s; pulse period: 0.5 s)

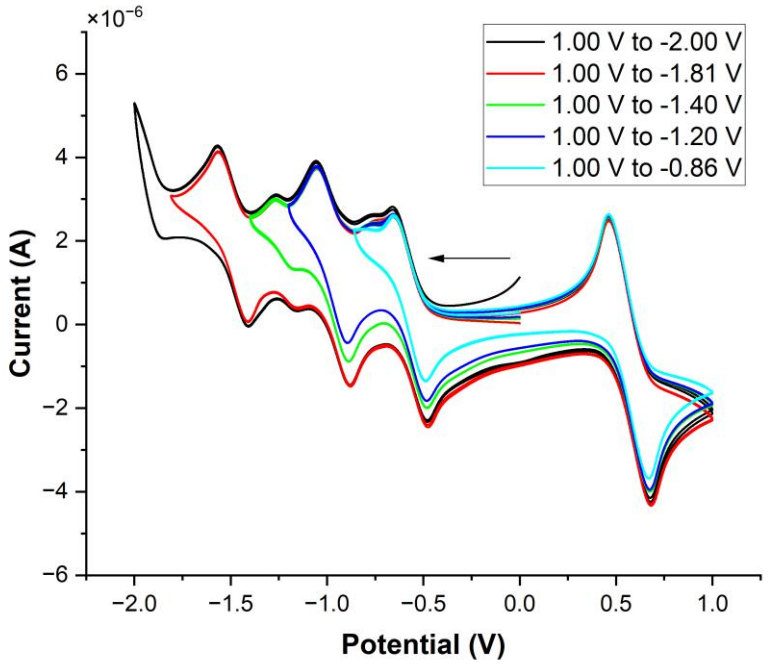

Fig. S107 CV of compound **3ed**. (scanning rate: 50 mV s^{-1})

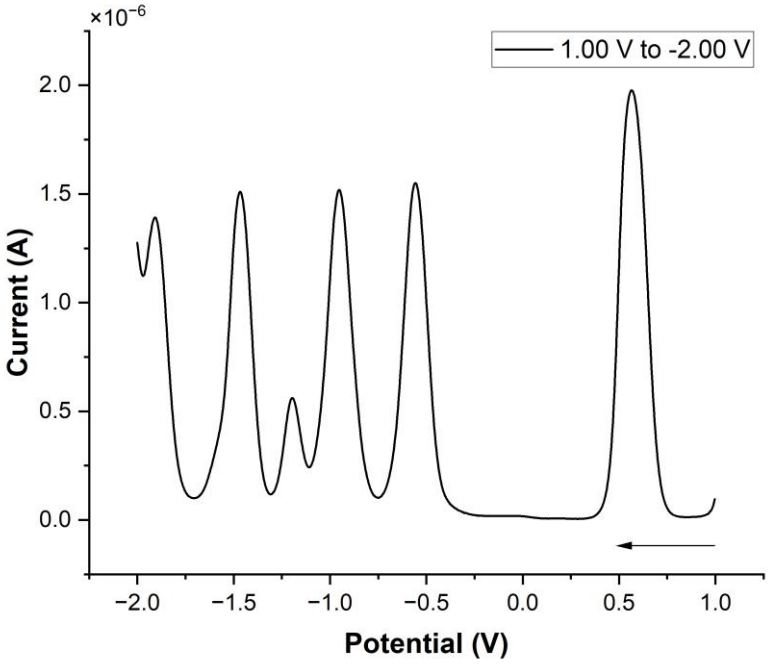

Fig. S108 DPV of compound **3ed**. (pulse amplitude: 50 mV; pulse width: 0.05 s; pulse period: 0.5 s)

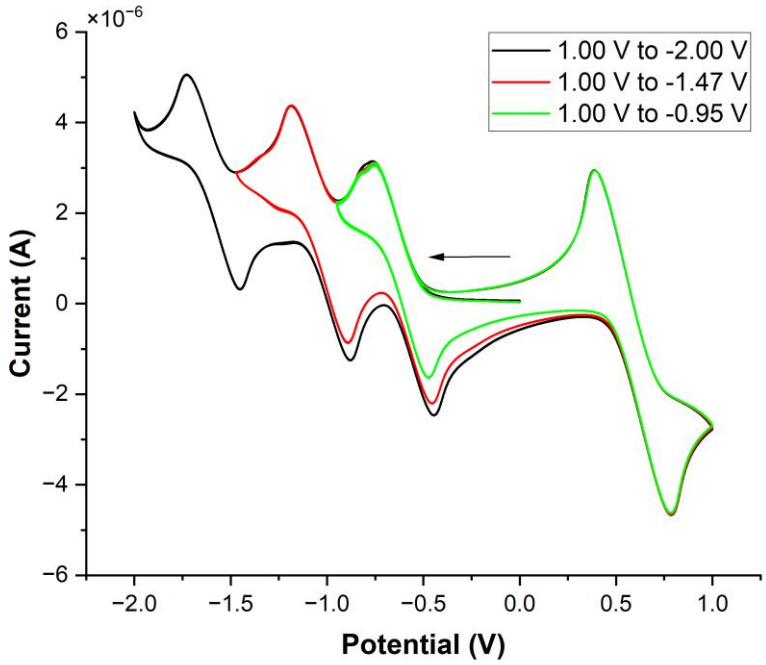

Fig. S109 CV of compound **3fd**. (scanning rate: 50 mV s^{-1})

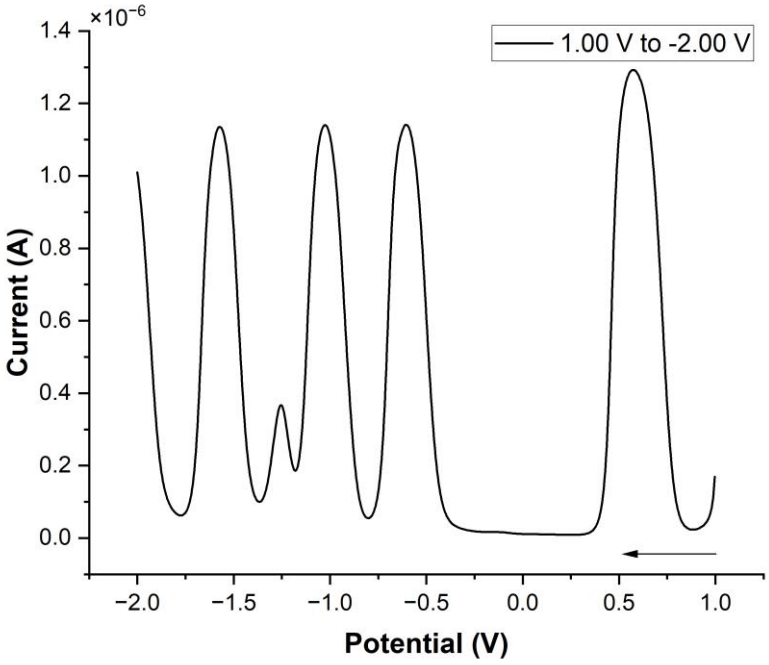

Fig. S110 DPV of compound **3fd**. (pulse amplitude: 50 mV; pulse width: 0.05 s; pulse period: 0.5 s)

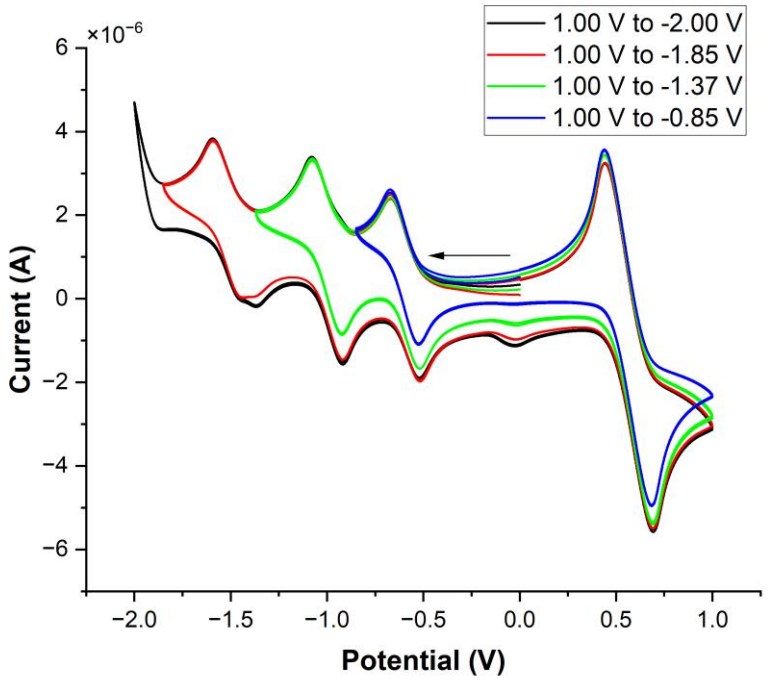

Fig. S111 CV of compound **3gd**. (scanning rate: 50 mV s^{-1})

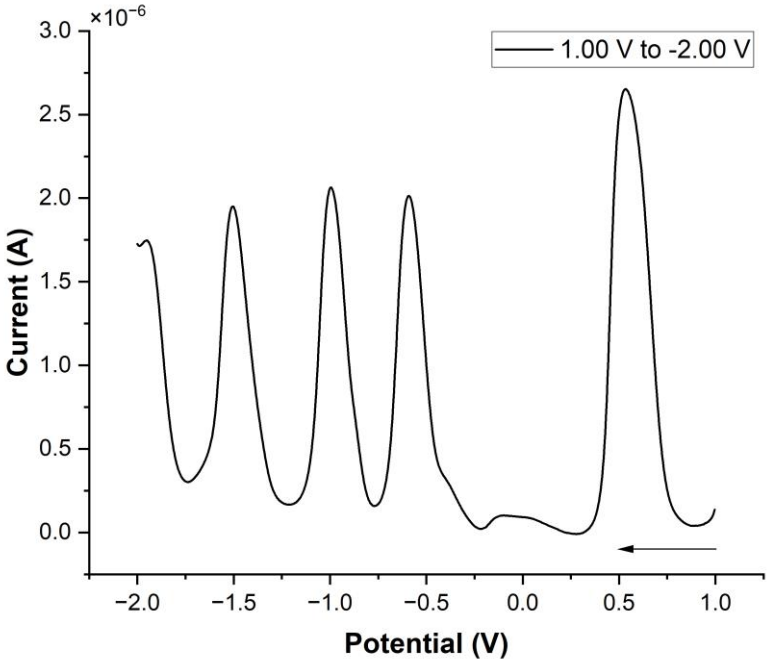

Fig. S112 DPV of compound **3gd**. (pulse amplitude: 50 mV; pulse width: 0.05 s; pulse period: 0.5 s)

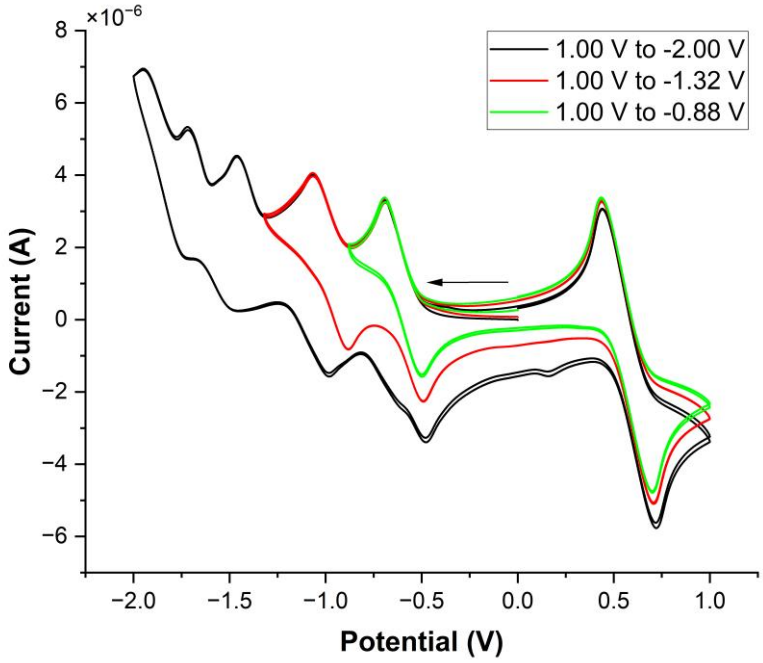

Fig. S113 CV of compound **3ha**. (scanning rate: 50 mV s^{-1})

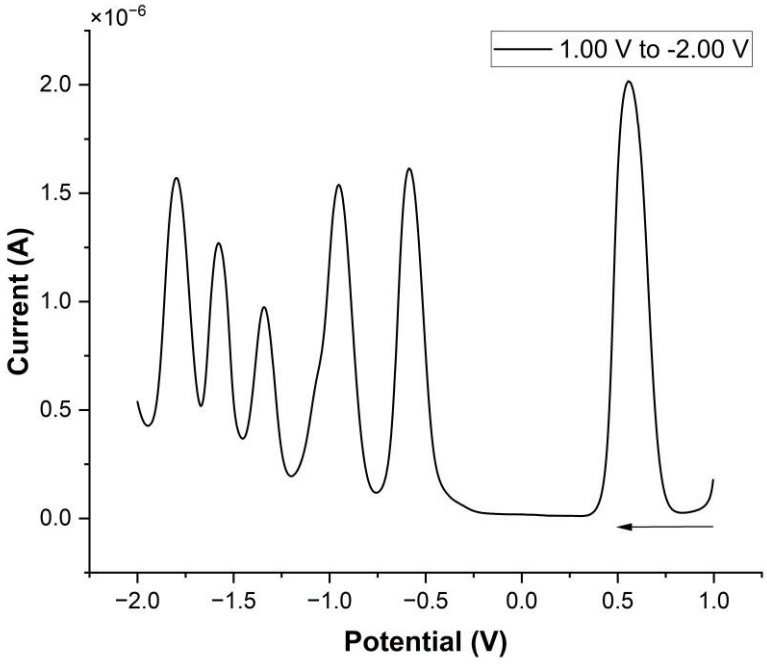

Fig. S114 DPV of compound **3ha**. (pulse amplitude: 50 mV; pulse width: 0.05 s; pulse period: 0.5 s)

9. Device fabrication and photovoltaic parameters

Pre-patterned indium-doped tin oxide (ITO) glass substrates were cleaned by sequential sonication in glass detergent, deionized water, acetone, and isopropyl alcohol for at least 20 min each, followed by drying under a nitrogen stream and ultraviolet-ozone treatment for 15 min. A PEDOT:PSS layer was spin-coated onto the ITO substrate (4500 rpm, 30 s) from an aqueous dispersion and annealed at 150 ◦C for 15 min in air. The active layers were prepared from chloroform solutions (15 mg/mL total concentration) containing either a binary blend of 5-(5-(4,8-bis(4-chloro-5-(2-ethylhexyl)thiophen-2-yl)-6-methylbenzo[1,2-b:4,5-b']dithiophen-2-yl)-4-(2-butyloctyl)thiophen-2-yl)-8-(4-(2-butyloctyl)-5-methylthiophen-2-yl)dithieno[3',2':3,4;2",3":5,6]benzo[1,2-c][1,2,5]thiadiazole (D18-Cl) and 2,2'-((2Z,2'Z)-((12,13-bis(3-ethylheptyl)-3,9-diundecyl-12,13-dihydro-[1,2,5]thiadiazolo[3,4-e]thieno[2",3":4',5']thieno[2',3':4,5]pyrrolo[3,2-g]thieno[2',3':4,5]thieno[3,2-b]indole-2,10-diyl)bis(methaneylylidene))bis(5,6-difluoro-3-oxo-2,3-dihydro-1H-indene-2,1-diylidene))dimalononitrile (N3) (1:1.4 by weight) or a ternary blend of D18-Cl, N3 and fullerene (1:1.4:0.05 by weight). Each solution was stirred at 65 °C for 2 h. Then, the above active blend in chloroform was spin-coated onto the PEDOT:PSS layer. *N,N′*-bis[7-(dimethylamino)-4-azaheptyl]-3,4,9,10-perylenetetracarboxylic diimide (PDINN, 1 mg/mL) in MeOH solution was spin-coated onto the active layer (3800 rpm for 30 s) as the electron transfer layer. The fabrication of all layers was carried out in a nitrogen-filled glove box (Mikrouna Co., Ltd.). Ag (~100 nm) was evaporated onto PDINN through a shadow mask (pressure ca. 3×10^{-4} Pa). The effective area for the devices was 4 mm^2. Current density-voltage (*J–V*) were measured using a Keysight B2901BL source meter coupled with a xenon-lamp solar simulator (Enlitech, AM 1.5G, 100 mW cm^{-2}). The light intensity was calibrated with a certified Si reference cell (SRC-2020, 2 cm×2 cm, Enlitech).

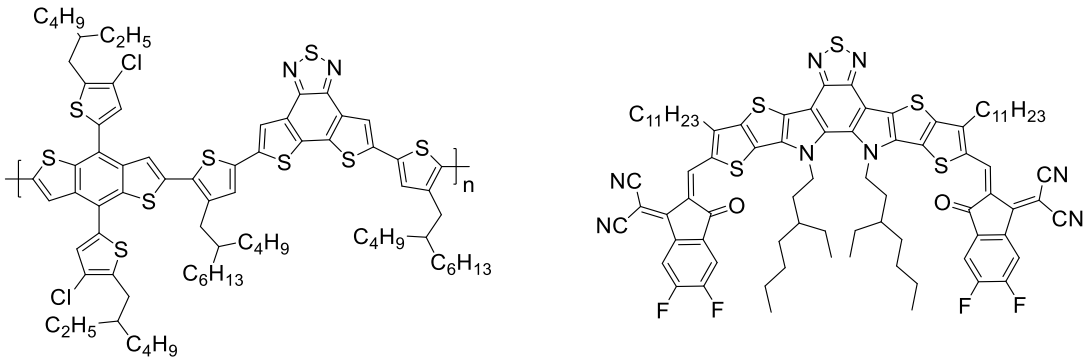

Fig. S115 The structures of D18-Cl and N3.

Table S3 Photovoltaic parameters for organic solar cells.

Active Layer	V_{OC} (V)	J_{SC} (mA cm^{-2})	FF (%)	PCE (%)[a]
D18-Cl:N3	0.878	27.15	74.42	17.75 (17.72 ± 0.03)
D18-Cl:N3:PCBM	0.886	27.41	74.09	17.99 (17.87 ± 0.12)
D18-Cl:N3:**3ah**	0.882	27.37	76.38	18.44 (18.23 ± 0.15)

[a]The average values in parentheses were calculated from 5 individual devices.

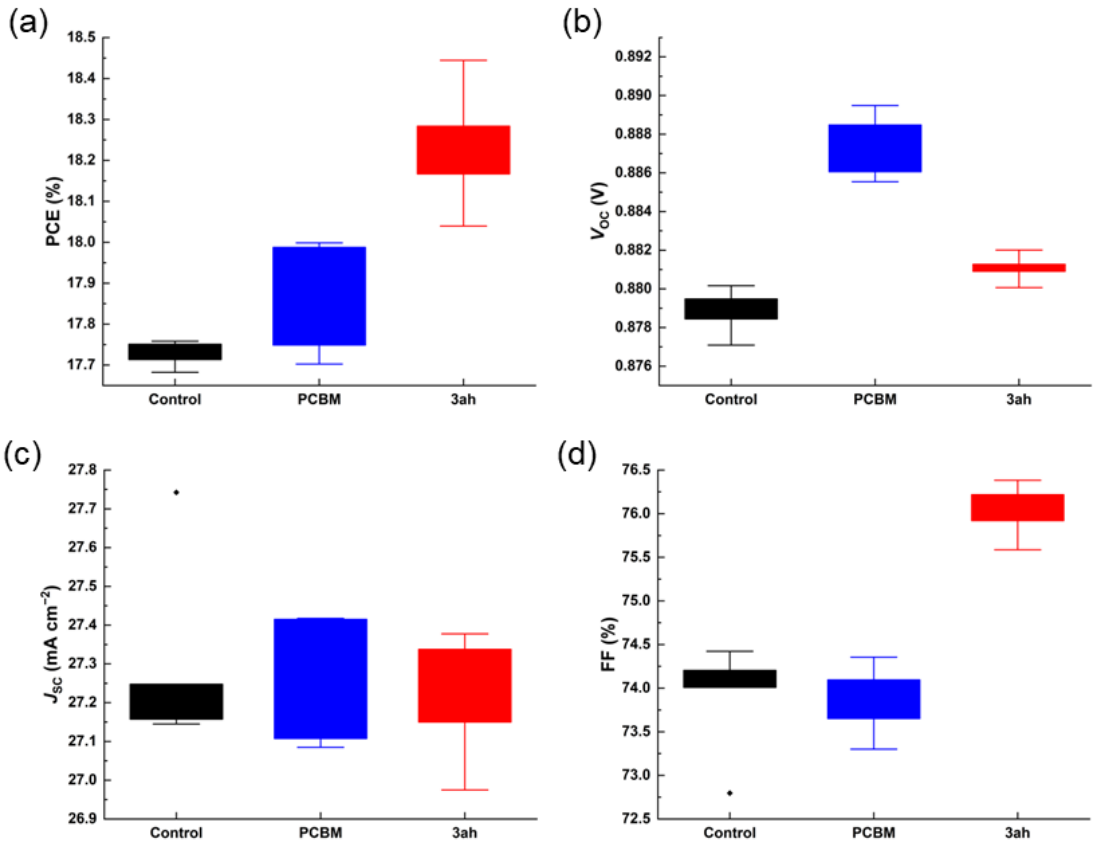

Fig. S116. Statistical distributions of photovoltaic parameters for OSCs based on D18-Cl:N3 (black), D18-Cl:N3:PCBM (blue) and D18-Cl:N3:**3ah** (red). (a) PCE, (b) V_{OC}, (c) J_{SC}, (d) FF.

10. References

1 Y.-T. Su, Y.-L. Wang and G.-W. Wang, *Chem. Commun.*, 2012, **48**, 8132–8134.
2 Y. He, H.-Y. Chen, J. Hou and Y. Li, *J. Am. Chem. Soc.*, 2010, **132**, 1377–1382.
3 J. G. Wijmans and R. W. Baker, *J. Membr. Sci.*, 1995, **107**, 1–21.
4 T. Johnson and S. Thomas, *Polymer*, 1999, **40**, 3223–3228.